AUTOIGNITION IN NONPREMIXED FLOW

by

A. Liñán and F.A. Williams

IDEA Final Technical Report
March, 1993

SUMMARY

The objective of this investigation has been to improve understanding of autoignition processes in nonpremixed flow fields of the types encountered in Diesel-engine ignition, through theoretical analyses that employ asymptotic methods of applied mathematics. The work was intended to develop formulas and equations that can be used in activities of applied research, such as code development, aimed at providing tools useful for the design of Diesel engines. The formulas may also be used directly for ignition estimates.

Characteristic time scales were identified for these ignition problems. Their relative magnitudes were employed to define different regimes of ignition and to obtain simplified partial differential equations that describe ignition in these regimes. Effects of turbulence on ignition were addressed. Special attention was devoted to unsteady mixing layers, involving both variable strain and variable pressure, for which ignition-time formulas were derived. In addition, ignition analyses were completed for variable-volume chambers with arbitrary initial spatial variations of temperature and composition, to determine pressure histories produced by ignition-front propagation.

These studies were based on one-step, Arrhenius approximations for the chemical kinetics and were restricted to ignition stages that precede ordinary flame propagation. Additional work considered triple-flame propagation that can occur in mixing layers after ignition, with this same chemical-kinetic description, and asymptotic analysis of n-heptane ignition on the basis of a four-step, semi-empirical model for the chemical kinetics. In this latter study, the region of negative effective overall activation energy, between 800 K and 1100 K, was identified as exhibiting unusual ignition dynamics, and the asymptotic ignition-time formulas were shown to give good agreement with predictions of numerical integrations.

This research has helped to strengthen the foundations of ignition theory for nonuniform media. It provided simplified descriptions of ignition processes that can be employed in studies of Diesel combustion that are oriented more towards development than are the present investigations. The asymptotic methods employed in this work thus appear capable of providing quite useful results.

1 INTRODUCTION

1.1 STATEMENT OF PROGRAM OBJECTIVES AND WORK

This program was designed to involve theoretical analyses of partial differential equations that describe autoignition in Diesel engines, employing asymptotic methods in applied mathematics, principally activation-energy asymptotics (AEA). It was intended to apply the AEA approach to various specific problems encountered in Diesel autoignition. The work initially was divided into five tasks, as listed below:

1. Derivation of ignition delay times in a nonpremixed flow field for a one-step reaction. This problem concerned autoignition in the time-dependent mixing between stagnant, isobaric, gaseous fuel and oxidizer regions at different temperatures. The AEA approach was to be applied to obtain critical conditions for ignition to occur and expressions for ignition times.

2. Unsteady effects, time scales. Time scales associated with various Diesel processes were to be considered, such as droplet vaporization times under subcritical conditions, fuel diffusion times, mixing-layer development times, spray penetration times, turbulent eddy times, and times associated with pressure increases resulting from piston motion. These times were to be compared with homogeneous ignition times and flame propagation times to ascertain the most significant autoignition processes to be analyzed by AEA. Conditions were to be identified for first occurrence of ignition along the centerline of the transient fuel jet, in the mixing layer at the edge of the jet, or in the recirculation flow in the bulk of the chamber. The unsteady effect of compressive heating on the autoignition time was to be calculated by AEA through inclusion of the appropriate $\partial p/\partial t$ term in the equation for energy conservation. Unsteady effects associated with flame propagation in the non-homogeneous system immediately following the autoignition event also were to be considered by AEA, with special emphasis on non-planar edge effects, to ascertain whether flames develop or decay. Considerations of the unsteady effects were intended to improve understanding of autoignition process in nonuniform flows.

3. Turbulent fluctuations of the scalar and the flow. Turbulence produces fluctuations of both velocity and scalar fields. These fluctuations affect autoignition processes occurring in the Diesel chamber. Influences of these fluctuations on autoignition were to be addressed. Questions to be considered included whether the ignition chemistry occurs independently within the smallest eddies or over larger eddies affected by turbulent diffusion from smaller eddies. Influences of the fluctuations on the initial nonuniform flame propagation away from ignition points also were to be investigated. The approaches were to make extensive use of AEA.

4. The influence of pressure transients. Pressure transients are thought to be of high potential importance to autoignition processes. In addition to the homogeneous effect of compressive heating there can be effects of pressure oscillations resulting, for example, from acoustic amplification. Investigations of these influences of pressure transients were to be included in the program by adding the appropriate terms to the conservation equations then proceeding with the AEA analysis.

5. The influence of radiation. Radiant energy transfer possibly could affect autoignition times through rapid, selective deposition of energy in regions favorable for ignition chemistry. The strongest effects of radiation often are associated with soot, which can both emit and absorb radiant energy efficiently. Because of the possible importance of radiation, it is desirable to include radiant absorption and emission terms in the equation for energy conservation when autoignition analyses by AEA are pursued. The last phase of the research initially was intended to incorporate these radiation effects. Of special interest is the possibility of radiation being emitted in one part of the Diesel chamber and absorbed in another part. These nonhomogeneity influences were to be considered.

For the most part, the research did indeed involve pursuit of these five tasks for one-step, Arrhenius chemistry, as originally envisioned. However, at a later stage it was decided, in agreement with N. Peters and K.-P. Schindler, to deemphasize the fifth task and instead to consider asymptotic analyses of n-heptane ignition with a four-step kinetic model. This decision was prompted by development of the four-step model after initiation of the program and by estimates indicating that, especially during ignition transients, radiation is less important than initially envisioned. Our studies showed that self-ignition occurs nearly simultaneously at many points in the chamber and extends to the rest of the chamber through self-ignition fronts enhanced by the pressure rise rather than by the ordinary flame propagation that generates radiant energy flux from the high-temperature products and soot that it produces. Thus, although radiation may be expected to play an important role in the heating and vaporization of droplets entering the chamber after ignition or of the larger droplets that do not vaporize during ignition, the effects of radiation during the ignition process itself appear to be small. On the other hand, there was a strong need to investigate the implications of the four-step model by asymptotic methods, and therefore this task was added, largely as a replacement for task 5.

1.2 RELATIONSHIPS TO OTHER PROGRAMS

As stated above, the results of the present program are intended to be used by other programs that are of a more applied character. The closest immediate research interactions of the present work were with the program of Peters at Aachen (and thereby, indirectly, with the program of Warnatz) and with the program of Bray and Rogg at Cambridge. In particular, the work under all tasks involved coordination and sometimes collaboration with the work of the group of Peters. The four-step model investigated in the present research came from the work of Peters, for example. The

work under the second task, related to flame propagation in nonhomogeneous systems, involved collaboration with the Cambridge group. For example, the numerical approach for calculating the triple flames was developed and executed by Rogg; it involved discussions and interpretations by Liñán. The interactions throughout the program occurred through numerous technical discussions at IDEA and other meetings.

1.3 THE FOLLOWING CHAPTERS

The following chapters present summary technical discussions of research performed under the various tasks listed above. Chapter 2 sets the general stage by addressing items mainly in tasks 2 and 3, but also with consideration of task 4. Chapter 3 reports results of research on task 1, simultaneously including pressure-transient effects (task 4) and mixing-layer aspects of task 2. Chapter 4 pertains to tasks 2, 3 and 4, expanding on turbulence effects and bringing the application to non-homogeneous, variable-volume chambers. Chapter 5 details the triple-flame study alluded to in task 2. Finally, Chapter 6 concerns the study of the four-step chemistry that replaced task 5. Chapter 7 summarizes conclusions and recommendations for future work.

2 TURBULENCE INTERACTIONS IN DIESEL IGNITION

2.1 INTRODUCTION

Ignition in turbulent mixing regions may be influenced by the turbulence in different ways, depending on the relative time scales involved. The wide range of chemical times encountered in autoignition processes such as those in diesel engines cause turbulent ignition problems to be especially difficult.[1] The developing knowledge concerning the behaviors of laminar mixing regions in turbulent flows[2] provides a basis for beginning to address difficult problems of this kind. Many different approaches to describing turbulent combustion processes now exist,[1-3] and some of these methods may be brought to bear on the ignition problem. To investigate such possibilities, conservation equations underlying nonpremixed turbulent ignition are written here, and through identification of various scales some conclusions are drawn concerning different possible ignition regimes.

2.2 SPECIES AND ENERGY CONSERVATION

The well-known equations for conservation of total mass and of momentum underlie the description of the turbulent flow. To focus on the ignition process per se, these equations are taken to be given, and attention is directed to the equations for conservation of chemical species and of energy. The chemistry will be described by the one-step reaction between fuel F and oxidizer O,

$$F + \nu_O O \rightarrow \text{Products} + q, \tag{1}$$

having the mass rate of production of fuel

$$w_F = -\rho B Y_F^n Y_O^m \exp\left(-E/RT\right). \tag{2}$$

Parameters here are the activation energy E, the reaction orders m and n, the mass of oxidizer consumed per unit mass of fuel consumed ν_O, and the heat released per unit mass of fuel consumed q. Variables are the mass fractions Y_i, temperature T and density ρ. Use will be made of the equation of state of an ideal gas,

$$\rho = p\overline{W}/RT, \tag{3}$$

where p is pressure and $\overline{W}$ the average molecular weight of the mixture. The function B, the reciprocal of a time related to a characteristic chemical time, depends weakly on Y_i and T and is proportional to $p^{\ell-1}$ where ℓ is the pressure exponent of the reaction rate.

The equations for species and energy conservation may be written as[4]

$$\rho\left(\frac{\partial Y_i}{\partial t} + \mathbf{v}\cdot\nabla Y_i\right) = \frac{1}{L_i}\nabla\cdot\left(\frac{k}{c_p}\nabla Y_i\right) + w_i, \qquad i = F, O \tag{4}$$

and

$$\rho\left(\frac{\partial T}{\partial t} + \mathbf{v}\cdot\nabla T\right) = \nabla\cdot\left(\frac{k}{c_p}\nabla T\right) + \frac{1}{c_p}\frac{\partial p}{\partial t} + w_T, \tag{5}$$

where

$$w_O = \nu_O w_F, \qquad w_T = -(q/c_p)\, w_F. \tag{6}$$

Here the specific heat at constant pressure c_p has been assumed constant, as have the Lewis numbers

$$L_F = \frac{k}{\rho c_p D_F}, \qquad L_O = \frac{k}{\rho c_p D_O} \tag{7}$$

in the Fick's-law approximation, but variations of the thermal conductivity k are permitted, subject to these restrictions. The energy equation here involves the further significant assumptions of low Mach numbers and negligible radiant energy transfer, resulting in p depending only on t (e.g. through engine compression) in the first approximation.

These equations are influenced by the turbulent velocity field $\mathbf{v}$ and need appropriate initial and boundary conditions before further progress in analysis can be made. The boundary conditions of interest are those for nonpremixed combustion such that, for all time, two different types of inflow boundaries can be identified, a fuel inlet in which the flux fraction of fuel everywhere is the constant Y_{Fo} and the flux fraction of oxidizer is zero, and an air inlet in which the flux fraction of oxidizer everywhere is the constant Y_{Oo} and the flux fraction of fuel is zero. Gas temperatures in the fuel and air inlet streams are denoted by the constants T_F and T_O, respectively. Since two-phase flow is not addressed here, the fuel boundary is taken to surround liquid fuel, so that gaseous fuel vapor composes the inlet stream; a number of additional interesting turbulence phenomena that require further consideration will arise when liquid fuel streams are considered. In addition to the inflow boundaries there are outflow boundaries at which the species and energy fluxes are not specified but rather to be determined, and there are impermeable boundaries at which the species fluxes are zero although energy fluxes may be nonzero (cold walls). The initial conditions also will pertain to nonpremixed combustion and will be considered to be consistent with what may be expected from boundary fluxes, thereby effectively maintaining a two-stream problem.

2.3 MIXTURE FRACTIONS

In two-stream nonpremixed systems of the type just described, it is convenient to introduce mixture fractions, defined to be unity in the fuel streams and zero in the oxidizer streams. When Lewis numbers are unity one unique mixture fraction exists; otherwise there are more than one. Two are

$$Z = \left(\frac{Y_F}{L_F} - \frac{Y_O}{\nu_O L_O} + \frac{Y_{Oo}}{\nu_O L_O}\right) \Big/ \left(\frac{Y_{Fo}}{L_F} + \frac{Y_{Oo}}{\nu_O L_O}\right) \tag{8}$$

and

$$\tilde{Z} = \left(Y_F - \frac{Y_O}{\nu_O} + \frac{Y_{Oo}}{\nu_O}\right) \Big/ \left(Y_{Fo} + \frac{Y_{Oo}}{\nu_O}\right). \tag{9}$$

At stoichiometric conditions $Z = Z_S$ and $\tilde{Z} = \tilde{Z}_S$, where

$$Z_S = (1+S)^{-1}, \qquad \tilde{Z}_S = \left(1+\tilde{S}\right)^{-1}, \tag{10}$$

in which the stoichiometric mixture ratios are

$$S = (L_O \nu_O Y_{Fo}) / (L_F Y_{Oo}), \qquad \tilde{S} = (\nu_O Y_{Fo}) / (Y_{Oo}), \tag{11}$$

the first Lewis-number weighted. From Eq. (4) it can be shown (by subtracting the equation for i = F from ν_O^{-1} times that for i = O) that

$$\rho \left(\frac{\partial \tilde{Z}}{\partial t} + \mathrm{v} \cdot \nabla \tilde{Z} \right) = \frac{1}{L} \nabla \cdot \left(\frac{k}{c_p} \nabla Z \right), \tag{12}$$

where the stoichiometry-weighted Lewis number is

$$L = \left(Y_{Fo} + \frac{Y_{Oo}}{\nu_O} \right) / \left(\frac{Y_{Fo}}{L_F} + \frac{Y_{Oo}}{\nu_O L_O} \right). \tag{13}$$

Although Eq. (12) is free from the chemical source, it involves two different functions unless $L_F = L_O$ (in which case $\tilde{Z} = \mathrm{Z}$).

2.4 ENTROPY-RELATED TEMPERATURE RATIO

For ignition by compression the term involving $\partial p / \partial t$ in Eq. (5) is important. This term detracts from the symmetry between Eqs. (4) and (5) and motivates introduction of a transformation prior to turbulence analysis. The nondimensional ratio of the local temperature to the isentropic temperature in the air stream is called here the entropy-related temperature ratio and is defined as

$$\theta = [T / T_O(0)] \, [p(0)/p(t)]^{(\gamma-1)/\gamma}, \tag{14}$$

where the process is assumed slow enough that the pressure depends only on t in the leading approximation, and the reference initial time $t = 0$ is selected for choosing the constant air-feed temperature $T_O(0)$ and pressure $p(0)$ for completing the nondimensionalization. Here the ratio of specific heats is

$$\gamma = 1 - R / \left(\overline{W} c_p \right), \tag{15}$$

which is assumed to be constant. By definition $\theta = 1$ in the air stream at $t = 0$, and adiabatic intake is assumed, so that $\theta = 1$ in the air inlet stream for all t. A similar assumption for the fuel stream gives $\theta = \theta_F =$ constant there, where

$$\theta_F = T_F(0) / T_O(0). \tag{16}$$

Substitution into Eq. (5) gives

$$\rho \left(\frac{\partial \theta}{\partial t} + \mathrm{v} \cdot \nabla \theta \right) = \nabla \cdot \left(\frac{k}{c_p} \nabla \theta \right) + \frac{\rho \omega}{\tau_q}, \tag{17}$$

where the function ω is nondimensional and of order at most unity and τ_q a characteristic heat-release time, with

$$\omega / \tau_q \equiv w_T / \left\{ \rho T_O(0) \, [p(t)/p(0)]^{(\gamma-1)/\gamma} \right\}. \tag{18}$$

Equation (17) is seen to bear a closer resemblance to Eq. (4) than does Eq. (5). This may be observed directly by writing Eq. (4) for $i = F$ in terms of the normalized fuel mass fraction

$$Y = Y_F / Y_{Fo} \tag{19}$$

(unity in the fuel stream and zero in the oxidizer stream), yielding

$$\rho\left(\frac{\partial Y}{\partial t} + \mathbf{v}\cdot\nabla Y\right) = \frac{1}{L_F}\nabla\cdot\left(\frac{k}{c_p}\nabla Y\right) - \frac{\rho\epsilon\omega}{\tau_q} \tag{20}$$

where the nondimensional function of time

$$\epsilon = \left[c_p T_O\left(0\right) / \left(qY_{Fo}\right)\right]\left[p\left(t\right)/p\left(0\right)\right]^{(\gamma-1)/\gamma} \tag{21}$$

in practice always remains small compared with unity.

2.5 INSTANTANEOUS SCALAR DISSIPATION

Equations (12), (17) and (20) may be taken to be the relevant conservation equations for nondimensional species concentrations and energy, with Y_i and T related to the variables appearing therein through Eqs. (8), (9), (14) and (19). In nonpremixed systems it is possible to adopt a curvilinear coordinate system in which one of the coordinates is aligned with ∇Z and to treat Z and the other two coordinates, denoted by the two-component vector $\mathbf{x}_\perp$ with corresponding gradient $\nabla_\perp$, as independent variables.[2–4] The transformation $(\mathbf{x}, t) \rightarrow (Z, \mathbf{x}_\perp, t)$ formally converts Eq. (17) into

$$\begin{aligned}\frac{\partial\theta}{\partial t} + \mathbf{v}_\perp\cdot\nabla_\perp\theta &= \frac{1}{2}L\chi\frac{\partial^2\theta}{\partial Z^2} + \frac{\omega}{\tau_q} \\ &+ \frac{1}{\rho}\nabla_\perp\cdot\left(\frac{k}{c_p}\nabla_\perp\theta\right) + \frac{\partial\theta}{\partial Z}\left[\frac{\partial}{\partial t}\left(L\tilde{Z} - Z\right) + \mathbf{v}\cdot\nabla\left(L\tilde{Z} - Z\right)\right],\end{aligned} \tag{22}$$

where $\mathbf{v}_\perp$ is the two-component velocity vector composed of the $\mathbf{x}_\perp$ components of $\mathbf{v}$, the instantaneous scalar dissipation has been defined as

$$\chi = 2 \mid \nabla Z \mid^2 k / \left(\rho c_p L\right), \tag{23}$$

and use has been made of Eq. (12). The usefulness of Eq. (22) is that it aids in effecting a transformation from physical space to state-variable space and thereby facilitates solution of various problems. Often gradients of θ and Z are sufficiently well aligned, and Lewis numbers are close enough to unity, that the last line of Eq. (22) can be neglected. Interpretations can be illustrated by considering special cases that satisfy this condition.

Equation (22) indicates that finding χ as a function of Z can be helpful in addressing nonpremixed combustion problems. Equation (12) is needed for this purpose but in general is incomplete because $\tilde{Z} \neq Z$. By putting

$$\tilde{Z} = Z + \left[\left(L-1\right)/L\right] z, \tag{24}$$

where, from Eqs. (8), (9) and (13), the normalized mixture-fraction deviation z is given by

$$z = \frac{Y_F\left(1-\frac{1}{L_F}\right)+\left(\frac{Y_{Oa}}{\nu_O}-\frac{Y_O}{\nu_O}\right)\left(1-\frac{1}{L_O}\right)}{Y_{Fo}\left(1-\frac{1}{L_F}\right)+\frac{Y_{Oa}}{\nu_O}\left(1-\frac{1}{L_O}\right)} - \frac{\frac{Y_F}{L_F}+\left(\frac{Y_{Oa}}{\nu_O}-\frac{Y_O}{\nu_O}\right)\frac{1}{L_O}}{\frac{L_{Fa}}{L_F}+\frac{Y_{Oa}}{\nu_O L_O}}, \tag{25}$$

Eq. (12) can be written as

$$\nabla\cdot\left(\frac{k}{c_p}\nabla Z\right) - L\rho\left(\frac{\partial Z}{\partial t}+\mathbf{v}\cdot\nabla Z\right) = (L-1)\,\rho\left(\frac{\partial z}{\partial t}+\mathbf{v}\cdot\nabla z\right). \tag{26}$$

Here $z = 0$ in both the fuel and oxidizer streams by definition, and for illustrative purposes the right-hand side of Eq. (26), which describes the deviation of $\tilde{Z}$ from Z that is produced by convective effects, will be neglected.

To solve the resulting simplified form of Eq. (26) in laminar mixing problems use is made of mass conservation in the form

$$\partial\rho/\partial t + \partial\left(\rho v\right)/\partial x + \rho a = 0, \tag{27}$$

where x is the coordinate normal to the mixing layer, v is the component of $\mathbf{v}$ in the x direction, and a is the strain rate or velocity gradient, found from conservation of momentum in the direction tangent to the mixing layer to obey

$$\rho\left(\frac{\partial a}{\partial t}+v\frac{\partial a}{\partial x}+a^2\right) = \rho_O\left(\frac{\partial a_O}{\partial t}+a_O^2\right) + Pr\frac{\partial}{\partial x}\left(\frac{k}{c_p}\frac{\partial a}{\partial x}\right), \tag{28}$$

in which Pr denotes the (constant) Prandtl number, and the subscript O implies evaluation in the oxidizer stream. Sufficiently near the oxidizer stream $\rho \approx \rho_O\,(t)$ and $a \approx a_O\,(t)$, which may be used in Eq. (27) to give

$$v = -\left[a_O + d\left(\ell n\rho_O\right)/dt\right]\left(x - x_O\right), \tag{29}$$

where v would be zero at $x = x_O$. With this approximation, the transformations

$$\eta = \left(x - x_O\right)/\delta, \qquad \tau = \int_0^t \left[\left(k/\rho c_p\right)_O/\delta^2\right] dt, \tag{30}$$

where the selection

$$d\left(\ell n\delta\right)/d\tau = 1 - d\left(\ell n\rho_O\right)/d\tau - \delta^2 a_O/\left(k/\rho c_p\right)_O \tag{31}$$

is made for the evolution of the boundary-layer thickness, reduce Eq. (26) near the oxidizer stream to

$$\partial Z/\partial\tau - \eta\partial Z/\partial\eta = \partial^2 Z/\partial\eta^2/L. \tag{32}$$

If changes in ρ and a across the entire mixing layer may be neglected, then in addition to the oxidizer-side boundary condition that $Z = 0$ at $\eta = \infty$, the fuel-side boundary condition that $Z = 1$ at $\eta = -\infty$ may be applied to Eq. (32), the solution

to which then soon becomes time-independent in the transformed coordinates and is given by

$$Z = \frac{1}{2}\mathrm{erfc}\left(\eta\sqrt{L/2}\right). \tag{33}$$

Use of this solution in Eq. (23) gives

$$\begin{aligned}\chi &= \left[(k/\rho c_p)_O/\pi\delta^2\right]\exp\left[-2\mathrm{erfc}^{-1}(2Z)\right] \\ &\approx \left[4Z^2(k/\rho c_p)_O/\delta^2\right]\left[\mathrm{erfc}^{-1}(2Z)\right]^2,\end{aligned} \tag{34}$$

where the last equality is obtained from an expansion for small values of Z. The focus on the air-side solution is appropriate for ignition because temperatures generally are higher there and also for combustion because $Z_S \ll 1$.

Equation (34) is an expression for χ as a function of Z in which special cases may be addressed by considering different expressions for the boundary-layer thickness δ. For the unstrained time-dependent mixing layer Eqs. (30) and (31) give

$$\delta = \left[2\int_0^t (k\rho/c_p)_O\,dt\right]^{1/2}/\rho_O = \left[2t\,(k/\rho c_p)_O\right]^{1/2}, \tag{35}$$

in which the last equality applies only when $(k\rho/c_p)_O$ is independent of time. For the steady, strained mixing layer Eq. (31) gives

$$\delta = \left[(k/\rho c_p)_O/a_O\right]^{1/2}. \tag{36}$$

Taking large density variations into account in the steady-flow problem can be shown to still lead to Eq. (34) with δ given by Eq. (36). Extensions to problems involving curvature effects in $\nabla^2 Z$ also can be considered.[2] In all cases a characteristic fluid-mechanical mixing time can be defined as

$$\tau_m = \delta^2/(k/\rho c_p)_O, \tag{37}$$

so that Eq. (34) becomes

$$\chi = \left(4Z^2/\tau_m\right)\left[\mathrm{erfc}^{-1}(2Z)\right]^2. \tag{38}$$

In the two simplest cases identified above, $\tau_m = 2t$ and $\tau_m = a_O^{-1}$.

2.6 SIMPLIFIED IGNITION FORMULATION

An attractive formulation of ignition problems may be obtained by introducing the approximations identified after Eq. (22). Equation (22) then becomes

$$\partial\theta/\partial t = \frac{1}{2}L\chi\partial^2\theta/\partial Z^2 + \omega/\tau_q, \tag{39}$$

in which ω/τ_q is to be obtained from Eqs. (2), (6) and (18). Equation (14) relates θ to T, while Eq. (2) shows that Y_F and Y_O also are needed. Equation (8) relates Y_O to Z and Y_F, while Eq. (19) gives Y_F in terms of Y, which, from Eq. (20), obeys

$$\partial Y/\partial t = \frac{1}{2}(L/L_F)\chi\partial^2 Y/\partial Z^2 - \epsilon\omega/\tau_q, \tag{40}$$

by the same transformations and approximations that produced Eqs. (22) and (39). Since ϵ from Eq. (21) is small, the reaction term in Eq. (40) often can be neglected, resulting in Eq. (33) for Y with L replaced by L_F, so that

$$Y = \frac{1}{2}\mathrm{erfc}\left[(L_F/L)^{1/2}\,\mathrm{erfc}^{-1}\,(2Z)\right], \tag{41}$$

in which Eqs. (11) and (13) show that $L_F/L = \tilde{S}\,(1+S)\,/\left[S(1+\tilde{S})\right]$. In an approximation such as this, Eq. (39) becomes the key differential equation for describing ignition, the quantities appearing therein all being related to θ and Z by algebraic equations that have been given. By use of Eqs. (2), (6), (8), (11), (14), (18) and (19), in Eq. (39) the quantities ω and τ_q may be expressed as

$$\omega = (QY)^n\,[1 + SY(1+S)Z]^m\,e^{-\beta\left[(P\theta)^{-1}-1\right]} \tag{42}$$

and

$$\tau_q^{-1} = \frac{qY_o^n}{c_pT_O(0)}\left[\frac{p(0)}{p(t_O)}\right]^{(\gamma-1)/\gamma} B(T_O(t_O), Y_{Oo}, p(t_o))Y_{F_o}^n Y_{O_o}^m e^{-\beta}, \tag{43}$$

where

$$\beta = \frac{E}{RT_O(0)}\left[\frac{p(0)}{p(t_o)}\right]^{(\gamma-1)/\gamma} \tag{44}$$

and

$$P(t) = \left[\frac{p(t)}{p(t_o)}\right]^{(\gamma-1)/\gamma}, \qquad [Q(t)]^n = \frac{B\,(T, Y_O, p)\,/\,(PY_o^n)}{B\,(T_O\,(t_o)\,, Y_{Oo}, p\,(t_o))}, \tag{45}$$

in which t_o is a time at which ignition begins and Y_o a representative value of Y in the reaction region at that time. The functions P and Y_oQ are of order unity, while β is the large parameter in activation-energy asymptotics. The parameters S, L and L_F also are large in the problems of interest.

2.7 CHARACTERISTIC TIMES

Two characteristic times that have now appeared in the problem are the characteristic mixing time τ_m of Eq. (37) and the characteristic heat-release time τ_q of Eq. (43). It is interesting to observe from Eq. (38) that the reciprocal of the instantaneous scalar dissipation, χ^{-1}, is related to τ_m; in the ignition region Z is small so that χ^{-1} is typically 10 to 100 times τ_m. For a steady strained mixing layer, τ_m is of the order of the shear-layer thickness divided by a velocity difference, while for the unstrained mixing layer it is essentially simply the time t from initiation of the layer.

Time variations of these characteristic times and of other quantities are important in ignition. A relevant compression time can be defined as

$$\tau_c = [d(\ell np)/dt]^{-1}_{t=t_o}, \tag{46}$$

and a time scale for variation of strain can be defined as

$$\tau_s = [d(\ell n a_O)/dt]^{-1}_{t=t_o}. \tag{47}$$

Here τ_c will be of the order of the ratio of a chamber dimension to a characteristic piston velocity, while τ_s will be of the order of the ratio of a chamber dimension to a characteristic gas velocity difference, giving, typically, $\tau_m < \tau_s < \tau_c$; as τ_s approaches τ_m the mixing layer becomes unsteady and Eq. (35) supplants Eq. (36). The strongest time variation of a characteristic time will be that of τ_q, through the $e^{-\beta}$ factor in Eq. (43). During compression τ_q will decrease from a value large compared with τ_c to a value often small compared with τ_m. The character of the ignition process differs depending on whether the ignition time t_o corresponds to $\tau_q \sim \tau_c$ or $\tau_q \sim \tau_m$, for example. The occurrence of these different ignition regimes will be determined by parameters such as β, S and L. In this way, a number of different ignition behaviors may be found for different systems.

Time scales in turbulence range from a large-eddy turnover time τ_l to a Kolmogorov time

$$\tau_k = \tau_\ell/\sqrt{R}, \tag{48}$$

where R denotes the turbulence Reynolds number, typically on the order of 100. Like τ_s the value of τ_ℓ may be expected to be of the order of the ratio of a chamber dimension to a gas velocity difference. The influence of turbulence on ignition must depend on the relative magnitudes of these times and of those defined above. Besides τ_k and τ_ℓ turbulence may involve times associated with ordered flow structures, such as large-eddy pairing times τ_p, relevant to spread rates of turbulent jets and typically larger than τ_ℓ. Thus, turbulent-time inequalities such as $\tau_k < \tau_\ell < \tau_p$ parallel the inequalities suggested above. Considerations of descriptions of the turbulence help to identify interactions between turbulence and ignition.

2.8 TURBULENCE DESCRIPTIONS

The relative simplicity of Eq. (39) suggests attempting to describe turbulence fields with mixture fraction treated as an independent variable. That is precisely what methods calculating evolution of probability density functions (pdf's) do.[1-3] Equation (39) implies that it is necessary to include χ as an independent variable in these methods as well, or at least to introduce approximations for $\chi(Z)$, such as Eq. (38) with a modeled τ_m. These mixing questions in fact constitute the most challenging aspect of these pdf-evolution methods, and satisfactory solutions to such problems are not yet available.

Presumed-pdf methods are simpler[1-3] and might be extended for achieving estimates of χ. Such an approach would apply moment methods directly to Eq. (26). Because of the strong variation of ω, it is inappropriate to do this in Eq. (17), although it could be done in Eq. (20) if ϵ is small enough.

An important question concerns the extent of thorough small-scale turbulent mixing that occurs prior to the ignition time t_o. It may be possible to separate the turbulence into fast and slow parts and to average over the fast parts, deriving for the

slow parts Eq. (17) for averaged quantities. While this may work for ν, ρ and (k/c_p), the strong dependence of ω on θ in Eq. (42) points towards significant influences of even rapid θ fluctuations on ignition times.[2-4] A scale β^{-1} may be established for fluctuations θ' of the magnitude of θ, such that the average $\omega(\theta)$ equals $\omega(\bar{\theta})$ only for averages involving $\theta' \ll \beta^{-1}$. This limits averaging to a high-frequency part of the Kolmogorov subrange. Further study of this problem is needed.

An alternative is to attempt to employ a description like Eq. (39), instead of Eq. (17), directly in an ignition analysis. A turbulent $\chi(Z,t)$ may be introduced, with a time dependence obeying suitable turbulence statistics, and Eq. (39) may then be investigated for extracting a $\theta(Z,t)$ that in some cases may not be monotonic in t. The estimate in Eq. (38) may relate the statistics of χ to those of τ_m. Equation (39) suggests that if $(L\chi)^{-l}$ is small compared with an ignition time then a steady mixing-layer type of balance is approached in the ignition process, while otherwise a time-dependent balance between $\partial\theta/\partial t$ and ω/τ_q may prevail. Appreciable development of turbulence descriptions of histories of χ conditioned on Z is needed in further pursuit of this line of investigation.

2.9 CONCLUSIONS

The formulation of the nonpremixed turbulent ignition problem developed here serves to emphasize the importance of the mixture fraction and the instantaneous scalar dissipation in ignition. Ignition typically occurs in flow regions having small values of the mixture fraction, and turbulence statistics of scalar dissipation in such regions appear to be of critical importance to the ignition process.

The entropy-related temperature ratio, the ratio of the temperature to the isentropic temperature, is an attractive variable for use in describing diesel ignition. It automatically handles the troublesome compression work $\partial p/\partial t$, yielding a formulation more readily interpretable through available knowledge of turbulent combustion.

Further study of relative values of the characteristic times that have been defined here is needed for identifying the most likely ignition regimes in diesel engines.

2.10 REFERENCES

1. P.A. Libby and F.A. Williams, Turbulent Reacting Flows, Springer-Verlag, Berlin, 1980, p. 232.

2. N. Peters, "Laminar Diffusion Flamelet Models in Non-Premixed Turbulent Combustion", Progress in Energy and Combustion Science 10, 319-339 (1984).

3. F.A. Williams, "Turbulent Combustion", Chapter III of The Mathematics of Combustion, J.D. Buckmaster, editor, SIAM, Philadelphia, 1985, pp. 97-131.

4. F.A. Williams, Combustion Theory, Second Edition, Addison-Wesley, Menlo Park, CA, 1985.

3 IGNITION IN AN UNSTEADY MIXING LAYER SUBJECT TO STRAIN AND VARIABLE PRESSURE

3.1 INTRODUCTION

Diesel combustion involves transient injection of a liquid fuel stream at high pressure into a chamber containing oxidizing gas in turbulent motion, with the chamber pressure increasing as a consequence of the volume decrease produced by piston motion.[1] Computations of such processes show regions of variable strain rates where vaporized fuel and oxidizer mix, such as at the front of the injected fuel jet.[2] To predict when ignition will occur in processes of this kind, it is helpful to have results of analyses of ignition in unsteady, strained, variable-pressure mixing. The intent of the present paper is to offer such results on the basis of activation-energy asymptotics for one-step processes.[3] Analyses of this kind can be useful in that they provide parametric descriptions of ignition times, not tied to specific values of transport and reaction-rate parameters.

The nonpremixed combustion to be considered here results in diffusion flames of the type analyzed previously[4] for steady, strained, counterflow configurations involving reactants with Lewis numbers of unity. That analysis[4] identified four regimes, one of which, the ignition regime, is relevant to the problems addressed here. Because of the low diffusion coefficients of fuels typically encountered in Diesel combustion, there is interest in analyzing mixtures with Lewis numbers different from unity. Although Lewis-number effects in such diffusion flames have been considered previously,[5–7] these studies did not treat the ignition regime. The present investigation is focused exclusively on the ignition regime and admits nonunity Lewis numbers.

Unlike the analyses cited above, the present study also admits time-dependent behavior. Time-dependent reactant consumption with strain has been treated earlier[8] for Lewis numbers of unity in the diffusion-controlled limit of large Damköhler numbers, where ignition events do not occur. Also, ignition in time-dependent, unstrained mixing layers has been analyzed previously[9] by activation-energy asymptotics for reactants with Lewis numbers of unity. The present work may be considered to generalize these last results[9] to different Lewis numbers and to time-dependent problems with strain. In addition to working out the solutions for the cases that appear to be of the greatest practical interest, the present writeup will indicate the additional cases that may arise and the asymptotic methods for solving those problems.

Niioka[10] took the first step towards generalizing the previous[9] analysis to include strain. Although he restricted his attention to Lewis numbers and reaction orders of unity and to a particular initial-value problem, his analysis by activation-energy asymptotics clearly showed the delay in ignition that is caused by the imposition of strain. The present work extends that of Niioka to different Lewis numbers and reaction orders and to more general initial and boundary conditions, as well as showing how compression can modify and simplify the ignition-stage analysis.

The general formulation is given in the following section, and analyses for various cases are addressed in subsequent sections.

3.2 FORMULATION

Attention is directed to the ignition of two steams, one of fuel and the other of oxidizer. These two streams flow opposite to each other and form a mixing layer that will be analyzed in a reference system that moves with the dividing fluid surface. Consideration is restricted to the stagnation region, where the flow and concentration field can be described in terms of a similarity solution involving only the variable time t and the transverse coordinate y. The temperatures of the fuel and oxidizer streams, T_F and T_O, will be considered to be different and changing with time because of the compression work associated with the variable stagnation-point pressure $P_s(t)$, all time scales being assumed long compared with acoustic times. If x is the coordinate along a locally planar mixing layer measured from the stagnation point and u the corresponding velocity component, which is associated with the strain, then this velocity takes the values $u = A_O x$ and $u = A_F x$ in the air and fuel streams, respectively, related to variations P' of pressure from its stagnation-point value according to

$$-\frac{\partial P'}{\partial x} = \rho_O \left(\frac{dA_O}{dt} + A_O^2 \right) x = \rho_F \left(\frac{dA_F}{dt} + A_F^2 \right) x, \tag{1}$$

where ρ_F and ρ_O are the densities of the fuel and oxidizer streams. Equation (1) relates the apparently different strain rates of the two streams, since there are no x-dependent pressure changes across the mixing layer. Inside the mixing layer $u = xA(y,t)$, where A must satisfy boundary conditions consistent with the second equality in Eq. (1).

The conservation equation for the density ρ, the variable strain rate A, the temperature T, the mixture fraction Z and the mass fractions of fuel Y_F and of oxidizer Y_O are, respectively,

$$\frac{\partial \rho}{\partial t} + \frac{\partial \rho v}{\partial y} + \rho A = 0, \tag{2}$$

$$\rho \left(\frac{\partial A}{\partial t} + v\frac{\partial A}{\partial y} + A^2 \right) = \rho_O \left(\frac{dA_O}{dt} + A_O^2 \right) + Pr \frac{\partial}{\partial y} \left(\frac{\lambda}{c_p} \frac{\partial A}{\partial y} \right), \tag{3}$$

$$\rho \left(\frac{\partial T}{\partial t} + v\frac{\partial T}{\partial y} \right) = \frac{\partial}{\partial y} \left(\frac{\lambda}{c_p} \frac{\partial T}{\partial y} \right) + \frac{1}{c_p} \frac{dP_s}{dt} - \frac{q}{c_p} w_F, \tag{4}$$

$$\rho \left(\frac{\partial Z}{\partial t} + v\frac{\partial Z}{\partial y} \right) = \frac{\partial}{\partial y} \left(\frac{\lambda}{c_p} \frac{\partial Z}{\partial y} \right), \tag{5}$$

$$\rho \left(\frac{\partial Y_F}{\partial t} + v\frac{\partial Y_F}{\partial y} \right) = \frac{1}{L_F} \frac{\partial}{\partial y} \left(\frac{\lambda}{c_p} \frac{\partial Y_F}{\partial y} \right) + w_F, \tag{6}$$

$$\rho \left(\frac{\partial Y_O}{\partial t} + v\frac{\partial Y_O}{\partial y} \right) = \frac{1}{L_O} \frac{\partial}{\partial y} \left(\frac{\lambda}{c_p} \frac{\partial Y_O}{\partial y} \right) + \nu_O w_F, \tag{7}$$

where Pr denotes the Prandtl number and L_k the Lewis number for species k, all assumed constant, λ represents the (variable) thermal conductivity and $c_p = \sum_{k=1}^{N} c_{pk} Y_k$ the specific heat at constant pressure, taken here to be constant, an approximation that may be reasonable because of the relatively small temperature changes that typically occur prior to thermal runaway in the ignition process. In these equations,

the mass rate of consumption of fuel is denoted by w_F, the mass of oxidizer consumed per unit mass of fuel is represented by the stoichiometric coefficient ν_O, and the heat released per unit mass of fuel consumed is identified by q. Equations (2), (3) and (4) express conservation of mass, the x component of momentum and energy, respectively; the y component of momentum conservation serves only to determine the small pressure changes in the direction normal to the mixing layer, and therefore it need not be considered. With Lewis numbers differing from unity there does not exist a unique mixture fraction, but it is convenient to employ the thermal diffusivity in selecting a mixture-fraction definition, as is done in Eq. (5). The equation of state for an ideal gas is employed,

$$P_s/\rho T = R^o/\overline{W}, \tag{8}$$

under the assumption that the average molecular weight $\overline{W} = \left(\sum_{k=1}^{N} Y_k/W_k\right)^{-1}$ is constant; R^o denotes the universal gas constant. The reaction rate is assumed of the Arrhenius form

$$w_F = -\rho B Y_F^n Y_O^m \exp\left(-E/R^o T\right), \tag{9}$$

where m and n are reaction orders, E the overall activation energy, and B a pressure-dependent prefactor having units of reciprocal time.

The variable pressure $P_s(t)$ (increasing with time) will be considered to be known, as will the variable strain rate $A_O(t)$. The boundary conditions are

$$T \to T_O(t),\ Z \to 0,\ Y_F \to 0,\ Y_O \to Y_{O_o} \text{ and } A \to A_O(t) \text{ as } y \to \infty, \tag{10a}$$

and

$$T \to T_F(t),\ Z \to 1,\ Y_F \to Y_{F_o},\ Y_O \to 0 \text{ and } A \to A_F(t) \text{ as } y \to -\infty, \tag{10b}$$

with A_F, T_F and ρ_F related to A_O, T_O, and ρ_O by

$$\rho_F T_F = \rho_O T_O = P_s \overline{W}/R^o, \tag{11a}$$

$$\rho_F \left(\frac{dA_F}{dt} + A_F^2\right) = \rho_O \left(\frac{dA_O}{dt} + A_O^2\right), \tag{11b}$$

and

$$\rho_F c_p \frac{dT_F}{dt} = \rho_O c_p \frac{dT_O}{dt} = \frac{dP_s}{dt}. \tag{11c}$$

The origin of the y coordinate system is chosen so that

$$v = 0 \text{ at } y = 0. \tag{12}$$

In addition to these boundary conditions, initial conditions are needed to define a well-posed problem. Typical initial conditions are those associated with a sharp interface between the fuel and the air at time $t = 0$,

$$T = T_O(0),\ Z = 0,\ Y_F = 0,\ Y_O = Y_{O_o} \text{ and } A = A_O(0) \text{ for } y > 0, \tag{13a}$$

and

$$T = T_F(0),\ Z = 1,\ Y_F = Y_{F_o},\ Y_O = 0 \text{ and } A = A_F(0) \text{ for } y < 0. \tag{13b}$$

This completes the set of equations that in principle determine v, A, T, Z, Y_F, Y_O and ρ as functions of space and time.

3.3 LENGTH AND TIME SCALES

Since ignition often occurs near the high-temperature oxidizer stream, it is convenient to employ properties of this stream in defining nondimensional length and time variables. A time-dependent boundary-layer thickness $\delta(t)$ may be taken to obey the ordinary differential equation

$$\delta\frac{d\delta}{dt} + \delta^2\left(A_O + \frac{dln\rho_O}{dt}\right) = \alpha_O, \tag{14}$$

where the thermal diffusivity of the oxidizer stream is

$$\alpha_O = \lambda_O/(\rho_O c_p). \tag{15}$$

An appropriate nondimensional length variable is then

$$\eta = y/\delta. \tag{16}$$

A corresponding time variable is

$$\tau = \int_0^t \left(\alpha_O/\delta^2\right) dt. \tag{17}$$

It is straightforward to transform Eqs. (2)-(7) from (y,t) to (η,τ) as independent variables. That the resulting system will be useful for most of the ignition problems of interest here can be seen from the following simplified development of the mixture-fraction equation for inert mixing fields.

Consider the case of nearly equal temperatures and molecular weights of both streams. In this case during the ignition transients the change in temperatures produced by the chemical reaction is still small, and then Eq. (3) has the solution $A = A_O(t) = A_F(t)$, constant in y, and Eq. (2) simplifies to

$$v = -\left(A_O + \frac{dln\rho_O}{dt}\right) y \tag{18}$$

because in the ignition transient we can neglect the spatial variations in ρ, as well as those of T. Equation (5) then reduces to

$$\frac{\partial Z}{\partial t} - \left(A_O + \frac{dln\rho_O}{dt}\right) y\frac{\partial Z}{\partial y} = \alpha_O\frac{\partial^2 Z}{\partial y^2}, \tag{19}$$

which upon introduction of Eq. (16) becomes

$$\left(\delta^2/\alpha_O\right) Z_t - \eta\left\{\left(\delta^2/\alpha_O\right)\left(\frac{\delta_t}{\delta} + A_O + \frac{dln\rho_O}{dt}\right)\right\} Z_\eta = Z_{\eta\eta}, \tag{20}$$

where the subscripts t and η identify partial derivatives. Equation (20) clearly motivates the selection given in Eq. (14). With this formula and Eq. (17), the further transformation from t to τ reduces Eq. (20) to the simple form

$$Z_\tau - \eta Z_\eta = Z_{\eta\eta}, \tag{21}$$

corresponding to a mixing layer under a constant strain of unity. Because the boundary conditions for Eq. (21) are constant, $Z \to 1$ as $\eta \to -\infty$ and $Z \to 0$ as $\eta \to \infty$, the solution soon becomes τ-independent and is then given by

$$Z = \frac{1}{2}\mathrm{erfc}\left(\eta/\sqrt{2}\right). \tag{22}$$

Similar treatments of Eqs. (6) and (7) for frozen flow in the cases $L_F \neq L_O \neq 1$ readily yield

$$Y_F/Y_{Fo} = \frac{1}{2}\mathrm{erfc}\left(\eta\sqrt{L_F/2}\right) \equiv Z_F \tag{23a}$$

and

$$1 - Y_O/Y_{Oo} = \frac{1}{2}\mathrm{erfc}\left(\eta\sqrt{L_O/2}\right) \equiv Z_O. \tag{23b}$$

These results show how Eq. (14) defines the evolution of the boundary-layer thickness.

Equation (14) may be integrated formally to show that δ^2 may be expressed in the form

$$\delta^2 = C\rho_O^{-2}\exp\left\{-2\int_0^t A_O dt\right\}, \tag{24}$$

where

$$\frac{dC}{dt} = 2\alpha_O\rho_O^2\exp\left\{2\int_0^t A_O dt\right\}, \tag{25}$$

and $C = C_0 = \delta_0^2\rho_O^2(0)$ at $t = 0$, where δ_0 is a characteristic value of δ at that time. Integration of Eq. (25) gives

$$C = C_0 + 2\int_0^t \alpha_O(t')\,\rho_O^2(t')\exp\left\{2\int_0^{t'} A_O(t'')\,dt''\right\}dt', \tag{26}$$

which may be used in Eq. (24) to provide an explicit expression for $\delta(t)$ that involves integrals. These results allow for arbitrary time variations of strain through A_O and of pressure through ρ_O and α_O. Often the characteristic times for pressure variations are long compared with A_O^{-1} and with the characteristic time for A_O variation, so that in these results α_O becomes constant and ρ_O disappears, and the term in Eq. (4) involving the time derivative of the pressure then also becomes negligible; in this case, when solving Eqs. (2)-(7), P_s, T_O and ρ_O are parameters, not functions of the short time scale relevant to the description of the transient mixing layer.

3.4 SIMPLIFICATIONS FOR CONSTANT RATE OF STRAIN

An important limiting case is that of constant rate of strain, A_O constant, or strain changing over times large compared with A_O^{-1}. For this case, Eqs. (24) and (26) yield simply $\delta^2 = \alpha_O/A_O = \text{constant}$. If the strain time A_O^{-1} is also small compared with the characteristic compression time, then the term $c_p^{-1}\partial P_s/\partial t$ can be left out of Eq. (4), together with the remaining time derivative terms in Eqs. (2) -(7), so that the system becomes expressible as

$$\frac{d\rho v}{dy} + \rho A = 0, \tag{27}$$

$$\rho\left(v\frac{dA}{dy}+A^2\right)=\rho_O A_O^2+Pr\frac{d}{dy}\left(\frac{\lambda}{c_p}\frac{dA}{dy}\right), \tag{28}$$

$$\rho v\frac{dY_F}{dy}=\frac{1}{L_F}\frac{d}{dy}\left(\frac{\lambda}{c_p}\frac{dY_F}{dy}\right)+w_F, \tag{29}$$

$$\rho v\frac{dY_O}{dy}=\frac{1}{L_O}\frac{d}{dy}\left(\frac{\lambda}{c_p}\frac{dY_O}{dy}\right)+\nu_O w_F, \tag{30}$$

$$\rho v\frac{dT}{dy}=\frac{d}{dy}\left(\frac{\lambda}{c_p}\frac{dT}{dy}\right)-\frac{q}{c_p}w_F, \tag{31}$$

and

$$\rho T=P_s\overline{W}/R^o,\quad w_F=-\rho B Y_F^n Y_O^m e^{-E/R^oT}, \tag{32}$$

a system of ordinary differential equations (those describing the steady stagnation-point boundary-layer flow) to be solved with the boundary conditions of Eq. (10), where now A_O and A_F are taken as constant and related by

$$\rho_F A_F^2=\rho_O A_O^2, \tag{11b'}$$

while T_F and T_O are related to P_s by Eqs.(11a) and (11c), namely,

$$T_O/T_{Oo}=(P_s/P_{so})^{(\gamma-1)/\gamma}=T_F/T_{Fo}, \tag{33}$$

while

$$A_F^2/A_O^2=\rho_O/\rho_F=\rho_{Oo}/\rho_{Fo}. \tag{34}$$

The system of equations given by Eqs. (27)-(32), with the boundary conditions of Eqs. (10), (33) and (34), will have, for large activation energies, a nearly frozen solution for values of the pressure smaller than a critical value, P_I, such that when $P_s=P_I$ is reached during the compression process, spontaneous ignition will take place in the mixing layer. There is a second critical pressure, $P_E<P_I$, such that if $P_s>P_E$ the above system of equation has fast-burning diffusion-controlled solutions, for which the chemical reaction is confined to a thin reaction sheet. In the pressure interval $P_E<P_s<P_I$ the problem of Eqs. (27)-(32) and (10) has three solutions the nearly frozen one, the near-equilibrium, diffusion-controlled solution, and a third intermediate unstable solution. These changes with pressure arise mainly through Eq. (33) and the strong dependence of the reaction rate on temperature in Eq. (32); direct pressure dependences, as through B, are much less important. Because of the quasisteady character of the problem, the critical pressures P_E and P_I are expressed most conveniently in terms of corresponding critical Damköhler numbers. Analyses that determine critical Damköhler numbers for ignition, thereby giving P_I, deserve further discussion here.

For the special case of unity Lewis numbers and unity reaction orders, the relevant ignition analysis has been published previously[4], in the so-called thermal-diffusion approximation in which for simplicity the density and transport coefficients are treated as being constants. Although inaccurate after flame development, this approximation is not too bad for ignition because the fractional temperature increases are small, of

order R^oT/E. That earlier study demonstrated the existence of two ignition regimes, one for which $(T_{Oo} - T_{Fo})$ is of the order of $R^oT_{Oo}^2/E$ or smaller, and the other for which $(T_{Oo} - T_{Fo}) \gg R^oT_{Oo}^2/E$. In the former regime, significant heat release occurs throughout the entire mixing layer during ignition, and reactant consumption is negligible prior to ignition, while in the latter regime heat release is significant only at the oxidizer edge of the mixing layer where the temperature and rates are highest, and fuel depletion may be important during ignition because the fuel concentration is small in the ignition region. This same classification of ignition regimes applies under the more general conditions addressed here, and it applies for time-dependent mixing as well.[9]

For the ignition regime in which $(T_{Oo} - T_{Fo})$ is of the order of $R^oT_{Oo}^2/E$ or smaller, use of activation-energy asymptotics results in a two-point boundary-value problem for a second-order ordinary differential equation, the numerical integration of which gives the maximum temperature as a function of a reduced Damköhler number, showing no solutions above a critical Damköhler number for ignition and two solutions below, that of the higher temperature being unstable. These solutions and ignition Damköhler numbers have been calculated and plotted for unity reaction orders with Lewis numbers of unity.[4] Although it would be straightforward to perform such calculations for reaction orders and Lewis numbers different from unity, no such results are currently available. Results for these extended parameter ranges will not be calculated herein either, because this regime typically is not very relevant to Diesel ignition.

However, results for the extended parameter ranges *are* presented here for the ignition regime in which $(T_{Oo} - T_{Fo}) \gg R^oT_{Oo}^2/E$. Not only is this inequality usually satisfied for Diesel autoignitions, but also L_F usually is sufficiently large that the previous[4] approximations may be thought to become inaccurate. Results for this regime have been derived earlier[4,9] for reaction orders and Lewis numbers of unity, taking the effect of fuel depletion during the ignition process fully into account. The results to be given here do not allow for fuel depletion, and it could be of interest to extend the analysis to include that effect. The analysis is given in Appendix A, where the condition necessary for fuel depletion to be neglected is derived, and where the equations needed for developing the more general theory are written. In the meantime, use of Fig. 16 and Eq. (A-11) of the previous paper[4] along with the present results provide an indication of the effects of both fuel depletion and Lewis numbers.

The results of the analysis in Appendix A are plotted in Figs. 1 and 2. Figure 1 determines the nondimensional increment of the maximum temperature above that for frozen mixing as a function of the reduced Damköhler number defined in Eq. (A-22), for various values of the relevant parameter nL_F. This nondimensional increment is defined as

$$\varphi_m = \frac{R^o}{E}\left\{T_m - [T_O - (T_O - T_F)\,Z]\right\}, \tag{35}$$

where T_m is the maximum temperature, and Z is given by Eq. (22). The lower branches of the curves in Fig. 1 are the stable solutions, and the turning points give the maximum values of Δ, the Damköhler numbers Δ_I for ignition. If reactant depletion had been included, and if the heat release were small enough that it could

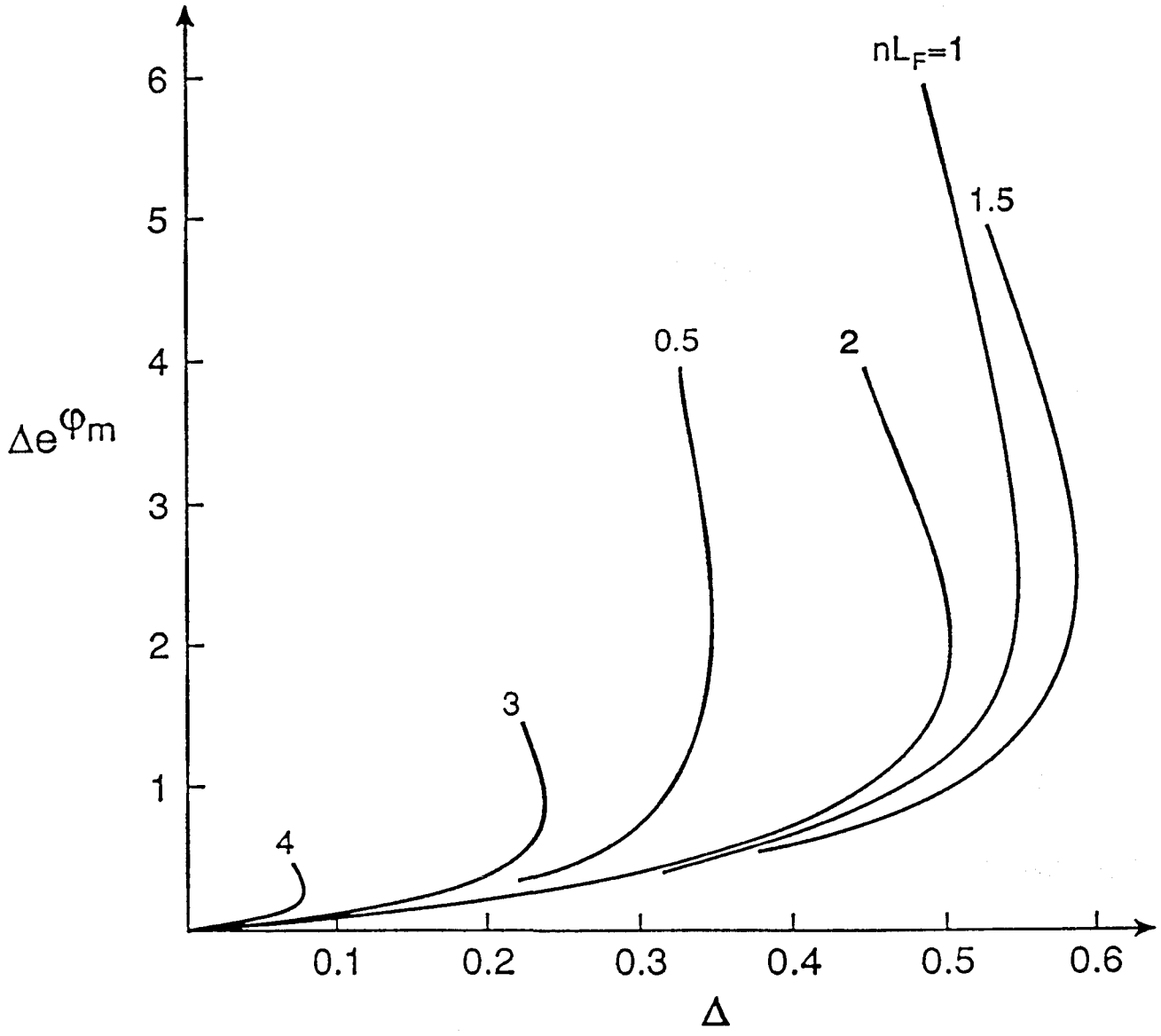

Figure 1. Results of numerical integration for ignition temperature increments as functions of the relevant Damköhler number, for various values of the reaction order and Lewis number of the fuel, with constant rate of strain.

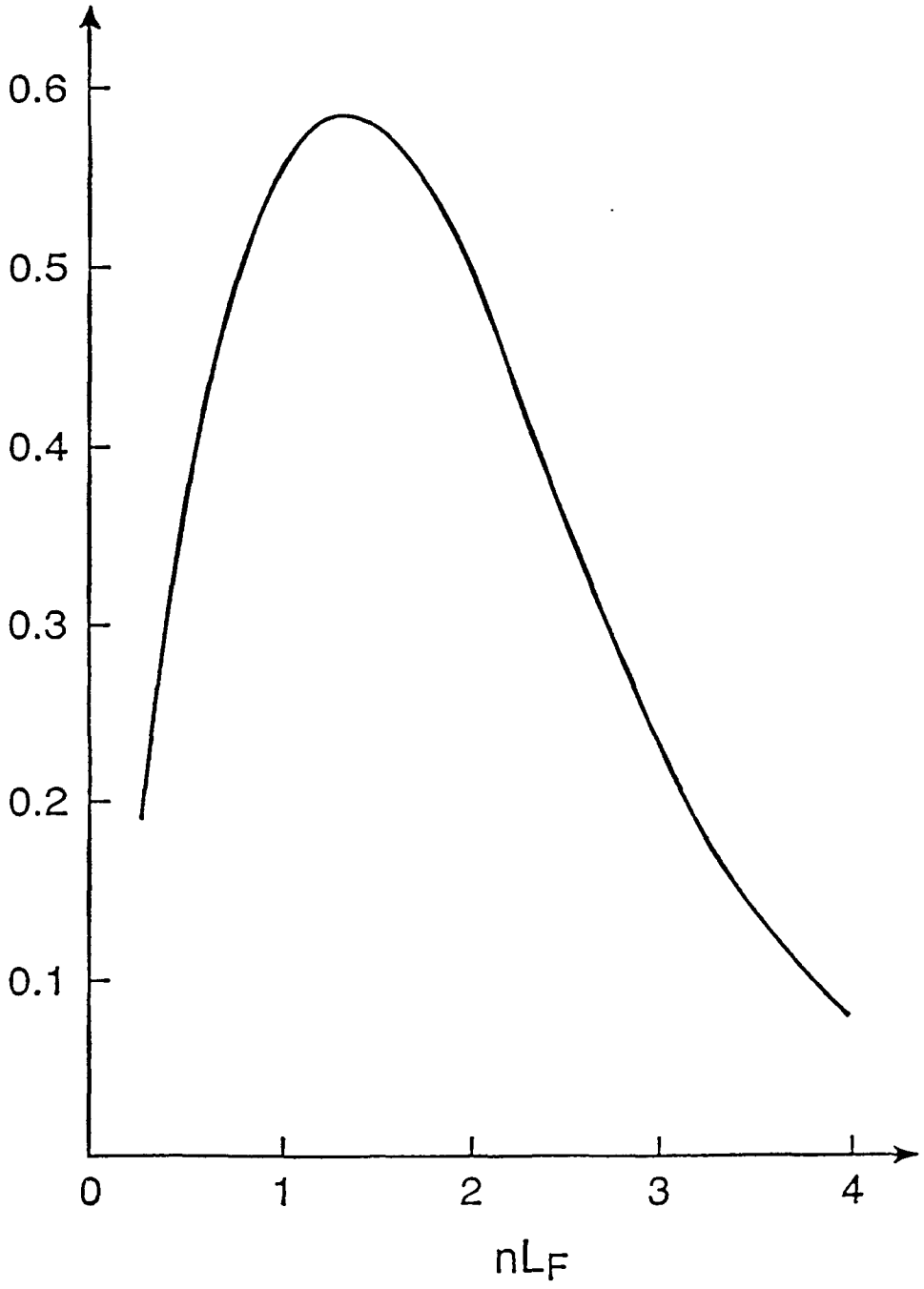

Figure 2. Ignition Damköhler Numbers as functions of the product of the fuel reaction order and Lewis number, for constant rate of strain.

contribute a maximum temperature increment no greater than a critical value dependent on the parameters of the problem, then φ_m would increase monotonically with Δ instead of exhibiting the abrupt ignition behavior of Fig. 1. In practice, the heat release generally is larger than this, and the behavior seen in Fig. 1 is representative.

The ignition Damköhler numbers are shown as a function of nL_F in Fig. 2. The result for $nL_F = 1$ has been obtained previously[4] and has $\Delta_I = 0.536$. It is interesting to observe that $\Delta_I = 0.5$ for both $nL_F = 0.8$ and $nL_F = 2$. This indicates that for a wide range of values of nL_F of practical importance, $\Delta_I = 0.5$ is a good approximation. This value is obtained entirely analytically for $nL_F = 2$ in Appendix A.

3.5 SIMPLIFICATIONS FOR UNSTRAINED MIXING LAYERS WITH VARIABLE PRESSURE

For unstrained mixing layers, $A_O = 0$, and Eqs. (24) and (26) show that

$$(\rho_O \delta)^2 = [\rho_O(0)\delta_0]^2 + 2\int_0^t \alpha_O(t')\rho_O^2(t')dt'. \tag{36}$$

If $\alpha_O \rho_O^2$ is constant, then Eq. (36) implies that $(\rho_O \delta)^2$ increases linearly with time, as in a diffusion process. Although it is possible to work with the η and τ of Eqs. (16) and (17) as independent variables, greater simplification is achieved (especially in the absence of strain) by introducing a mass coordinate for the unsteady mixing layer. Therefore, a characteristic time t_0 is selected, to be defined later, and the nondimensional variables

$$\sigma = t/t_0 \ , \ \zeta = (t_0 \alpha_{O0} \rho_{O0}^2)^{-1/2} \int_0^y \rho dy \tag{37}$$

are introduced, where the subscripts 0 on α_O and ρ_O mean that they are to be evaluated at $t = 0$. In terms of σ and ζ, Eqs. (4), (6) and (7) formally become

$$\frac{\partial T}{\partial \sigma} - \frac{\partial}{\partial \zeta}\left(k\frac{\partial T}{\partial \zeta}\right) = \frac{\gamma - 1}{\gamma}\frac{T}{P_s}\frac{dP_s}{d\sigma} - \frac{q}{c_p}t_0\frac{w_F}{\rho} \tag{38}$$

and

$$\frac{\partial Y_F}{\partial \sigma} - \frac{1}{L_F}\frac{\partial}{\partial \zeta}\left(k\frac{\partial Y_F}{\partial \zeta}\right) = \frac{\partial (Y_O/\nu_O)}{\partial \sigma} - \frac{1}{L_O}\frac{\partial}{\partial \zeta}\left[k\frac{\partial (Y_O/\nu_O)}{\partial \zeta}\right] = t_0\frac{w_F}{\rho}, \tag{39}$$

where a Chapman-Rubesin type of parameter is

$$k = (\lambda\rho/c_p) \,/\, \left(\alpha_{O0}\rho_{O0}^2\right), \tag{40}$$

and the ratio of specific heats, γ, obeys

$$(\gamma - 1)/\gamma = R^o/\left(\overline{W}c_p\right), \tag{41}$$

use having been made of Eq. (8). Equations (10) and (13) readily provide boundary and initial conditions for Eqs. (38) and (39).

A detailed treatment of the resulting ignition problem has been given earlier[9] for the special case $k = L_F = L_O = 1, dP_s/d\sigma = 0$. It is interesting to note[11] that

pressure variations are readily taken into account in the analysis by working with the entropy-related function

$$S = T/P_s^{(\gamma-1)/\gamma} \tag{42}$$

instead of T. Although in ideal gas mixtures k is proportional to P_s at constant T and composition, this pressure effect on the transport coefficients often is small enough to be neglected, and the approximation $k = 1$ may be introduced for simplicity. With this approximation, use of Eq. (42) in Eq. (38) results in

$$\frac{\partial S}{\partial \sigma} - \frac{\partial^2 S}{\partial \zeta^2} = -\frac{q t_0 w_F}{c_p \rho P_s^{(\gamma-1)/\gamma}} \quad , \tag{43}$$

to be solved along with Eq. (39) for $k = 1$. If $\rho\lambda/c_p$ is constant at constant pressure (a fairly reasonable approximation for ideal gases), then k is a function only of P_s, which in turn is a function only of σ, so the factor $k(\sigma)$ may be taken outside the derivative in Eqs. (38) and (39), and introduction of the revised time variable $\int_0^\sigma k d\sigma$ automatically takes into account the time variations of the diffusivities and results in a problem having the same functional form as that for $k = 1$. With this simple generalization in mind, equations are written here only for $k = 1$. It may be noted that the mass and time coordinates introduced here are also useful[12] for $A_O \neq 0$, even though, for simplicity, they were not introduced in the preceding development.

The increase of P_s with increasing σ can enhance ignition by increasing temperatures, as seen in Eq. (11c). If this is an important effect, then it is convenient to select t_0 to be the characteristic time over which fractional pressure change of order unity occur, in particular making $[(\gamma-1)/\gamma]\, d(lnP_s)/d\sigma$ of order unity in Eq. (38). If the pressure changes are slow enough to constitute small perturbations, then it is more convenient to select t_0 to be a relevant chemical time, as was done previously.[9] In any case, normalized nondimensional variables can be introduced as

$$\theta = S/S_O \quad , \quad \psi_F = Y_F/Y_{Fo}, \quad \psi_O = Y_O/Y_{Oo}, \tag{44}$$

and the partial differential equations

$$\frac{\partial \theta}{\partial \sigma} - \frac{\partial^2 \theta}{\partial \zeta^2} = F \, , \quad \frac{\partial \psi_F}{\partial \sigma} - \frac{1}{L_F}\frac{\partial^2 \psi_F}{\partial \zeta^2} = \frac{\partial(\psi_O/s)}{\partial \sigma} - \frac{1}{L_O}\frac{\partial^2(\psi_O/s)}{\partial \zeta^2} = -G \tag{45}$$

derived, subject to boundary conditions

$$\psi_F \to 0, \psi_O \to 1, \theta \to 1 \text{ as } \zeta \to \infty; \psi_F \to 1, \psi_O \to 0, \theta \to \theta_F \text{ as } \zeta \to -\infty \tag{46}$$

and to similar initial conditions, as obtained from Eqs. (10) and (13). Here $s = \nu_O Y_{Fo}/Y_{Oo}$,
$G = (P_s/P_{s0})^{(\gamma-1)/\gamma}\,[(c_p T_{O0})/(qY_{Fo})]\, F$, and, from Eq. (9),

$$F = \left(\frac{P_s}{P_{s0}}\right)^{-(\gamma-1)/\gamma} \frac{qBY_{Fo}^n Y_{Oo}^m t_0}{c_p T_{O0}} \psi_F^n \psi_O^m \exp\left[-\left(\frac{E}{R^o T_{O0}}\right)\left(\frac{P_s}{P_{s0}}\right)^{-(\gamma-1)/\gamma}\left(\frac{1}{\theta}\right)\right]. \tag{47}$$

Equation (11) is employed in deriving the boundary conditions for θ, and $\theta_F \equiv T_F/T_O$, which is constant by virtue of Eqs. (11a) and (11c), the adiabaticity condition in the

external streams. The problem defined by Eqs. (45) and (46) offers a most convenient way to address the unstrained ignition and exhibits the relevant nondimensional parameters, θ_F, s, L_F, L_O and the parameters appearing in F and G.

When ignition is produced by compression, there is an inert initial stage during which F and G are negligibly small. The solutions to Eqs. (45) and (46) during this inert stage are

$$\theta = 1 - (1 - \theta_F)\frac{1}{2}\mathrm{erfc}\left(\frac{\zeta/2}{\sqrt{\sigma}}\right), \tag{48}$$

$$\psi_F = \frac{1}{2}\mathrm{erfc}\left(\frac{\zeta}{2}\sqrt{\frac{L_F}{\sigma}}\right), \psi_O = 1 - \frac{1}{2}\mathrm{erfc}\left(\frac{\zeta}{2}\sqrt{\frac{L_O}{\sigma}}\right). \tag{49}$$

Within the context of activation-energy asymptotics, this inert stage ends at a time σ_c, and the large parameter of expansion, β, is defined by

$$\beta = E/(R^\circ T_{Oc}) \ , \ T_{Oc} \equiv T_{Oo}\left[P_s(\sigma_c)/P_{so}\right]^{(\gamma-1)/\gamma}. \tag{50}$$

A first approximation to the compression-produced ignition time σ_c may be obtained by substituting Eqs. (48) and (49) into Eq. (47) then putting $F = F_c$, where

$$F_c \equiv \left[(\gamma - 1)/\gamma\right]\left[d(lnP_s)/d\sigma\right]_{\sigma=\sigma_c}, \tag{51}$$

which is the order of magnitude of F when the chemistry begins to become important. A more thorough analysis involves application of activation-energy asymptotics in a short ignition stage near $\sigma = \sigma_c$, as has been done for $L_F = L_O = 1$ in an earlier report.[11] Again, there are two regimes, one in which $\beta(1 - \theta_F)$ is an order unity or smaller, and the other in which $\beta(1 - \theta_F)$ is large. In the first of these, the heat release in the ignition stage occurs throughout the mixing layer (with negligible reactant depletion), and in the second it is localized at the oxidizer edge of the layer (with fuel depletion possibly important). The character of the analysis resembles that of Appendix A, although the details are quite different.

An equation for the departure of θ from the inert solution given in Eq. (48) is readily derived from the first expression in Eq. (45) by suitably expanding F of Eq. (47) for the ignition stage. When $\beta(1 - \theta_F)$is of order unity or smaller and compression is not dominant in producing ignition, the resulting partial differential equation must be solved numerically; such solutions have been plotted previously[9] for $L_F = L_O = 1$ and $m = n = 1$. When $\beta(1 - \theta_F)$ is large, there are simplifications that circumvent numerical solutions of partial differential equations.[9] When the ignition is produced by compression, the relevant stretched nondimensional time variable of order unity in the ignition state is[11] $F_c\beta(\sigma - \sigma_c)$, and diffusive effects during the ignition stage are small, of order β^{-1}, so that ordinary differential equations in the stretched time variable are obtained.[11] These equations have solutions that can exhibit thermal runaway at a particular time, identified with ignition, as shown in Appendix B, where the details of the procedures differ in the two different ignition regimes.

3.6 SIMPLIFICATIONS FOR COMPRESSION-PRODUCED AUTOIGNITION WITH VARIABLE STRAIN

Thus far, steady-state problem with constant rates of strain and time-dependent problems without strain have been addressed. The general class of problems defined

by Eqs. (2)-(13) can exhibit a wide variety of different ignition behaviors. Consider first situations in which effects of compression are negligible. The results of Appendix A show that when strain rates are too high, ignition does not occur. As strain rates are relaxed, a condition is reached at which ignition can occur, and it then becomes relevant to ask about ignition times. For values of Δ of Fig. 1 slightly above the critical value Δ_I of Fig. 2, ignition occurs, but it may require a long time because it is delayed by effects of strain. Under such conditions multiple-stage analyses, analogous to those needed for ignition in homogeneous systems near critical conditions,[13] would be appropriate for calculating ignition times. Problems of this kind would be soluble but challenging. At sufficiently large values of Δ, in the first approximation strain can be neglected in calculating ignition times, and the procedures discussed in the preceding section can be applied. It would be straightforward to add small strain rates as perturbations to these methods, to investigate the delay in the ignition time produced by small strain, but this has not been done. Only a few results for mixing-layer ignition times are available at constant pressure without strain.[9]

Pressure variations may be expected to complicate the problem even more. For small rates of pressure variation, their effects may be included as perturbations in constant-pressure analyses. Large rates of pressure variation cannot, but the analysis of Appendix B suggests that sufficiently rapid compression can simplify ignition-stage analyses by converting the problems to ordinary differential equations in time. Although Appendix B concerns only strain-free ignition, it may be anticipated that a similar approach will apply in the presence of strain, so long as the compression effects are strong enough and the rate of strain is not so large as to prevent ignition or to delay it excessively. It will be of interest to indicate here how variable strain can be included in such analyses of compression-produced ignition.

For illustrative purposes, the approximations leading to Eq. (18) are retained, and reactant depletion is neglected, so that Eq. (23) applies after the transient mixing development. Introduction of the independent variables in Eqs. (16) and (17) and the dependent variables of Eq. (44) then reduce Eq. (4) to

$$\frac{\partial \theta}{\partial \tau} - \eta \frac{\partial \theta}{\partial \eta} - \frac{\partial^2 \theta}{\partial \eta^2} = F, \tag{52}$$

where F is given by Eq. (47) with t_0 put equal to δ^2/α_O. Boundary and initial conditions are as in Eq. (46).

For compression-produced autoignition, there is an inert initial stage during which F is negligible in Eq. (52). During this stage, θ will vary from the solution given in Eq. (48) (with ζ and σ replaced by η and τ) to $1 - (1 - \theta_F)\, Z$, where Z is given by Eq. (22). The inert stage ends at a critical time τ_c at which the source term in Eq. (52) becomes important. In the vicinity of $\tau = \tau_c$, the evolution occurs over a short time in an ignition stage, during which a time variable like that of Appendix B is of order unity. It is clear that the β of Eq. (50) is the relevant expansion parameter in the description of the ignition stage by activation-energy asymptotics, and in this stage at leading order Eq. (52) becomes

$$d\theta/d\tau = F. \tag{53}$$

Appropriate stretched variables are basically those of Eq. (B-1), with $\sigma - \sigma_c$ replaced by $\tau - \tau_c$ provided that the F_c of Eq. (51) is now defined to involve $d(lnP_s)/d\tau$. The ignition analysis will then parallel that of Appendix B entirely. The only differences are that the inert solutions ψ_F and ψ_O are now more general functions than those of Eq. (49), and the matching condition $\phi_{-\infty}$ of Eq. (B-5) becomes instead $\beta[\theta_I(\eta, \tau_c) - 1]$, where $\theta_I(\eta, \tau)$ is the more general inert solution indicated above.

If the rate of strain in large enough and varies slowly enough for the solutions in Eqs. (22) and (23) to become accurate before ignition occurs, then the results are like those in Eqs. (B-9) to (B-12), with $\zeta_m/\left(2\sqrt{\sigma_c}\right)$ replaced by $\eta_m/\sqrt{2}$, and with the additional factor

$$f = \delta^2/(\alpha_O t_c) \tag{54}$$

appearing on the left-hand sides of Eqs. (B-10) and (B-12). The condition for the validity of Eqs. (22) and (23) at the time of ignition is that f is small. Placing the factor $f < 1$ in Eq. (B-12), for example, increases the value of T_{Oc} at ignition, thereby delaying ignition through the influence of the strain. Use of Eqs. (24) and (26) in Eq. (54) allows compression-produced autoignition times to be evaluated in the presence of time-varying strain under these conditions.

3.7 CONCLUSIONS

It may be concluded that, under many situations of interest in Diesels, ignition times may be estimated relatively straightforwardly from formulas like Eq. (B-12), provided that the rate parameters appropriate for a one-step, Arrhenius description of the ignition chemistry are available. These estimates may account not only for time-dependent mixing but also for influences of variable strain in the mixing layer. Strain delays ignition and in extreme cases may prevent it from occurring. The most favorable locations in mixing layers for ignition to occur therefore are positions of low rates of strain. The shortest compression-produced ignition times are those of Appendix B for strain-free conditions.

In the presence of strain, there are criticality conditions for ignition to occur, as shown in Appendix A. These conditions may be expressed in terms of a critical reduced Damköhler number of Eq. (A-22), having a value of about 0.5. Effects of time-varying strain on ignition times may be calculated through the time-varying mixing-layer thickness δ, given by Eqs. (24) and (26). Thus, many aspects of influences of strain and its variations on autoignition may be estimated.

The general formulation in Eqs. (2) to (13) encompasses a wide variety of ignition phenomena. Many of these phenomena have not been analyzed here. For example, situations in which variations of the strain rate A through the mixing layer are important, as described by Eq. (3), have not been treated. Other outstanding problems have been identified in the preceding discussions. There are a number of problems in which pressure variations have only small influences on ignition, and these tend to necessitate consideration of partial differential equations during ignition stages. These problems have not been emphasized here; the focus has been on compression-produced ignition. Strong compression simplifies the analysis by ultimately reducing the problems to ordinary differential equations in time. Thus, perhaps unexpectedly,

many Diesel ignition problems are simpler than other ignition problems.

3.8 REFERENCES

1. T. Kamimoto and H. Kobayashi, "Combustion Processes in Diesel Engines," Progress in Energy and Combustion Science 17, 163-189 (1991).

2. T. Takagi, C.-Y. Fang, T. Kamimoto and T. Okamoto, "Numerical Simulation of Evaporation, Ignition and Combustion of Transient Sprays," Combustion Science and Technology 75, 1-12 (1991).

3. A. Liñán and F.A. Williams, Fundamental Aspects of Combustion, Oxford University Press, New York, 1993.

4. A. Liñán, "The Asymptotic Structure of Counterflow Diffusion Flames for Large Activation Energies," Acta Astronautica 1, 1007-1039 (1974).

5. C.K. Law and S.H. Chung, "Steady State Diffusion Flame Structure with Lewis Number Variations," Combustion Science and Technology 29, 129-145 (1982).

6. S.H. Chung and C.K. Law, "Structure of Convective Diffusion Flames with General Lewis Numbers," Combustion and Flame 52, 59-79 (1983).

7. K. Seshadri and C. Treviño, "The Influence of the Lewis Numbers of the Reactants on the Asymptotic Structure of Counterflow and Stagnant Diffusion Flames," Combustion Science and Technology 64, 243-261 (1989).

8. G.F. Carrier, F.E. Fendell and F.E. Marble, "The Effect of Strain Rate on Diffusion Flame," SIAM Journal on Applied Mathematics 28, 463-500 (1975).

9. A. Liñán and A. Crespo, "An Asymptotic Analysis of Unsteady Diffusion Flames for Large Activation Energies," Combustion Science and Technology 14, 95-117 (1976).

10. T. Niioka, "Ignition Time in the Stretched-Flow Field," Eighteenth Symposium (International) on Combustion, The Combustion Institute, Pittsburgh, Pennsylvania, 1981, pp. 1807-1813.

11. A. Liñán, "The Effect of Pressure Transients in Diffusion Flames," INTA Report on AFOSR Grant 73-2535, March, 1975, unpublished.

12. F.A. Williams, Combustion Theory, Second Edition, Addison-Wesley, Menlo Park, CA, 1985, pp. 489-495.

13. D.R. Kassoy and A. Liñán, "The Influence of Reactant Consumption on the Critical Conditions for Homogeneous Thermal Explosions," Quarterly Journal of Mechanics and Applied Mathematics 31, 99-112 (1978).

APPENDIX 3A – ANALYSIS OF IGNITION FOR CONSTANT RATE OF STRAIN

The thermal-diffusive approximation is adopted, so that $A = A_O = A_F, \rho = \rho_O = \rho_F$ and $\lambda/(\rho c_p) = \alpha_O = \alpha_F$. The mixing-layer thickness becomes $\delta = \sqrt{\alpha_O/A_O}$, as indicated above Eq. (27). Relevant parameters are

$$s = \nu_O Y_{Fo}/Y_{Oo} \ , \ \alpha = q/(c_p T_O) \ , \ \beta = E/(R^o T_O), \qquad (A-1)$$

all three of which typically are large. For example, the air-to-fuel stoichiometric mass ratio for hydrocarbons is of order $s \approx 15$, the ratio α/s is approximately $(T_{af} - T_O)/T_O \approx 6$, where T_{af} is the adiabatic flame temperature, and the nondimensional activation energy is perhaps $\beta \approx 20$ in ignition. In activation-energy asymptotics, the small parameter of expansion is β^{-1}.

The inert solution for the temperature field is

$$T = T_O + (T_F - T_O)\, Z, \qquad (A-2)$$

where Z is given by Eq. (22). The inert solutions for the concentration fields are similarly given by Eq. (23). The expansions

$$T = T_O \left(1 - cZ + \beta^{-1}\varphi + \ldots\right), \qquad (A-3a)$$

$$Y_F = Y_{Fo} \left(Z_F + \alpha^{-1}\beta^{-1} y_F + \ldots\right), \qquad (A-3b)$$

$$Y_O = Y_{Oo} \left(1 - Z_O + s\alpha^{-1}\beta^{-1} y_O + \ldots\right) \qquad (A-3c)$$

are sought, where the nonnegative nondimensional temperature difference is

$$c = (T_O - T_F)/T_O. \qquad (A-4)$$

Introduction of Eq. (16) and of these nondimensionalizations and expansions into Eqs. (29)-(32) leads to the system of equations

$$\eta \frac{dy_F}{d\eta} + \frac{1}{L_F}\frac{d^2 y_F}{d\eta^2} = \eta \frac{dy_O}{d\eta} + \frac{1}{L_O}\frac{d^2 y_O}{d\eta^2}$$
$$= -\eta \frac{d\varphi}{d\eta} - \frac{d^2\varphi}{d\eta^2} = D\left[Z_F + y_F/(\alpha\beta)\right]^n (1 - Z_O)^m e^{\varphi - \beta c Z}, \qquad (A-5)$$

subject to the boundary conditions that φ, y_F and y_O approach zero as $\eta \to \pm\infty$. Here the relevant Damköhler number is

$$D = \alpha\beta A_O^{-1} B Y_{Fo}^{n-1} Y_{Oo}^m e^{-E/(R^o T_O)}. \qquad (A-6)$$

In the reaction-rate term in Eq. (A-5), expansions have been introduced in which terms that are not of leading order in any ignition regime have been dropped.

When βc is of order unity or smaller, reaction occurs everywhere in the mixing layer, and unless α is unreasonably small $y_F/(\alpha\beta)$, which describes the effect of fuel

depletion, is of higher order in the reaction term in Eq. (A-5) and can be neglected in the first approximation. In this case, Eqs. (22) and (23) enable the equation for φ in Eq. (A-5) to be solved to yield $\varphi(\eta)$ for given values of $\beta c, m, n, L_F, L_O$ and D; the functions $y_F(\eta)$ and $y_O(\eta)$ can be calculated later. The solution for $\varphi(\eta)$ will exist only for $D < D_I$, where D_I is the ignition Damköhler number, of order unity. This two-valued solution can be determined numerically for different values of $\beta c, m, n, L_F$ and L_O, and D_I can similarly be calculated as a function of these parameters. Parametric results for $m = n = L_F = L_O = 1$ are available.[4]

When βc is large, the reaction rate is negligibly small except where $\beta c Z$ is of order unity. It is therefore useful to introduce the variable

$$\xi = \beta c Z. \qquad (A-7)$$

For large ξ, away from the oxidizer side of the mixing layer, the chemistry is frozen, and the solutions are

$$\varphi = \varphi_m (1 - Z) \quad , \quad y_F = y_{Fm} (1 - Z_F) \quad , \quad y_O = y_{Om} (1 - Z_O), \qquad (A-8)$$

where the peak values, φ_m, y_{Fm} and y_{Om}, are to be determined by matching with the solution in the reaction region, where ξ is of order unity.

In the reaction zone Z is small and therefore can be approximated from Eq. (22) as

$$Z = e^{-\eta^2/2} \left(\eta \sqrt{2\pi}\right). \qquad (A-9)$$

The value of η in the reaction zone, denoted by η_r, may be estimated from Eqs. (A-7) and (A-9) by putting $\xi = 1$, giving

$$e^{-\eta_r^2/2} \left(\eta_r \sqrt{2\pi}\right) = (\beta c)^{-1}. \qquad (A-10)$$

The values of Z_F and Z_O also are small there, so that $1 - Z_O \approx 1$ in Eq. (A-5), and the expansions

$$Z \approx \frac{e^{-\eta_r^2/2}}{\sqrt{2\pi}\eta_r} e^{-\eta_r(\eta - \eta_r)} \quad , \quad Z_F \approx \frac{e^{-\eta_r^2} L_F/2}{\sqrt{2\pi L_F}\eta_r} e^{-\eta_r(\eta - \eta_r)L_F}, \qquad (A-11)$$

or, from Eqs. (A-7) and (A-10)A, equivalently,

$$\xi = e^{-\eta_r(\eta - \eta_r)} \qquad (A-12)$$

and

$$Z_F = Z_{Fr} \zeta^{L_F} \qquad (A-13)$$

may be employed, where

$$Z_{Fr} = (\beta c)^{-L_F} \left(\sqrt{2\pi}\eta_r\right)^{L_F - 1}. \qquad (A-14)$$

These exponential profiles, in η, of ξ and Z_F, given by Eqs. (A-12) and (A-13), result from approximating in the reaction zone the convective velocity η appearing in the first-derivative terms in Eq. (A-5) by a constant value η_r; they are justified by

the moderately large value of η_r. The same approximation can be used when writing the conservation equation for φ in the reaction zone, so that Eq. (A-5) with fuel depletion neglected becomes

$$\eta\frac{d\varphi}{d\eta}+\frac{d^2\varphi}{d\eta^2}+DZ_{Fr}^{n}\xi^{nL_F}e^{\varphi-\xi}=0, \qquad (A-15)$$

to be solved with the boundary conditions

$$\varphi\to\varphi_m \text{ as } \eta-\eta_r\to-\infty, \quad \varphi\to 0 \text{ as } \eta-\eta_r\to\infty, \qquad (A-16)$$

the former obtained from matching to Eq. (A-8). Here φ_m is an eigenvalue to be determined as part of the solution as a function of D.

In this same approximation, Eq. (A-5) gives for the fuel concentration

$$\eta_r\frac{dy_F}{d\eta}+\frac{1}{L_F}\frac{d^2y_F}{d\eta^2}-DZ_{Fr}^{n}\xi^{nL_F}e^{\varphi-\xi}=0, \qquad (A-17)$$

with the boundary conditions

$$y_F\to y_{Fm} \text{ as } \eta-\eta_r\to-\infty, \quad y_F\to 0 \text{ as } \eta-\eta_r\to\infty, \qquad (A-18)$$

where y_{Fm} must be determined as part of the solution. From Eqs. (A-15) to (A-18) we obtain the equations

$$\eta_r\left(\varphi+y_F\right)+\frac{d}{d\eta}\left(\varphi+y_F/L_F\right)=\eta_r\left(\varphi_m+y_{Fm}\right)=0 \qquad (A-19)$$

so that $y_{Fm}=-\varphi_m$. Thus, with φ_m of order unity, the fuel consumption in the reaction term in Eq. (A-5) can be neglected when describing the ignition process, so long as $(\alpha\beta)^{-1}\ll Z_{Fr}$, that is, from Eq. (A-14),

$$\alpha\beta\left(\beta c\right)^{-L_F}\left(\eta_r\sqrt{2\pi}\right)^{L_F-1}\gg 1. \qquad (A-20)$$

Usually α is large enough to insure that Eq. (A-20) is satisfied and that therefore fuel depletion can be neglected.

When solving Equation (A-15) it is useful to use ξ defined by equation (A-7) as the independent variable; Eq. (A-15) then becomes

$$\frac{d^2\varphi}{d\xi^2}+\Delta\xi^{nL_F-2}e^{\varphi-\xi}=0, \qquad (A-21)$$

where $\Delta=\eta_r^{-2}DZ_{Fr}^{n}$, or

$$\Delta=\eta_r^{-2}\left\{\left(\eta_r\sqrt{2\pi}\right)^{L_F-1}\left(\beta c\right)^{-L_F}\right\}^{n}\alpha\beta BA_O^{-1}Y_{Fo}^{n-1}Y_{Oo}^{m}e^{-E/R^oT_O}, \qquad (A-22)$$

is the reduced Damköhler number, of order unity, under near-ignition conditions for $\beta c\gg 1$. It may be recalled that η_r in Eq. (A-22) is determined by Eq. (A-10). Equation (A-21) must be solved with the boundary conditions

$$\varphi=0 \text{ at } \xi=0, \quad \varphi\to\varphi_m \text{ as } \xi\to\infty, \qquad (A-23)$$

where the increment in temperature φ_m must be calculated as a function of Δ for different values of the parameter nL_F. Because we can expect φ_m to be a two-valued function of Δ for Δ smaller than an ignition value Δ_I, and no solution to exist for values of $\Delta > \Delta_I$, it is more convenient to pose the problem as that of finding the value of the Damköhler number Δ that results in a given value of the temperature increment φ_m. The function $\Delta = \Delta(\varphi_m, nL_F)$ will exhibit a maximum $\Delta_I = \Delta_I(nL_F)$ that characterize the ignition conditions.

In the particular case $nL_F = 2$, the solution can be obtained in closed form by using $\Psi = \varphi - \xi$ as the independent variable. A first integral of Eq. (A-21) in this case is

$$\Psi_\xi^2 - \Psi_\xi^2(0) = 2\Delta\left(1 - e^\Psi\right) \qquad (A-24)$$

where $\Psi_\xi^2(0) = 1 - 2\Delta$. Thus $\Delta \leq 1/2$; the ignition value of Δ for $nL_F = 2$ is $\Delta_I = 1/2$. The stable, lower branch of the curve $\varphi(\xi, \Delta)$ is then given by

$$\xi = \int_\Psi^0 \left\{1 - 2\Delta e^\Psi\right\}^{-1/2} d\Psi$$

or

$$\varphi = \Psi + \xi = 2ln\left(\frac{1 + \sqrt{1 - 2\Delta e^\Psi}}{1 + \sqrt{1 - 2\Delta}}\right), \qquad (A-25)$$

and

$$\varphi_m = 2ln\left\{2/\left(1 + \sqrt{1 - 2\Delta}\right)\right\}. \qquad (A-26)$$

Fortuitously, the value $nL_F = 2$ often may be reasonably accurate for many hydrocarbon fuels in air.

APPENDIX 3B – ANALYSIS OF IGNITION BY COMPRESSION IN THE UNSTRAINED MIXING LAYER

Let

$$\phi = \beta(\theta - 1), \quad \upsilon = F_c\beta(\sigma - \sigma_c), \tag{B-1}$$

where β and F_c are defined in Eqs. (50) and (51). Substitution into Eqs. (45) and (47) and expansion to leading order for the ignition stage then gives

$$d\phi/d\upsilon = \Lambda\Psi_F^n\Psi_O^m e^{\phi+\upsilon} \tag{B-2}$$

where

$$\Lambda = \frac{qB_cY_{Fo}^nY_{Oo}^mt_ce^{-E/(R^oT_{Oc})}}{F_cc_pT_{Oo}(P_{sc}/P_{so})^{(\gamma-1)/\gamma}}. \tag{B-3}$$

The manner in which $\phi + \upsilon$ arises in the exponent is through the expansion

$$\begin{aligned}&\frac{E}{R^oT_{Oo}}\left(\frac{P_{sc}}{P_{so}}\right)^{-(\gamma-1)/\gamma}\left[1-\frac{1}{\theta}\left(\frac{P_{sc}}{P_s}\right)^{(\gamma-1)/\gamma}\right]\\ =\ &\frac{E}{R^oT_{O\upsilon}}\left\{1-\left(1-\frac{\phi}{\beta}+\ldots\right)[1-F_c(\sigma-\sigma_c)+\ldots]\right\},\end{aligned} \tag{B-4}$$

which shows that the υ term is the effect of the T_O increase caused by compression. The matching condition for Eq. (B-2) is found from Eq. (48) to be

$$\phi \to -\beta(1-\theta_F)\frac{1}{2}\,\mathrm{erfc}\left(\frac{\zeta/2}{\sqrt{\sigma_c}}\right) \equiv \phi_{-\infty} \text{ as } \upsilon \to -\infty. \tag{B-5}$$

If Ψ_F and Ψ_O are independent of ϕ and υ, for example, given by Eq. (49), then the integral of E. (B-2) is

$$e^{-\phi_{-\infty}} - e^{-\phi} = \Lambda\Psi_F^n\Psi_O^m e^{\upsilon}, \tag{B-6}$$

which has $\phi \to \infty$ (thermal runaway) when

$$\upsilon = -\phi_{-\infty} - ln(\Lambda\Psi_F^n\Psi_O^m), \tag{B-7}$$

the minimum value of which (over all values of ζ) is selected to be zero so that, by definition, the thermal runaway first occurs at $\sigma = \sigma_c$. If the subscript m is employed to denote the value of ζ at which the minimum occurs, then from Eqs. (49), (B-5) and (B-7) it is found that

$$\begin{aligned}&\exp\left\{\beta(1-\theta_F)\frac{1}{2}\mathrm{erfc}\left(\frac{\zeta_m/2}{\sqrt{\sigma_c}}\right)\right\}\\ =\ &\Lambda\left[\frac{1}{2}\mathrm{erfc}\left(\frac{\zeta_m}{2}\sqrt{\frac{L_F}{\sigma_c}}\right)\right]^n\left[1-\frac{1}{2}\mathrm{erfc}\left(\frac{\zeta_m}{2}\sqrt{\frac{L_O}{\sigma_c}}\right)\right]^m\end{aligned} \tag{B-8}$$

and

$$n\sqrt{L_F}\left[\frac{1}{2}\mathrm{erfc}\left(\frac{\zeta_m}{2}\sqrt{\frac{L_F}{\sigma_C}}\right)\right]^{-1}$$
$$-\ m\sqrt{L_O}\left[1-\frac{1}{2}\mathrm{erfc}\left(\frac{\zeta_m}{2}\sqrt{\frac{L_O}{\sigma_c}}\right)\right]^{-1}=\beta\left(1-\theta_F\right), \qquad (B-9)$$

the last of which is obtained by differentiation ($dv/d\zeta = 0$ at the location $\zeta = \zeta_m$ of the minimum) and serves to determine the value of ζ_m. With t_c not yet defined precisely, it is possible to select $\sigma_c = 1$ and then determine t_c by substituting Eqs. (51) and (B-3) into Eq. (B-8). The result is

$$\frac{\gamma q B c Y_{F_o}^n Y_{O_o}^m e^{-E/(R^oT_{Oc})}}{(\gamma-1)\,c_pT_{Oc}\left[d\left(lnP_s\right)/dt\right]_{t=t_c}}\left[\frac{1}{2}\mathrm{erfc}\left(\frac{\zeta_m}{2}\sqrt{L_F}\right)\right]^n\left[1-\frac{1}{2}\mathrm{erfc}\left(\frac{\zeta_m}{2}\sqrt{L_O}\right)\right]^m$$
$$=\ \exp\left\{\frac{E\left(T_{Oc}-T_{Fc}\right)}{R^oT_{Oc}^2}\left[\frac{1}{2}\mathrm{erfc}\left(\frac{\zeta_m}{2}\right)\right]\right\}, \qquad (B-10)$$

which with ζ_m determined by Eq. (B-9) provides t_c mainly through the variation of $e^{-E/(R^oT_{Oc})}$, in which $T_{Oc} = T_{Oo}\left(P_{sc}/P_{so}\right)^{(\gamma-1)/\gamma}$ according to Eq. (50).

For large values of $\beta\left(1-\theta_F\right)$, Eq. (B-9) gives

$$\zeta_m = \left(2/\sqrt{L_F}\right)\mathrm{erfc}^{-1}\left\{\left(2n\sqrt{L_F}\right)/\left[\beta\left(1-\theta_F\right)\right]\right\}, \qquad (B-11)$$

where erfc^{-1} denotes the inverse of the complementary error function, and manipulations like those of Eqs. (A-9) and (A-10), also using $\beta\left(1-\theta_F\right) = E\left(T_{Oo}-T_{Fo}\right)/\left(R^oT_{Oo}T_{Oc}\right)$, reduce Eq. (B-10) to

$$\frac{\gamma q B_c Y_{F_o}^n Y_{O_o}^m e^{-E/(R^oT_{Oc})}}{(\gamma-1)\,c_pT_{Oc}\left[d\left(lnP_s\right)/dt\right]_{t=t_c}}\left[\frac{n\sqrt{L_F}R^oT_{Oo}T_{Oc}}{E\left(T_{Oo}-T_{Fo}\right)}\right]^n$$
$$=\ \exp\left\{\left(nL_F\right)^{1/L_F}\left[\frac{E\left(T_{Oo}-T_{Fo}\right)}{\sqrt{\pi}\zeta_m R^oT_{Oo}T_{Oc}}\right]^{(L_F-1)/L_F}\right\}, \qquad (B-12)$$

which is more direct than Eqs. (B-9) and (B-10) to employ for determining when ignition occurs.

If $\beta\left(1-\theta_F\right)$ becomes too large, then in the reaction region about $\zeta = \zeta_m$, identified above, the inert fuel concentration is so small that fuel consumption becomes significant during the ignition stage. It then becomes necessary to determine ψ_F from Eq. (45) during the ignition stage, matching to Eq. (49) as $v \to -\infty$. In the ignition stage at the reaction region, $\psi_O = 1$ to leading order, and

$$\chi \equiv \beta\psi_F qY_{Fo}/\left(c_pT_{Oc}\right) \qquad (B-13)$$

is of order unity, so that it becomes appropriate to redefine Λ to include the additional factor $\left[\left(c_pT_{Oc}\right)/\left(qY_{Fo}\beta\right)\right]^n$, obtaining from Eqs.(45) and (47)

$$-d\chi/dv = d\phi/dv = \Lambda\chi^n e^{\phi+v}, \qquad (B-14)$$

since diffusive effects are of higher order. Integration of the first of these equalities, subject to the matching conditions, gives

$$\chi = \frac{\beta q Y_{Fo}}{\sqrt{\pi L_F}\zeta c_p T_{Oc}} e^{-(\zeta^2/4)L_F} - \frac{\beta(1-\theta_F)}{\sqrt{\pi}\zeta} e^{-\zeta^2/4} - \phi \qquad (B-15)$$

under the present conditions, where the selection $\sigma_c = 1$ has again been made. The value of ζ in the reaction region is suitably large for the terms in Eq. (B-15) to be of order unity. A single ordinary differential equation (with ζ as a parameter) is obtained from the second equality in Eq. (B-14) when Eq. (B-15) is employed in the reaction term. The fuel depletion enters through the ϕ term in Eq. (B-15), which reduces χ as ϕ increases. The character of the solution to the resulting differential equation has been fully explored.[11] The reactant depletion can prevent thermal runaway and give rise to premixed-flame propagation away from an ignition point.

4 AUTOIGNITION OF NONUNIFORM MIXTURES IN VARIABLE-VOLUME CHAMBERS

4.1 INTRODUCTION

Combustion in Diesel engines is a complicated process involving turbulent, two-phase flows with transport processes and finite-rate chemistry.[1] Accurate descriptions of autoignition in variable-volume chambers are needed for improving methods of Diesel-engine design. There has been recent progress in both experimental and computational approaches to the investigation of Diesel autoignition.[1] In particular, computational methods have been applied with some success to the calculation of ignition in transient fuel sprays.[2,3]

Computation of *nonreacting* two-phase, turbulent flows with atomization and evaporation is a challenging problem. The computational difficulties are greatly increased when the rapid finite-rate chemistry that typically occurs during autoignition is included as well. Therefore, there is motivation for obtaining simplified descriptions of the influences of the autoignition chemistry on the overall combustion processes. The present work addresses the problem of obtaining such simplified descriptions. It is presumed here that experiment or numerical simulation has given the spatial distributions of temperature and fuel and oxidizer concentrations within the combustion chamber just prior to initiation of the compression and combustion processes leading to autoignition. An analytical approach based on activation-energy asymptotics is then developed to provide the ignition time and subsequent pressure history in terms of this initial input information. The results remove the necessity of including the autoignition chemistry in numerical simulations, enabling them to focus on the transport-controlled stages of evaporation and combustion that occur prior to and subsequent to ignition.

Attention is focused on spontaneous ignition that takes place as a result of the temperature rise that occurs when the chamber volume $V(t)$ is reduced. The ignition transient is assumed to be short compared with characteristic times of heat conduction across nonhomogeneities, so that heat-conduction and diffusion effects can be neglected during ignition. In addition, the ignition time is taken to be long compared with the time required for acoustic waves to propagate across the chamber, so that the chamber pressure $P(t)$ can be considered to be spatially uniform, a function only of time t. The activation energy of the model one-step reaction is presumed to be large enough that changes in reactant concentrations can be neglected in evaluating reaction rates. Finally, subsequent to ignition at any point, the ignition front is considered to propagate more rapidly than the velocity of a premixed laminar flame, measured in the product gas at the adiabatic flame temperature behind the ignition front. These hypotheses, which enable all molecular transport processes to be ignored, become invalid shortly after ignition, when premixed flames overtake ignition fronts or diffusion flames are left behind, but they may serve to describe the initial ignition pressure transient.

Subsequent to formulating the problem, in later sections we shall consider the initiation stage and the propagation stage for the ignition fronts, sequentially.

4.2 FORMULATION

Since molecular diffusion is absent, it is convenient to employ a Lagrangian description in which x is the initial position of the fluid particle. The initial distribution of the fuel mass fraction Y_F, the oxidizer mass fraction Y_O and temperature T are specified as $Y_{Fo}(\mathrm{x}), Y_{Oo}(\mathrm{x})$ and $T_o(\mathrm{x})$, respectively. Hot spots, points of maximum temperature, are of greatest importance in autoignition. Let the hot spots initially be located at positions x_i and have compositions Y_{Fi} and Y_{Oi} and maximum temperature T_i, with temperature curvature T_i'', such that the volume with temperature between $T_i - \Delta T$ and T_i is $(\Delta T/T_i'')^k$, where $k = 3/2$ unless the "spots" are cylindrical or planar, in which case $k = 1$ or $k = 1/2$, respectively. While deterministic simulations yield specific values for x_i and its associated parameters, in turbulent flows it should more often be better to generate the four-variable, joint probability-density functions $\mathcal{P}_i(Y_{Fi}, Y_{Oi}, T_i, T_i'')$, such that $\mathcal{P}_i \Delta Y_{Fi}\ \Delta Y_{Oi}\ \Delta T_i\ \Delta T_i''$ is the probability that any hot spot has values of parameters in the range ΔY_{Fi} about Y_{Fi} ΔY_{Oi} about Y_{Oi}, ΔT_i about T_i and $\Delta T_i''$ about T_i''. By definition, $\int_0^\infty \int_0^\infty \int_0^1 \int_0^1 \mathcal{P}_i dY_{Fi} dY_{Oi} dT_i dT_i'' = 1$. Similarly, the number of hot spots N in the chamber may be assigned a probability P_N, such that $\sum_{N=0}^{\infty} P_N = 1$. Both deterministic and probabilistic descriptions of the initial spatial distributions will be permitted in the following analysis.

Let D/Dt denote the material derivative following a fluid element. Then the equations for species and energy conservation become

$$DY_F/Dt = -BY_F^n Y_O^m e^{-E/R^oT}, \tag{1}$$

$$DY_O/Dt = -\nu_O BY_F^n Y_O^m e^{-E/R^oT} \tag{2}$$

and

$$\rho c_p DT/Dt = dp/dt + \rho q BY_F^n Y_O^m e^{-E/R^oT}, \tag{3}$$

where the reaction orders are n and m, E and R^o denote the activation energy and the universal gas constant, B is the effective frequency factor for fuel consumption and ν_O the stoichiometric oxidizer-to-fuel mass ratio, ρ represents density and c_p the specific heat at constant pressure, and q is the heat release per unit mass of fuel. In the gas phase, the ideal-gas equation of state is adopted,

$$p = \rho(R^o/W)T, \tag{4}$$

where W represents the average molecular weight, and this enables Eq. (3) to be rewritten as

$$D(lnT)/Dt = [(\gamma - 1)/\gamma]\, d(lnp)dt + [q/(c_pT)]\, BY_F^n Y_O^m e^{-E/R^oT}, \tag{5}$$

where the ratio of specific heats,

$$\gamma = (c_p - R^o/W)/c_p, \tag{6}$$

will be taken to be constant.

Subtraction of ν_O^{-1} times Eq. (2) from Eq. (1) removes the chemical term and enables integration to be performed to show that

$$Y_F - (Y_O - Y_{O\infty})/\nu_O = Z(\mathbf{x}), \tag{7}$$

where $Z(\mathbf{x})$ is the initial mixture fraction, $Y_{O\infty}$ is the oxidizer mass fraction in the inlet oxidizer stream, and the inlet fuel stream has been assumed to be pure fuel, as is generally true. This relationship enables the concentration factor in the reaction rate to be written in terms of Y_F as

$$Y \equiv Y_F^n Y_O^m = Y_F^n \left[Y_{O\infty} + \nu_O(Y_F - Z)\right]^m, \tag{8}$$

so that Eq. (1) becomes

$$dY_F/dt = -BYe^{-E/(R^oT)}. \tag{9}$$

It is convenient to write Eq. (5) in terms of an entropy-related variable as

$$D(lnS)/Dt = \left\{q/\left[c_p S p^{(\gamma-1)/\gamma}\right]\right\} BYe^{-E/\left[R^oSP^{(\gamma-1)/\gamma}\right]}, \tag{10}$$

where

$$S = T/P^{(\gamma-1)/\gamma}. \tag{11}$$

In working with S, the exponential of a constant times the entropy, the isentropic increase in T with increasing P during adiabatic compression comes automatically from Eq. (11) with S constant, and the additional compression term is not present in Eq. (10). Equations (9) and (10) are the differential equations that describe the autoignition process addressed here. They are to be integrated subject to the initial distributions at $t = 0$ specified earlier.

4.3 PRESSURE-VOLUME RELATIONS

If dV_o is the volume of a fluid element at time zero and dV the volume of the same element (of the same mass) at time t, then $\rho dV = \rho_o dV_o$, where $\rho_o(\mathbf{x})$ is the initial density. This relationship implies that the chamber volume V at time t is

$$V = \int\int_{V_o}\int (\rho_o/\rho) dV_o. \tag{12}$$

Under the assumption that the volume occupied by liquid is negligible compared with that occupied by gas, Eqs. (4) and (11) may be used in this expression to show that

$$(P/P_o)^{1/\gamma} = (V_o/V)\int\int_{V_o}\int (S/S_o)(W_O/W) dV_o/V_o. \tag{13}$$

Prior to chemistry occurring, $S = S_o$ and $W = W_o$, so that Eq. (13) provides the usual isentropic relationship. During this inert stage, a volume decrease produces a pressure increase and a temperature increase. At a time t_c, the maximum temperature reaches a critical value T_c for chemistry to begin, and the inert stage is terminated by a stage of transition to ignition.

4.4 THE IGNITION STAGE

Let S_c denote the maximum value of $S_o(\mathrm{x})$ within the chamber and P_c the pressure in the inert stage at time t_c. An appropriate small parameter for describing the ignition stage is then

$$\epsilon = R^o S_c P_c^{(\gamma-1)/\gamma}/E. \tag{14}$$

A distinguished limit is that in which $S_o(\mathrm{x})$ differs from S_c by an amount of order ϵ throughout the chamber,

$$S_o(\mathrm{x})/S_c = 1 - \epsilon s_o(\mathrm{x}), \tag{15}$$

with $s_o(\mathrm{x})$ nonnegative and of order unity. Typically, variations in $S_o(\mathrm{x})$ will be greater than this, so that $s_o(\mathrm{x})$ is large in much of the chamber and is of order unity only in a fraction of the initial volume V_o. In the latter case, the analysis of the ignition stage automatically receives no contribution from the fraction of the chamber in which $s_o(\mathrm{x})$ is large.

The expansions

$$(t - t_c)/t_c = \epsilon\tau,\ P/P_c = 1 + \epsilon p,\ V/V_c = 1 + \epsilon v,\ S/S_c = 1 + \epsilon(s - s_o) \tag{16}$$

are introduced, where p and v are functions of τ, while s depends on τ and x. The value of ϵ is presumed to be small enough that reactant consumption (and therefore changes in W) can be neglected during ignition. Therefore, only Eq. (10) needs to be considered. The expansion of Eq. (10) to leading order in ϵ is

$$Ds/D\tau = \delta Y e^{s - s_o + [(\gamma-1)/\gamma]p}, \tag{17}$$

where the Frank-Kamenetskii parameter is

$$\delta = \frac{t_c q B_c}{c_p T_c} e^{-E/R^o T_c}, \tag{18}$$

in which $T_c \equiv S_c P_c^{(\gamma-1)/\gamma}$, B_c denotes the value of B at pressure P_c, and in general qB_c/c_p may vary with x, so that δ varies, but not much, and for simplicity here it may be treated as a constant. The expansion of Eq. (13) shows that

$$p = \gamma(\overline{s} - v), \tag{19}$$

which may be used in Eq. (17) to express p in terms of the prescribed function v and the volume average of s, denoted by an overbar, namely,

$$\overline{s} = \int\!\!\int_{V_o}\!\!\int s dV_o/V_o. \tag{20}$$

Equations (17) and (19) show that the equation to be integrated is

$$Ds/D\tau = (\delta Y e^{-s_o}) e^{-(\gamma-1)v + (\gamma-1)\overline{s}} e^{s}, \tag{21}$$

subject to the matching condition $s \to 0$ as $\tau \to -\infty$. The initial position x is a parameter in this equation, while v and $\overline{s}$ are functions only of τ. In terms of the new time variable

$$\sigma = \delta \int_{-\infty}^{\tau} e^{-(\gamma-1)(v-\overline{s})} d\tau, \tag{22}$$

the solution to Eq. (21) is

$$s = -ln(1 - \sigma Y e^{-s_o}), \tag{23}$$

which exhibits thermal runaway when

$$\sigma Y e^{-s_o} = 1. \tag{24}$$

Since Eq. (23) gives s explicitly as a function of σ and $Y(\mathbf{x})e^{-s_o(\mathbf{x})}$, it may be used in Eq. (20) to evaluate the average $\overline{s}$ as a function of σ, after which the function

$$F(\sigma) = \int_0^\sigma e^{-(\gamma-1)\overline{s}} d\sigma \tag{25}$$

may be calculated. From Eqs. (18) and (22), the ignition time may then be determined from

$$t_c = [c_p T_c/(qB_c)]\, e^{E/R^o T_c} F(\sigma_c) / \int_{-\infty}^{0} e^{-(\gamma-1)v} d\tau, \tag{26}$$

where $\sigma_c = (Ye^{-s_o})_c^{-1}$, in which $(Ye^{-s_o})_c$ denotes the maximum value of this product within the chamber. Since $Y < 1$ according to Eq. (8) and $s_o \geq 0$ according to Eq. (15) and the definition of S_c, it is seen that $\sigma_c > 1$; although Y often is quite small where $S = S_c$, neglect of reactant consumption in the present analysis requires $\epsilon \ll Y$ and thereby limits σ_c. In Eq.(26), T_c and B_c are functions of t_c, determined through the inert-stage pressure P_c at $t = t_c$. Therefore, Eq. (26) is an implicit relationship for t_c.

After $\overline{s}(\sigma)$ is found from Eqs. (20) and (23), Eq. (19) determines the pressure history during the ignition stage and shows that, at the ignition time, $p = \gamma\overline{s}(\sigma_c)$. In regions where s_o is large, say of order ϵ^{-1} or larger, Eq. (23) shows that $s = 0$, so that according to Eq. (20), in this last expression $\overline{s}(\sigma_c)$ is the product of the fraction of the initial volume over which s_o is of order unity with the average over this lesser volume.

Equation (26) can be used only when the integral in the denominator is of order unity, so that compressional heating during the ignition transient enhances ignition. In the simplest case, $-t_c(dV/dt)/V_c \equiv \dot{v}$ is constant and of order unity during the ignition stage, so that the denominator in Eq. (26) is $[(\gamma-1)\dot{v}]^{-1}$. If the integral becomes larger than order ϵ^{-1}, then a different scaling is needed in Eq. (16), such that the first equation is replaced by $(t-t_1)/(t_c-t_1) = \tau$, and the ϵv term is removed as being negligibly small. Here t_1 is the time at which the volume change became negligible, so that $V_c = V_1$ and, according to Eq. (13), $P_c = P_1$, giving $S_c = S_1$ and $T_c = T_1$. The parameter δ is redefined by replacing t_c by $(t_c - t_1)/\epsilon$ in Eq. (38). The v term is absent in Eqs (19), (21) and (22), and in Eq. (22) the lower limit of the integral is now zero. The solution again is given by Eq. (23), where now Eq. (22) implies that $\delta\tau = F(\sigma)$. Since $\tau = 1$ at ignition by the definition of τ, Eq. (26) is replaced by

$$t_c - t_1 = R^o c_p T_c^2 e^{E/R^o T_c} F(\sigma_c)/(EqB_c). \tag{27}$$

In a homogeneous system, $s_o = 0$ and $\overline{s} = s$, so that Eqs. (23) and (25) give

$$F(\sigma) = [1 - (1 - \sigma Y)^\gamma]/(\gamma Y), \tag{28}$$

and (with c_v the specific heat at constant volume) Eq. (27) becomes

$$t_c - t_1 = R^o c_v T_c^2 e^{E/R^o T_c}/(EqB_c Y), \tag{29}$$

the well-known[4] Frank-Kamenetskii result for constant-volume ignition.

4.5 THE IGNITION-FRONT PROPAGATION STAGE

The preceding results determine when ignition first occurs and give pressure histories over a period of fractional changes in pressure of an amount of order ϵ during the ignition transient. Subsequent to that ignition stage is a stage of ignition-front propagation, during which ignition waves spread from the ignition points. During this stage, ignitions may also develop at other points that at time t_c have values of their entropy parameter S below S_c by an amount of order larger than ϵ, but because of its greater heat release, the ignition propagation generally dominates the pressure rise, so that these subsequent ignitions may be neglected. The value of ϵ is assumed here to be small enough that, after ignition occurs, combustion goes to completion in a negligibly short time across the ignition front, consuming all of the fuel or oxidizer, depending on which is the deficient reactant. In Diesel-engine applications, cooling by processes such as fuel vaporization generally causes oxidizer-rich regions to be hotter, so that fuel is the deficient reactant in the ignition regions. For this reason, the present formulation takes the fuel consumption as determining the heat release; heat release controlled by oxidizer depletion can be treated in a similar fashion.

Multiplication of Eq. (9) by $q/(c_p T)$, followed by addition to Eq. (10), results in a source-free total-enthalpy equation that can be written as

$$DS/Dt + \left\{q/[c_p P^{(\gamma-1)/\gamma}]\right\} DY_F/Dt = 0. \tag{30}$$

A fluid element at initiation position x that burns at a time $t_b(\mathrm{x})$, at which the pressure is $P_b(\mathrm{x})$, will experience an increase in S upon burning by an amount $qY_{Fo}/\left[c_p P_b^{(\gamma-1)/\gamma}\right]$, according to the integral of Eq. (30) across the short increment of time required for the element to burn. In the first approximation, DS/Dt vanishes both before and after burning, because the reaction rate is negligible in Eq. (10) before burning, and $Y = 0$ in Eq. (10) after burning. Therefore, the solution for S at leading order is

$$S = \begin{cases} S_o(\mathrm{x}) & ,t < t_b(\mathrm{x}) \\ S_o(\mathrm{x}) + qY_{Fo}(\mathrm{x})/\left[c_p P_b(\mathrm{x})^{(\gamma-1)/\gamma}\right] & ,t > t_b(\mathrm{x}). \end{cases} \tag{31}$$

Use of Eq. (31) in Eq. (13) gives

$$\left(\frac{P}{P_o}\right)^{1/\gamma} = \frac{V_o}{V}\left\{1 + \frac{1}{V_o}\int\int\int_{V_b}\left[\frac{qY_{Fo}W_o}{c_p S_o W_b P_b^{(\gamma-1)/\gamma}} + \frac{W_o}{W_b} - 1\right] dV_o\right\}, \tag{32}$$

where $W_b(\mathrm{x})$ denotes the average molecular weight of the burnt gas, and $V_b(t)$ is the initial volume of the fluid comprising the burnt gas at time t. Henceforth, for brevity

the approximation $W_b = W_o$ will be employed, since changes in mean molecular weights for ignition-front propagation usually are small.

In the previous section, an expansion of Eq. (13) was employed, near time t_c, in which fractional departures of P and V from P_c and V_c were of order ϵ. Once the fraction $f \equiv V_b(t)/V_o$ of the initial fluid volume comprising burnt gas exceeds ϵ, terms of order ϵ in the expansion of Eq. (13) become negligible, and for f small compared with unity but large compared with ϵ, Eq. (32) provides the expansion

$$P/P_c = 1 + \gamma f \langle G \rangle, \tag{33}$$

where $\langle\rangle$ identifies the average over the x of the burnt gas alone, and

$$G(\mathrm{x}) = qY_{Fo}(\mathrm{x}) / \left[c_p S_o(\mathrm{x}) P_b(\mathrm{x})^{(\gamma-1)/\gamma}\right], \tag{34}$$

which is the fractional increase in S upon burning. The volume change no longer contributes to the pressure change in Eq. (33), since a sudden increase in volume compression would be unrealistic and is not considered. To obtain the pressure history during this stage, it is necessary to find f and $\langle G \rangle$ as functions of time.

The evolution of f is determined by the rate of propagation of the ignition front from each ignition point. In the vicinity of any ignition point i, Eq. (11) enables the center value S_{oi} and curvature parameter S''_{oi} to be evaluated readily from the given values T_i and T''_i, defined at the beginning of Section 2. The dominant factor in any ignition-time formula is

$$e^{E/\left[R^o S P^{(\gamma-1)/\gamma}\right]} = e^{E/\left[R^o S_{oi} P^{(\gamma-1)/\gamma}\right]} e^{E S''_{oi} V_i^{1/k} / \left[R^o S_{oi}^2 P^{(\gamma-1)/\gamma}\right]}, \tag{35}$$

in which V_i is the burnt-gas volume in the initial (x) space at the ignition time t_i. Equation (35) is obtained from an expansion of S^{-1} for small values of $S''_{oi} V_i^{1/k}/S_{oi}$, which must be valid for V_i to be characterized only by S''_{oi}, without needing additional terms in the Taylor expansion. From Eq. (35) and Eq. (26), for example, it may be inferred that V_i is related approximately to t_i and the ignition time t_{ci} for the center of spot i by the formula

$$V_i = \left\{ \left[R^o S_{oi}^2 P_i^{(\gamma-1)/\gamma} / (E S''_{oi}) \right] ln\,(t_i/t_{ci}) \right\}^k, \tag{36}$$

where $P_i \equiv P(t_i)$. The approach leading to Eq. (36) is a simplification of much more detailed analyses[5,6,7] of related problems. The fraction $f_i(t) \equiv V_i(t)/V_o$ may be calculated from Eq. (35) by putting $t_i = t$, after which, by summing over all burnt-gas regions, $f(t)$ is found from $f = \sum_{i=1}^{N} f_i$.

The average $\langle G \rangle$ may be obtained from the average $\langle G \rangle_i$ taken over each burnt-gas volume according to

$$\langle G \rangle = \sum_{i=1}^{N} f_i \langle G \rangle_i / f. \tag{37}$$

To find $\langle G \rangle_i$, it is necessary only to employ Eq. (35), which gives

$$\langle G \rangle_i = \int\int\int_{V_i} \left\{ qY_{Fi} / \left[c_p S_{oi} P_{bi}^{(\gamma-1)/\gamma} \right] \right\} dV_i / V_i. \tag{38}$$

When terms of order ϵ and f are neglected, Eq. (38) shows that, to leading order, simply

$$\langle G\rangle_i = qY_{Fi}/\left[c_pS_cP_c^{(\gamma-1)/\gamma}\right], \tag{39}$$

so that Eq. (37) becomes

$$\langle G\rangle = \sum_{i=1}^{N} qY_{Fi}f_i/(c_pT_cf). \tag{40}$$

Use of Eqs. (36) and (40) in Eq. (33) produces the result

$$P/P_c = 1 + \sum_{i=1}^{N}\left[\gamma qY_{Fi}/(c_pT_c)\right]\left\{\left[R^oT_cT_i/(ET_i'')\right]^k/V_o\right\}\left[(t-t_{ci})/t_{ci}\right]^k, \tag{41}$$

where an expansion for small values of f and $(t-t_{ci})/t_{ci}$ has been employed.

For deterministic problems, Eq. (41) directly yields the pressure history during the stage of ignition-front propagation. When the hot-spot distributions can be described only probabilistically and the prescription given at the beginning of Section 2 is employed, then the average pressure history during this stage is found from Eq. (41) to be

$$\frac{\overline{P}}{P_c} = 1 + \left[\sum_{N=0}^{\infty}\left(\frac{NP_N}{V_o}\right)\right]\left[\int_0^\infty\int_0^\infty\int_0^1\int_0^1\left(\frac{\gamma qY_{Fi}}{c_pT_c}\right)\left(\frac{R^oT_cT_i}{ET_i''}\right)^{3/2}\mathcal{P}_i dY_{Fi}dY_{Oi}dT_idT_i''\right]\left(\frac{t-t_c}{t_c}\right)^{3/2}, \tag{42}$$

where fractional differences of order ϵ in ignition times of different spots have been neglected by putting $t_{ci}=t_c$, and the usual three-dimensional case of $k=3/2$ has been considered. Equation (42) shows that, after ignition, the hot-spot growth causes the pressure to increase with time in proportion to $(t-t_c)^{3/2}$. The first proportionality factor in Eq. (42) is the average number of hot spots per unit volume, and the second is the average of the product of the increase in pressure ratio of a gas element upon burning times the volume increase of the element in time $t-t_c$. For oxidizer-deficient spots, the quantity $\gamma qY_{Fi}/(c_pT_c)$ is replaced by $\gamma qY_{Oi}/(\nu_O c_pT_c)$ in Eq. (42); in either case, one of the integrals just gives a factor of unity, and only a trivariate probability-density function appears.

4.6 DISCUSSION

The ignition time t_c, as given by Eq. (26), marks the end of inert, compressional heating. During the ignition stage, the pressure history may be obtained from Eqs. (16), (19), (20), (22) and (23). That result may be used until $t=t_c$, after which time Eq. (23) would produce singularities in Eq. (20), which imply that an additive term of order $(f/\epsilon)qY_{Fo}/(c_pT_c)$ belongs in $\bar{s}$. Shortly thereafter, with burnt-gas volumes increasing according to Eq. (36), $\overline{P}/P_c$ as given by Eq. (42) becomes larger than $1+\epsilon p$, and subsequently Eq. (42) gives the pressure history. This equation then applies until, for some burnt-gas region, either V_i becomes too large for Eq. (36) to be accurate, or the rate of increase of V_i obtained from Eq. (36) becomes slower than that which would occur by premixed laminar-flame propagation. At such times, either distortion of shapes of burnt-gas regions or flame propagation sets in, leading eventually to

consumption of all premixed regions and to solely diffusion-flame combustion in the final stages. This description represents a simplification of more detailed ignition analyses of the type reported previously.[5-7] The simplifications introduced here are particularly suited to the Diesel problem.

An approximation that may be applied for computational purposes is to terminate use of these analytical results at a time t at which $dV_i^{1/3}/dt$ first decreases to the laminar burning velocity and to consume all remaining premixed reactants at that time. The numerical simulations may then be resumed in a purely nonpremixed mode of combustion, employing the mixture-fraction formulation suggested previously.[4]

To employ the approach suggested here that makes use of Eq. (42), the numerical simulations of the nonreacting flow prior to ignition must generate the requisite probability-density functions such as $\mathcal{P}_i$. Different degrees of complexity in the probabilistic formulation can be selected. For example, it is straightforward to allow $\mathcal{P}_i$ to be statistically dependent on the number N of hot spots, so that the integral does not factor out of the sum in Eq. (42). However, it seems unlikely that this degree of detail would be retained in practical computations. The simplest assumption would be that the distributions of Y_{Fi} and (T_i/T_i'') are statistically independent, so that the integrals become products of individual averages, and only the average fuel mass fraction $\overline{Y}_{Fi}$ at hot spots and their average curvature-tangent volumes $\overline{(T_i/T_i'')}$ need to be retained from the inert simulations, along with the parameters that appear in Eq (26).

4.7 CONCLUSIONS

This analysis has provided a way to obtain the ignition time t_c in Diesel-type combustion and has indicated that after ignition there is a stage in which the chamber pressure increases with time in proportion to $(t - t_c)^{2/3}$. The results may be used in conjunction with computational approaches to remove chemical kinetics from the problem by providing the necessary link between the initial, inert-mixing stage and the final, equilibrium nonpremixed-combustion stage.

4.8 REFERENCES

1. T. Kamimoto and H. Kobayashi, "Combustion Processes in Diesel Engines," Progress in Energy and Combustion Science 17, 163-189 (1991).

2. S.K. Aggarwal, "Ignition Behavior of a Multicomponent Fuel Spray," Combustion and Flame 76, 5-15 (1989).

3. T. Takagi, C.-Y. Fang, T. Kamimoto and T. Okamoto, "Numerical Simulation of Evaporation, Ignition and Combustion of Transient Sprays," Combustion Science and Technology 75, 1-12 (1991).

4. A. Liñán and F.A. Williams, Fundamental Aspects of Combustion, Oxford University Press, New York, 1993.

5. J.W. Dold, "Analysis of the Early Stage of Thermal Runaway," Quarterly Journal of Mechanics and Applied Mathematics 38, 361-387 (1985).

6. J.W. Dold, " Analysis of Thermal Runaway in the Ignition Process," SIAM Journal on Applied Mathematics 49, 459-480 (1988).

7. J.W. Dold and A.K. Kapila, "Ignition Theory," Proceedings of the Royal Society of London, to appear, 1993.

5 THE TRIPLE FLAME IN STRAINED LAMINAR MIXING LAYERS

5.1 INTRODUCTION

Laminar flames in turbulent flows are subjected to strain and develop curvature as consequences of the turbulent velocity fluctuations. Effects of both influences, combined with effects of differential diffusion of heat and reactants, cause the inner structure of the flames to respond, thereby leading in some cases to extinction. These phenomena have important implications on the modeling of turbulent reacting flows in the laminar-flamelet regime. To enhance their understanding a detailed knowledge of the laminar-flame structure as a function of various parameters, such as the rate of strain, the radius of curvature, the type of fuel, or the equivalence ratio, as well as its response to variations of these parameters is required. For instance, in turbulent diffusion flames on the flamelet level, so-called "triple flames" may form when after local flamelet extinction due to excessive straining the turbulence intensity decreases to values sufficiently low for re-ignition to take place. It is the purpose of the present work to model such laminar triple flames in turbulent flows.

Effects of strain on the ignition, structure and spread of laminar flames can be investigated in a stagnation-point flow configuration, such as the Tsuji counterflow geometry, in which a fuel stream and an oxidizer stream are directed towards each other. Although a number of theoretical, experimental and computational studies have been devoted to steadily burning premixed, partially premixed and non-premixed laminar counterflow flames, only a few studies have addressed the propagation of laminar flames in mixing layers produced by counterflowing streams of fuel and oxidizer. A photograph of a flame in mixing layer, is given by Phillips[1], for example. The flame structure is composed of an upward bending fuel-rich premixed flame, a downward bending fuel-lean premixed flame, and a trailing streamwise diffusion flame in which are burned the excess fuel and oxidizer not consumed in the upper and lower premixed flames. The region where the two premixed flames and the diffusion flame meet is referred to as a "triple point", and the flame itself as a "triple flame" or "tribrachial flame".

Liñán and Crespo[2] used asymptotic methods to analyze the transient mixing in a boundary layer of two initially separated coflowing streams of fuel and oxidizer, and demonstrated the existence of multiple burning regimes. Also using theoretical methods, Dold[3-6], Buckmaster and Matalon[7] and Wichman[8] carried out analyses of various limiting combustion regimes based on somewhat more general governing equations that were not subjected to the boundary-layer approximation. A numerical analysis of a laminar coflow diffusion flame, established in channels at the trailing edge of a splitter plate separating a fuel stream and an oxidizer stream, was performed by Ramanujam and Tien[9]. With notable exceptions,[5,6] in the above analyses effects of strain were not taken into account.

The intent of the present work is to analyze in more detail diffusion flame spread in a strained mixing layer generated by directing a fuel stream and an oxidizer stream towards each other. Attention is focused on the stagnation region. A general similarity formulation is derived which describes the complex three-dimensional process of flame spread by only two spatial coordinates. To solve the nonlinear governing

similarity equations, a numerical solution procedure based on self-adaptive mesh refinement is developed. For the limiting case in which a thermal-diffusional model results, the numerical procedure is used to calculate the structure of the flame and its burning velocity for various sets of values of parameters such as the strain rate and the air-fuel equivalence ratio.

5.2 THE GOVERNING EQUATIONS IN SIMILARITY FORM

As independent variables the time t and rectangular cartesian space coordinates x, y and z are adopted. Although herein we are interested only in steady phenomena and, therefore, will adopt time-independent boundary conditions, the time-dependent terms are retained in the governing equations to allow a transient approach to the steady solution of the problem. In seeking a similarity formulation, we assume that for all quantities, except the pressure p and the z velocity component w, spatial variations occur only with respect to the x and y direction. Specifically, the velocity field $\mathbf{v} \equiv (u, v, w)$ is assumed to be of the form

$$u = u(t, x, y), \qquad v = v(t, x, y), \qquad w = z\,A(t, x, y), \tag{1}$$

where $A = A(t, x, y)$ is the variable strain rate; the pressure p is taken as

$$p = p_O + p'(t, x, y) - A_O^2 \rho(t, x, y)(\frac{y^2}{2} + \frac{z^2}{2}) \tag{2}$$

where p_O and A_O denote the constant pressure and the constant strain rate, respectively, prevailing at the oxidizer boundary; the functional dependence of temperature and mass fractions is

$$T = T(t, x, y) \quad \text{and} \quad Y_i = Y_i(t, x, y), \tag{3}$$

respectively, $i = 1, \ldots, N$, where N denotes the number of chemical species in the system. Ideal-gas mixtures at low Mach numbers are considered. In particular, the pressure is taken as thermochemically constant with a value equal to p_0; tacitly this assumption has already been introduced in Eq. (2) in assuming that the density ρ is independent of z. Effects of body forces, viscous dissipation and thermal diffusion are neglected; ordinary diffusion is assumed to obey Fick's law with suitably defined diffusion coefficients D_i to be specified below. Thus, in terms of the accumulative-convective-diffusive transport operator

$$\begin{aligned} L(\phi;\Gamma) &\equiv \frac{\partial(\rho\phi)}{\partial t} + \frac{\partial(\rho u\phi)}{\partial x} + \frac{\partial(\rho v\phi)}{\partial y} + \rho\phi A - \frac{\partial}{\partial x}(\Gamma\frac{\partial\phi}{\partial x}) - \frac{\partial}{\partial y}(\Gamma\frac{\partial\phi}{\partial y}) \\ &= \rho\frac{\partial\phi}{\partial t} + \rho u\frac{\partial\phi}{\partial x} + \rho v\frac{\partial\phi}{\partial y} - \frac{\partial}{\partial x}(\Gamma\frac{\partial\phi}{\partial x}) - \frac{\partial}{\partial y}(\Gamma\frac{\partial\phi}{\partial y}), \end{aligned} \tag{4}$$

where ϕ denotes any of the quantities ρ, u, v, A, T or Y_i, the governing equations can be written as

$$L(1\,;1) = 0, \tag{5}$$

$$L(u\,;\mu) = -\frac{\partial p'}{\partial x} + U\,, \tag{6}$$

$$L(v\,;\mu) = -\frac{\partial p'}{\partial y} + \rho A_O^2 y + V, \tag{7}$$

$$L(A\,;\mu) = \rho(A_O^2 - A^2), \tag{8}$$

$$c_p L(T\,;\lambda) = (\nabla T)\sum_{i=1}^{N} c_{pi}(\rho D_i \nabla Y_i) - \sum_{i=1}^{N} h_i w_i, \tag{9}$$

$$L(Y_i\,;\rho D_i) = w_i, \tag{10}$$

$i = 1, \ldots N$. In addition to the quantities already defined, in Eqs. (6) - (10) μ denotes the dynamic viscosity of the mixture, λ its thermal conductivity, and c_p its constant-pressure specific heat capacity; c_{pi}, h_i and w_i denote the constant-pressure specific heat capacity, the specific enthalpy and the mass rate of production, respectively, of species i. The transport coefficients, thermodynamic properties and rates of production are defined as usual; their functional form will be specified below. The terms U and V appearing in the x and y momentum equation, respectively, are given by

$$\begin{aligned} U &= \frac{\mu}{3}\frac{\partial(\nabla\cdot\mathbf{v})}{\partial x} + \frac{\partial\mu}{\partial x}\left(\frac{\partial u}{\partial x} - \frac{2}{3}(\nabla\cdot\mathbf{v})\right) + \frac{\partial\mu}{\partial y}\frac{\partial v}{\partial x}, \\ V &= \frac{\mu}{3}\frac{\partial(\nabla\cdot\mathbf{v})}{\partial y} + \frac{\partial\mu}{\partial y}\left(\frac{\partial v}{\partial y} - \frac{2}{3}(\nabla\cdot\mathbf{v}) + \frac{\partial\mu}{\partial x}\frac{\partial u}{\partial y}\right. \end{aligned} \tag{11}$$

where

$$\nabla\cdot\mathbf{v} = \frac{\partial u}{\partial x} + \frac{\partial v}{\partial y} + A. \tag{12}$$

The simplifications $U = V = 0$ apply in the special case of constant density and constant viscosity.

The system of governing equations (5) - (10) and (13) is closed through the ideal-gas equation of state

$$\frac{p_0}{\rho} = R^0 T \sum_{i=1}^{N}\left(\frac{Y_i}{W_i}\right), \tag{13}$$

where R^0 denotes the universal gas constant and W_i the molecular weight (=molar mass) of species i.

The solution of the problem defined by Eqs. (5) - (10) and (13) requires appropriate boundary conditions to be imposed. At the fuel and oxidizer side, $y = -\infty$ and $y = +\infty$, respectively, the temperature and composition of either stream is specified. The value of the x velocity component u in either stream is equal to the constant but unknown flame speed u_F; u_F is an eigenvalue and must be determined as part of the solution. The y velocity component v in the fuel and oxidizer stream is $v_F = A_F y + a(x)$ and $v_O = A_O y + b(x)$, respectively; here $a(x)$ and $b(x)$ are unknown functions characterizing the flame's displacement due to the heat release; in general, $a(x)$ and $b(x)$ must be determined as part of the solution of the problem. The inviscid flow outside the stagnation region imposes the condition $\rho_O A_O^2 = \rho_F A_F^2$. Sufficiently far upstream ahead of the flame, and sufficiently far downstream behind the flame, the derivatives with respect to x of all dependent variables become negligibly small.

Thus, as boundary conditions at $x = -\infty$ we impose a frozen similarity solution satisfying the governing equations and boundary conditions at $y = \pm\infty$ with $\partial/\partial x = 0$, and at $x = +\infty$ we require zero x derivatives for all dependent variables.

5.3 SIMPLIFICATIONS

Subsequently we assume equal and constant specific heat capacities c_{pi} $(=c_p)$ and equal diffusion coefficients D_i $(=D)$ for all species, and constant a Prandtl and Lewis number of unity. Chemistry is assumed to occur via the global one-step reaction

$$\nu_F F + \nu_O O \rightarrow \nu_P P\,, \tag{14}$$

whose heat of reaction is $q = \nu_P W_P h_P - \nu_F W_F h_F - \nu_O W_O h_O$; here the ν_i and h_i denote the stoichiometric coefficient and (constant) specific enthalpy, respectively, of species i, $i = F, O$ or P. The rate of reaction (14) is assumed to be of the Arrhenius form

$$\omega = (\frac{\rho Y_F}{W_F})(\frac{\rho Y_O}{W_O}) B \exp(-E/R^0 T)\,, \tag{15}$$

where the symbols have their usual meaning. With these specifications the energy and species conservation equations (9) and (10) reduce to

$$L(T\,;\rho D) = -\frac{q}{c_p}\omega\,, \tag{16}$$

$$L(Y_F\,;\rho D) = -\nu_F W_F\,\omega\,, \tag{17}$$

$$L(Y_O\,;\rho D) = -\nu_O W_O\,\omega\,, \tag{18}$$

$$L(Y_P\,;\rho D) = \nu_P W_P\,\omega\,. \tag{19}$$

Note that the mass fraction of an inert species I, which may be present in the system, is given by $Y_I = 1 - Y_F - Y_O - Y_P$. It will be advantageous to introduce a conserved scalar Z,

$$Z = \frac{\frac{Y_F}{Y_{F,F}} s + (1 - \frac{Y_O}{Y_{O,O}})}{s + 1} \tag{20}$$

where

$$s = \frac{\nu_O W_O / Y_{O,O}}{\nu_F W_F / Y_{F,F}} \tag{21}$$

is the *air-fuel* equivalence ratio. The conserved scalar obeys the governing equation

$$L(Z\,;\rho D) = 0\,, \tag{22}$$

which must be solved subject to the upstream boundary condition

$$\begin{aligned} Z &= \frac{I(y)}{I(\infty)}, \\ I(y) &= \int_{-\infty}^{y} \frac{1}{\rho D} \exp\left(\int_{-\infty}^{y'} \frac{\rho u}{\rho D} \mathrm{d}y''\right) \mathrm{d}y', \end{aligned}$$

and subject to $Z \to 0$ as $y \to +\infty$, $Z \to 1$ as $y \to -\infty$ and $\partial Z/\partial x = 0$ as $x \to +\infty$.

We may combine equations (16) and (20) to obtain

$$L(Y_1) = -\nu_F W_F \omega \tag{23.a}$$

$$L(Y_2) = -\nu_O W_O \omega \tag{23.b}$$

where

$$Y_1 \equiv \frac{\nu_F W_F}{q/c_p} T + \phi_F Z + \varphi_F, \tag{24.a}$$

$$Y_2 \equiv \frac{\nu_O W_O}{q/c_p} T + \phi_O Z + \varphi_O \tag{24.b}$$

are coupling functions and ϕ_O, ϕ_F, φ_O, and φ_F are constants to be determined. By virtue of Eqs. (21), and upon requiring that at the boundaries Y_1 and Y_2 be identical to the fuel and the oxidizer mass fraction, respectively, we obtain

$$Y_F = \frac{\nu_F W_F}{q/c_p} [T + Z(T_O - T_F) - T_O] + Z(Y_{F,F} - Y_{F,O}) + Y_{F,O}\,, \tag{25.a}$$

$$Y_O = \frac{\nu_O W_O}{q/c_p} [T + Z(T_O - T_F) - T_O] + Z(Y_{O,F} - Y_{O,O}) + Y_{O,O}\,. \tag{25.b}$$

Upon eliminating Z from Eqs. (23), the coupling function

$$\phi_1 \frac{Y_F - Y_{F,O}}{\nu_F W_F} - \phi_2 \frac{Y_O - Y_{O,O}}{\nu_O W_O} - \frac{T - T_O}{q/c_p} = 0 \tag{26}$$

is obtained, where

$$\phi_1 = \left(\frac{T_O - T_F}{q/c_p} - \frac{Y_{O,O} - Y_{O,F}}{\nu_O W_O} \right) / \left(\frac{Y_{F,F} - Y_{F,O}}{\nu_F W_F} - \frac{Y_{O,O} - Y_{O,F}}{\nu_O W_O} \right), \tag{27.a}$$

$$\phi_2 = \left(\frac{T_O - T_F}{q/c_p} + \frac{Y_{F,F} - Y_{F,O}}{\nu_F W_F} \right) / \left(\frac{Y_{F,F} - Y_{F,O}}{\nu_F W_F} - \frac{Y_{O,O} - Y_{O,F}}{\nu_O W_O} \right), \tag{27.b}$$

Upon introducing the temperature T_f of the trailing diffusion-flame sheet,

$$T_f = T_O - \frac{q}{c_p} \left(\phi_1 \frac{Y_{F,O}}{\nu_F W_F} - \phi_2 \frac{Y_{O,O}}{\nu_O W_O} \right), \tag{28}$$

Eq. (24) can be written as

$$\phi_1 \frac{Y_F - Y_{F,O}}{\nu_F W_F} - \phi_2 \frac{Y_O - Y_{O,O}}{\nu_O W_O} + \frac{T - T_O}{T_f - T_O} \left(\phi_1 \frac{Y_{F,O}}{\nu_F W_F} - \phi_2 \frac{Y_{O,O}}{\nu_O W_O} \right) = 0 \tag{29}$$

5.4 NONDIMENSIONALIZATION

The problem is nondimensionalized by introducing the scaled variables

$$\tilde{t} = t\,A_O\,, \qquad \tilde{x} = x/\sqrt{D_O/A_O}\,, \qquad \tilde{y} = y/\sqrt{D_O/A_O} \tag{30.a}$$

and

$$\begin{aligned} &\tilde{A} = A/A_0, \quad \tilde{u} = u/\sqrt{D_O A_O}, \quad \tilde{v} = v/\sqrt{D_O A_O}, \quad \tilde{p}' = p'/\rho_O A_O D_O, \\ &\tilde{\rho} = \rho/\rho_O, \quad \tilde{Y}_F = Y_F/Y_{F,F}, \quad \tilde{Y}_O = Y_O/Y_{O,O}, \quad \tilde{T} = (T - T_O)/(T_f - T_O) \end{aligned} \tag{30.b}$$

In terms of these variables, the governing equations can be written as

$$\tilde{L}(1\,;1) = 0, \tag{31}$$

$$\tilde{L}(\tilde{u}\,;\tilde{\mu}\,Sc) = -\frac{\partial \tilde{p}'}{\partial \tilde{x}} + \tilde{U}Sc, \tag{32}$$

$$\tilde{L}(\tilde{v}\,;\tilde{\mu}\,Sc) = -\frac{\partial \tilde{p}'}{\partial \tilde{y}} + \tilde{\rho}\tilde{y} + \tilde{V}Sc, \tag{33}$$

$$\tilde{L}(\tilde{A}\,;\tilde{\mu}\,Sc) = \tilde{\rho}(1 - \tilde{A}^2) \tag{34}$$

$$\tilde{L}(\tilde{Y}_F\,;\tilde{\rho}\tilde{D}) = -\delta\beta^4\tilde{\rho}^2\tilde{Y}_F\tilde{Y}_O \exp\left(-\beta(1-\tilde{T})/[1-\alpha(1-\tilde{T})]\right), \tag{35}$$

$$\tilde{L}(\tilde{Z}\,;\tilde{\rho}\tilde{D}) = 0. \tag{36}$$

The boundary conditions are non-dimensionalized analogously. In Eqs. (29) - (34), the diffusion coefficient and dynamic viscosity have been non-dimensionalized with their respective values at the oxidizer side,

$$Sc = \mu_O/(\rho_O D_O) \tag{37}$$

is a Schmidt number,

$$\beta = \frac{E}{R^0 T_f}\frac{T_f - T_O}{T_f} \tag{38}$$

is the Zel'dovich number which is assumed to be large,

$$\alpha = \frac{T_f - T_O}{T_f} \tag{39}$$

a non-dimensional heat-release parameter, and

$$\delta = \frac{\nu_F \rho_O Y_{O,O} B}{A_O W_O}\exp(-E/R^0 T_f)/\beta^4 \tag{40}$$

a Damköhler number. The non-dimensional temperature and density are given by

$$\tilde{T} = 1 - \phi_3\tilde{Y}_F + \phi_4\tilde{Y}_O \tag{41}$$

$$\tilde{\rho} = (1-\alpha)/[1-\alpha(1-\tilde{T})]\,; \tag{42}$$

the non-dimensional oxidizer mass fraction is obtained from Eq. (18), viz.,

$$\tilde{Y}_O = 1 + s\tilde{Y}_F - (s+1)\tilde{Z}\,. \tag{43}$$

The quantities ϕ_3 and ϕ_4 appearing in Eq. (39) are given by

$$\phi_3 = \frac{\phi_1 Y_{F,F}/(\nu_F W_F)}{\phi_1 Y_{F,O}/(\nu_F W_F) + \phi_2 Y_{O,O}/(\nu_O W_O)}, \tag{44}$$

$$\phi_4 = \phi_2 Y_{O,O}/(\nu_O W_O)\phi_1 Y_{F,O}/(\nu_F W_F) + \phi_2 Y_{O,O}/(\nu_O W_O)\,. \tag{45}$$

5.5 THE THERMAL-DIFFUSIONAL MODEL

We now turn to the limiting case of a thermal-diffusional model, i.e., to the case in which $\alpha \rightarrow 0$. In this case we have $\tilde{\rho} = 1$, $\tilde{u} = \tilde{u}_F$, $\tilde{v} = -\tilde{y}$ and $\tilde{A} = 1$. Assuming $\tilde{D} = 1$, the set of governing equations reduces to

$$\tilde{u}_F \frac{\partial \tilde{Y}_F}{\partial \tilde{x}} - \tilde{y} \frac{\partial \tilde{Y}_F}{\partial \tilde{y}} = \frac{\partial^2 \tilde{Y}_F}{\partial \tilde{x}^2} + \frac{\partial^2 \tilde{Y}_F}{\partial \tilde{y}^2} - \delta \beta^4 \tilde{Y}_F \tilde{Y}_O e^{-\beta(1-\tilde{T})}, \tag{46}$$

$$\tilde{u}_F \frac{\partial \tilde{Z}}{\partial \tilde{x}} - \tilde{y} \frac{\partial \tilde{Z}}{\partial \tilde{y}} = \frac{\partial^2 \tilde{Z}}{\partial \tilde{x}^2} + \frac{\partial^2 \tilde{Z}}{\partial \tilde{y}^2}, \tag{47}$$

$$\tilde{T} = 1 - \tilde{Y}_F - \tilde{Y}_O, \tag{48}$$

$$\tilde{Z} = \frac{s\tilde{Y}_F + 1 - \tilde{Y}_O}{s+1}, \tag{49}$$

with the boundary conditions

$$\begin{aligned}
\tilde{y} &\rightarrow -\infty : \tilde{Y}_F = \tilde{Z} = 0, \\
\tilde{y} &\rightarrow +\infty : \tilde{Y}_F = \tilde{Z} = 1, \\
\tilde{x} &\rightarrow -\infty : \tilde{Z} = 1 \leq 2\ s + 1 \leq sY_{F,F} + 1 - Y_{O,O} erfc(\tilde{y}/\sqrt{2}), \\
\tilde{x} &\rightarrow +\infty : \text{zero } x \text{ gradients for all dependent variables.}
\end{aligned} \tag{50}$$

Recall that the non-dimensional flame speed $\tilde{u}_F$ is an eigenvalue which must be determined as part of the solution. The procedure to determine $\tilde{u}_F$ is described in the next section.

5.6 DIFFERENCE EQUATIONS

For ease of notation, in this paragraph the tilde is dropped from the nondimensional variables. Equations (42) and (43) are are used in (40) and (41) to eliminate $\tilde{Y}_O$ and $\tilde{T}$. With respect to the space variables x and y, the two strongly coupled equations (40) and (41) are discretized on a mesh M^n of grid points,

$$\mathrm{M}^n = \{(x_i^n, y_j^n)\ ;\ i = 1, \cdots, N_x^n,\ j = 1, \cdots, N_y^n\}. \tag{51}$$

Here the grid lines x_i^n = constant, $i = 1, \cdots, N_x^n$, and y_j^n = constant, $j = 1, \cdots, N_y^n$, are distributed in a non-equidistant manner using the adaptive-gridding procedure described below. In Eq. (47) and below the superscript n identifies quantities at time level t^n, $n = 0, 1, 2, \cdots$; if possible without ambiguity, for ease of notation this superscript will be omitted. For the first-order derivatives central differences are adopted, e.g. for the x derivative of a scalar dependent variable ϕ at the grid point with the coordinates (x_i, y_j), we write

$$\left(\frac{\partial \phi}{\partial x}\right)_{i,j} \approx \left[\frac{h_{i-1}}{h_i(h_i + h_{i-1})}\phi_{i+1,j} + \frac{h_i - h_{i-1}}{h_i h_{i-1}}\phi_{i,j} - \frac{h_i}{h_{i-1}(h_i + h_{i-1})}\phi_{i-1,j},\right] \tag{52}$$

where $h_i = x_i - x_{i-1}$, $i = 2, \cdots, N_x$. The second-order derivatives at grid point (x_i, y_j), e.g. in the x direction, are approximated by

$$\left(\frac{\partial^2 \phi}{\partial x^2}\right)_{i,j} \approx \frac{2}{h_i + h_{i+1}} \left[\frac{\phi_{i+1,j} - \phi_{i,j}}{h_i} - \frac{\phi_{i,j} - \phi_{i-1,j}}{h_{i-1}}\right]. \tag{53}$$

To bring the initially guessed solution of the problem into the domain of convergence of Newton's method applied to steady-state version of the governing equations, terms involving time derivatives are added to the governing equations. Since we are interested only in steady-state solutions, temporal accuracy of the solution is unimportant and, therefore, the time-derivatives are approximated by simple backward-Euler finite-differences. A fully implicit formulation is employed in order to successfully cope with the stiffness of system (40) - (43) which arises through the chemical source term in Eq. (40).

To determine the burning-rate eigenvalue $\tilde{u}_F$ for a given set of parameters β, δ and s, we first note that since the solution to the governing equations is translational invariant, the condition

$$T = T_{fix} \text{ at } i = i_{fix},\ j = j_{fix} \tag{54}$$

is imposed in order to "anchor" the flame in the computational domain. Secondly we note that the solution to a problem is independent of the the value selected for the temperature T_{fix} and of the location at which the temperature, and hence the flame, is fixed. Herein $T_{fix} = 0.5$ has been selected. The burning-rate eigenvalue is treated as an additional dependent variable that obeys the differential equations

$$\frac{\partial \tilde{u}_F}{\partial x} = \frac{\partial \tilde{u}_F}{\partial y} = 0\,. \tag{55}$$

For ease of notation, sequently the tilde and the subscript F will be dropped from $\tilde{u}_F$. Equations (51) are discretized according to If Newton's method is used to solve the governing equations in terms of the dependent variables $\tilde{Y}_F$, $\tilde{Z}$ and $\tilde{u}_F$, the discretization of these variable as described above leads to a Jacobian matrix with a block-pentadiagonal structure. Further aspects of the numerical approach are described by Rogg.[10]

5.7 RESULTS AND DISCUSSION

Shown in Fig. 3 is the computed burning–rate eigenvalue, i.e., the nondimensional flame speed $\tilde{u}_F$, as a function of the Zel'dovich number β with the Damköhler number δ kept fixed, $\delta = 0.19$. It is seen that for values of β less than approximately 12 $\tilde{u}_F$ depends strongly on β. This strong dependence is the consequence of the so–called "cold–boundary difficulty" [11] which, essentially, consists of a non–vanishing reaction rate at the cold, upstream boundary. Inspection of the r.h.s of Eq. (42) shows that the reaction rate becomes exponentially small for sufficiently large values of β. It is seen from Fig. 3 that for the problem under consideration $\beta > 12$ is sufficiently large.

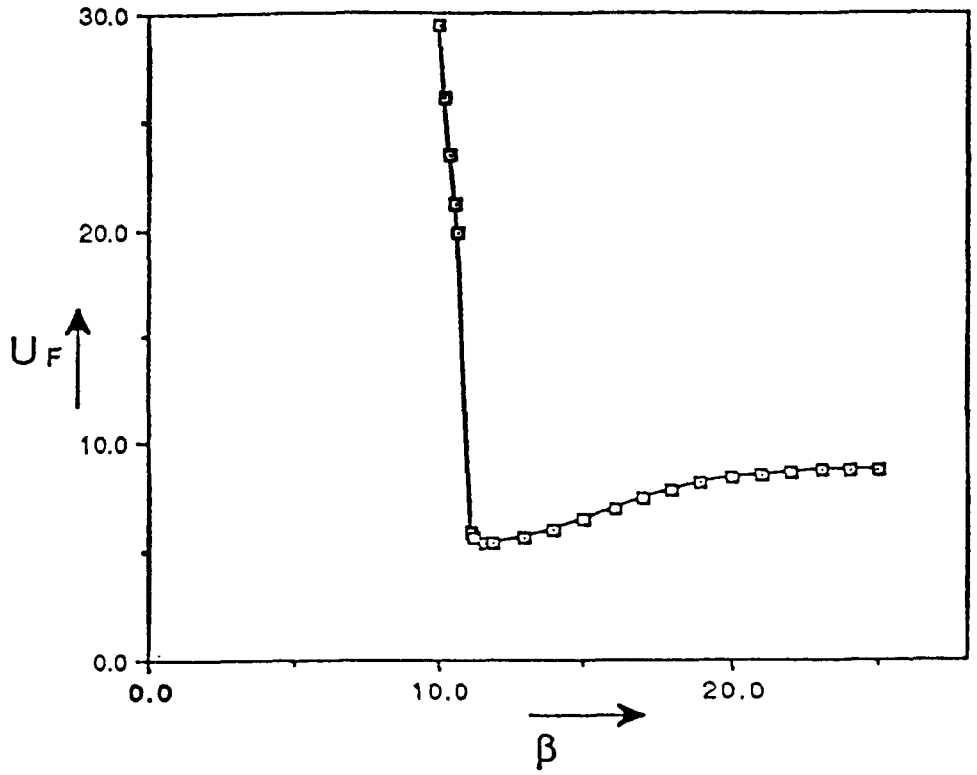

Figure 3: Computed burning-rate eigenvalue $\tilde{u}_f$ as a function of the Zel'dovich number: illustration of the cold-boundary difficulty. The difficulty is present for $\beta < 12$ and overcome for $\beta > 12$.

A value of 12 or greater for β is consistent with values typically used for this quantity in activation–energy asymptotics.

The results presented and discussed below were obtained for $s = 1$, where s is the air–fuel equivalence ratio defined in Eq. (19). Shown in Fig. 4 is the burning-rate eigenvalue $\tilde{u}_F$ as a function of the Damköhler number δ which according to Eq. (38) is proportional to the reciprocal of the rate of strain. Curves for $\beta = 15$ and $\beta = 25$ are shown. It is seen that $\tilde{u}_F$ decreases monotonically with decreasing δ, and for small values of δ becomes negative. The negative flame speed calculated for small values of the Damköhler number is in accordance with observations by Dold et. al[6].

It is also possible to construct contour plots of the nondimensional reaction rate

$$\Omega \equiv \delta \beta^4 \tilde{Y}_F \tilde{Y}_O e^{-\beta(1-\tilde{T})}, \tag{56}$$

the temperature $\tilde{T}$, and fuel mass fraction $\tilde{Y}_F$. In these plots the triple-flame structure is clearly visible: the two backward-bending premixed wings joint in the triple point with the trailing diffusion flame. At the leading edge in the vicinity of the triple point, the thickness of the premixed flames is approximately 0.5 mm; the thickness of the diffusion flame is approximately 0.2 mm. It is noteworthy that, as to be expected on physical grounds, the reaction rate attains its highest value in the triple point and decreases slightly towards the trailing diffusion flame. Many other cases have been obtained and reported by Rogg. [10]

5.8 CONCLUSIONS

The present work has developed a similarity formulation describing diffusion flame spread in strained mixing layers. In particular, the so-called triple-flame geometry has been considered. Rogg developed numerical, self-adaptive methods that are capable of solving the truly two-dimensional governing equations. Using these methods, for the limiting case of the thermal-diffusional model, the structure and speed of the triple flame were computed for various values of the rate of strain. It was found that at large Damköhler numbers, i.e., low rates of strain, the flame structure is indeed that of a triple flame propagating with a relatively large, positive speed. With decreasing rates of strain, the flame speed decreases and the flame structure evolves towards the structure of an ordinary diffusion flame. For sufficiently low rate of strain the propagation velocity of the diffusion flame becomes negative.

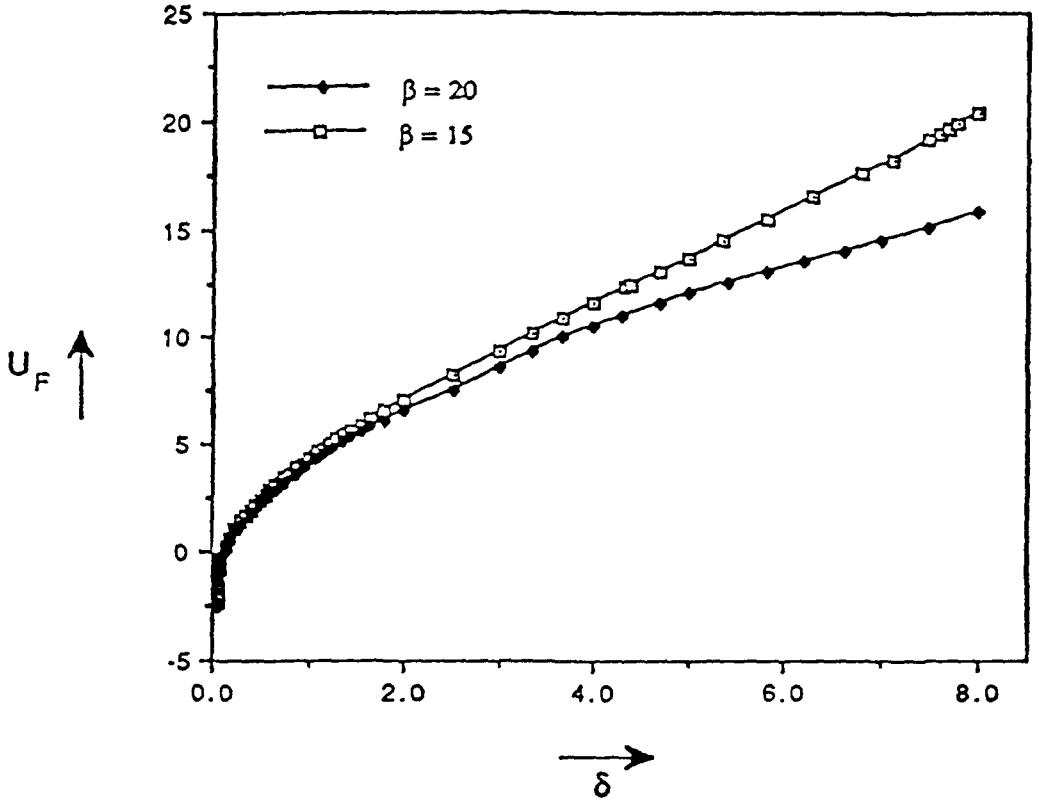

Figure 4: Computed burning-rate eigenvalue $\tilde{u}_f$ as a function of the Damköhler number δ for $\beta = 15$ and $\beta = 20$.

5.9 REFERENCES

1. H. Phillips, "Flame in a Buoyant Methane Layer," Tenth Symposium (International) on Combustion, pp. 1277-1283, The Combustion Institute, Pittsburgh (1965).

2. A. Liñán, A. Crespo, "An Asymptotic Analysis of Unsteady Diffusion Flames for Large Activation Energies," Combustion Science and Technology 14, 95-117 (1976).

3. J.W. Dold, "Flame Propagation in a Nonuniform Mixture: The Structure of Anchored Triple-Flames Flames," in Progress in Astronautics and Aeronautics, Vol. 113, A.L. Kuhl, J.R. Bowen, J.-C. Leyer, A. Borisov, (Eds.), American Institute of Aeronautics and Astronautics, New York, 240-248 (1988).

4. J.W. Dold, "Flame Propagation in a Nonuniform Mixture: Analysis of a Slowly Varying Triple Flame," Combustion and Flame 76, 71-88 (1989).

5. J.W. Dold, "Flame Propagation in a Mixing Layer," Paper presented at the Third International Seminar on Flame Structure, Alma-Ata, Kazakhstan, September 1989, to be published by Nauka (Siberian branch).

6. J.W. Dold, L.J. Hartley, D. Green, "Laminar Triple-Flamelet Structures in Non-premixed Turbulent Combustion," in Dynamical Issues in Combustion Theory, P.C. Fife, A. Liñán and F.A. Williams (Eds.), IMA Volumes in Mathematics and its Applications, Springer-Verlag, in press (1990).

7. J. Buckmaster, M. Matalon, "Anamolous Lewis Number Effects in Tribrachial Flames," Twenty-Second Symposium (International) on Combustion, pp. 1527-1535, The Combustion Institute, Pittsburgh (1988).

8. I. Wichman, "On the Quenching of a Diffusion Flame Near a Cold Wall," Combustion Science and Technology 64, pp. 295-313 (1989).

9. S. Ramanujam, J. S. T'ien, "A Numerical Study of Burke-Schumann Diffusion Flame Blow-Off and Extinction," Paper presented at the Second ASME-JSME Thermal Engineering Joint Conference, Honolulu (Hawaii), March 22-27 (1987).

10. B. Rogg, IDEA Program Report, 1992.

11. F. A. Williams, Combustion Theory, Second Edition, Addison-Wesley, Menlo Park, CA, 1985.

6 ASYMPTOTIC ANALYSES OF n-HEPTANE IGNITION WITH A FOUR-STEP KINETIC MODEL

6.1 INTRODUCTION

There is practical interest in auto-ignition of hydrocarbon fuels in air, for example in connection with Diesel-engine combustion. This has motivated experimental[1-3] and computational[2,4,5] studies of ignition times for model hydrocarbon fuels, as well as for fuel mixtures used in applications. One of the favorite model fuels is n-heptane because its chemical-kinetic behavior is relatively well characterized and similar to that of other alkanes. Recently[5] a four-step approximation to the detailed chemical kinetics has been developed for n-heptane ignition and has been shown to predict ignition times in reasonable agreement with those obtained using full chemistry. This approximation, empirically based but with qualitative motivation from the detailed chemistry, captures the two different types of ignition behaviors found at low and high temperatures in relatively simple Arrhenius expressions suitable for application of activation-energy asymptotics. The present work gives the relevant asymptotic analyses for homogeneous systems and indicates how those analyses may be extended to heterogeneous systems.

6.2 THE CHEMICAL MODEL

The chemical model to be considered in the analysis is[5]

$$F \rightarrow I, \tag{1}$$
$$I + 11O \rightarrow P, \tag{2}$$
$$F + 2O \rightleftharpoons J, \tag{3}$$
$$J + 9O \rightarrow P. \tag{4}$$

Here F stands for the fuel, nC_7H_{16}, O for the oxidizer, O_2, P for the product combination, $7CO_2+8H_2O$, I for one intermediate combination, taken to be $3C_2H_4+CH_3+H$, and J for the other intermediate combination, $OC_7H_{13}O_2H+H_2O$. The first two reactions are most important at higher temperatures, while the third and fourth describe a lower-temperature route. Only the third is reversible, and it has a large activation energy for the reverse step that serves to slow down the low-temperature path at high temperatures.

The rate ω_i of each step i is given by

$$\omega_1 = k_1 n_F \quad , \quad \omega_2 = k_2 n_O n_I, \tag{5}$$
$$\omega_3 = k_{3f} n_O n_F - k_{3b} n_J \quad , \quad \omega_4 = k_4 n_O n_J,$$

where k_i denotes the specific reaction-rate constant for step i (subscripts f and b identifying forward and backward steps 3), and n_j represents the concentration of species j. The first step and the reverse of the third step are unimolecular, while the others are bimolecular.

The Arrhenius forms

$$k_1 = A_1 e^{-T_a/T} \quad , \quad k_2 = A_2 e^{-(T_a/3)/T}, \qquad (6)$$
$$k_{3f} = A_{3f} e^{-T_a/T} \quad , \quad k_{3b} = A_{3b} e^{-T_b/T}, \; k_4 = A_4 e^{-T_c/T}$$

are employed, where the values of the prefactors are

$$A_1 = 2 \times 10^{10} \mathrm{s}^{-1} \quad , \quad A_2 = 2 \times 10^{12} (\mathrm{cm}^3/\mathrm{mol})\mathrm{s}^{-1} \qquad (7)$$
$$A_{3f} = 3 \times 10^{18} (\mathrm{cm}^3/\mathrm{mol})\mathrm{s}^{-1} \quad , \quad A_{3b} = 4 \times 10^{22} \mathrm{s}^{-1}, \; A_4 = 5 \times 10^{13} (\mathrm{cm}^3/\mathrm{mol})\mathrm{s}^{-1},$$

and the activation temperatures are

$$T_a = 21,650\,\mathrm{K}, \; T_b = 37,285\,\mathrm{K}, \; T_c = 13,230\,\mathrm{K}. \qquad (8)$$

The activation energy for the forward third step is the same as that of the first, while that for the second is one third of these. Ignition times for the temperature and pressure ranges $600\,\mathrm{K} \leq T \leq 1500\,\mathrm{K}$ and $1\,\mathrm{atm} \leq p \leq 40\,\mathrm{atm}$, obtained by numerical integrations with these rate parameters, compare quite favorably with those found from numerical integrations with full kinetics and from experiment.[5]

6.3 THERMODYNAMIC APPROXIMATIONS

The calculations that produced the ignition-time agreement also required thermodynamic data. Isobaric conditions were considered, with a constant average molecular weight and a constant molar heat capacity at constant pressure of 34.8 J/mol K, representative of the fuel-air mixtures under the conditions of interest. The heat released in each step i was characterized by a temperature rise T_i, defined as the ratio of the enthalpy change of that step to the molar heat capacity. The values obtained,

$$T_1 = -20,400\,\mathrm{K}, \; T_2 = 149,800\,\mathrm{K}, \; T_3 = 1,550\,\mathrm{K}, \; T_4 = 127,850\,\mathrm{K}, \qquad (9)$$

obey the thermodynamically required summation relation

$$T_1 + T_2 = T_3 + T_4 = 129,400\,\mathrm{K}. \qquad (10)$$

These same values are employed herein.

6.4 CONSERVATION EQUATIONS

The equations for species and energy conservation may be written as[6]

$$\rho\left(\frac{\partial X_j}{\partial t} + \mathbf{v}\cdot\nabla X_j\right) = \frac{1}{L_j}\nabla\cdot\left(\frac{\lambda}{c_p}\nabla X_j\right) + w_j, \; j = F, I, J, O, P \qquad (11)$$

and

$$\rho\left(\frac{\partial T}{\partial t} + \mathbf{v}\cdot\nabla T\right) = \nabla\cdot\left(\frac{\lambda}{c_p}\nabla T\right) + \frac{1}{c_p}\frac{dp}{dt} + w_T, \qquad (12)$$

under the present assumptions, where ρ is density and $\mathbf{v}$ velocity, $X_j = n_j/n$ denotes the mole fraction of species j, L_j its Lewis number (assumed constant) and w_j its

molar rate of production times the mean molecular weight $\overline{W}$, and p, λ and c_p are pressure, thermal conductivity and the specific heat at constant pressure, respectively. The ideal gas equation of state,

$$\rho = p\overline{W}/(R^{\circ}T) \equiv \overline{W}n \tag{13}$$

(with R° the universal gas constant) is employed. The source terms, under the present approximations, are

$$\begin{aligned} w_F = \overline{W}(-\omega_1 - \omega_3) \quad &, \quad w_I = \overline{W}(\omega_1 - \omega_2), \quad w_J = \overline{W}(\omega_3 - \omega_4), \\ w_O = \overline{W}(-11\omega_2 - 2\omega_3 - 9\omega_4) \quad &, \quad w_p = \overline{W}(\omega_2 + \omega_4), \end{aligned} \tag{14}$$

with ω_i given by Eq.(5), in which $n_j = X_j n$. In the energy conservation,

$$w_T = \overline{W}(T_1\omega_1 + T_2\omega_2 + T_3\omega_3 + T_4\omega_4). \tag{15}$$

Mass and momentum conservation complement Eqs. (11) and (12). Additional approximations appearing here are the Fick and Fourier laws, the assumption of negligible local radiant energy loss in the differential equation for energy conservation and the assumption of low Mach number, which allows p to be treated solely as a function of t.

6.5 TIME-DEPENDENT, STRAINED MIXING LAYERS

Before specializing to homogeneous, isobaric conditions, it is of interest to formulate the problem for unsteady mixing layers with strain. Following earlier work[7] the mass and tangential-momentum conservation equations for such problems can be written as

$$\partial\rho/\partial t + \partial(\rho v)/\partial x + \rho a = 0 \tag{16}$$

and

$$\rho\left(\frac{\partial a}{\partial t} + v\frac{\partial a}{\partial x} + a^2\right) = \rho_O\left(\frac{da_O}{dt} + a_O^2\right) + Pr\frac{\partial}{\partial x}\left(\frac{\lambda}{c_p}\frac{\partial a}{\partial x}\right), \tag{17}$$

where x is the coordinate normal to the mixing layer, v the component of velocity in the x direction, a the strain rate and Pr the Prandtl number (assumed constant). Here the subscript O denotes evaluation of a quantity in the oxidizer stream, and the subscript F will denote evaluation in the fuel stream. The tangential component of velocity is the product of $a(x,t)$ with the tangential distance from the plane of symmetry. The normal component of the equation for conservation of momentum is not written here because it serves only to determine the small variation of pressure in the direction normal to the mixing layer.

In this problem Eqs. (11) and (12) are simplified because changes in X_j and T in the direction parallel to the mixing layer are small and can be neglected. Ignition often will occur near the oxidizer stream, where Eq. (16) can be integrated with respect to x to give

$$v = -\left[a_O + d(ln\rho_O)/dt\right]x \equiv -Ax, \tag{18}$$

in which the origin of the x coordinate has been taken to be the position of zero normal velocity, extrapolated from the velocity profile in the oxidizer stream. If,

further, λ/c_p is approximated as constant in the region of interest, then Eqs. (11) and (12) become

$$\partial X_j/\partial t - Ax\partial X_j/\partial x - (D_T/L_j)\partial^2 X_j/\partial x^2 = W_j\,,\ j = F, I, J, O, P \tag{19}$$

and

$$\partial T/\partial t - Ax\partial T/\partial x - D_T\partial^2 T/\partial x^2 = [(\gamma-1)/\gamma]\,T d(lnp)dt + W_T, \tag{20}$$

where the thermal diffusivity is

$$D_T = \lambda/(\rho c_p), \tag{21}$$

the ratio of specific heats is

$$\gamma = c_p/\left[c_p - (R^o/\overline{W})\right], \tag{22}$$

and the source terms are

$$W_F = -k_1 X_F - k_{3f} n X_O X_F + k_{3b} X_J, \tag{23}$$

$$W_I = k_1 X_F - k_2 n X_O X_I, \tag{24}$$

$$W_J = k_{3f} n X_O X_F - k_{3b} X_J - k_4 n X_O X_J, \tag{25}$$

$$W_O = -11 k_2 n X_O X_I - 2k_{3f} n X_O X_F + 2k_{3b} X_J - 9k_4 n X_O X_J, \tag{26}$$

$$W_P = k_2 n X_O X_I + k_4 n X_O X_J, \tag{27}$$

$$W_T = T_1 k_1 X_F + T_2 k_2 n X_O X_I + T_3(k_{3f} n X_O X_F - k_{3b} X_J) + T_4 k_4 n X_O X_J. \tag{28}$$

Under these approximations, Eqs. (19) and (20) can be addressed without further reference to Eqs. (16) and (17); the functions $A(t)$ and $p(t)$ are treated as being prescribed in advance.

Initial and boundary conditions are needed to define a well-posed problem. The initial temperature and mole-fraction profiles must be specified,

$$X_j(x,0) = X_{jo}(x),\ \ T(x,0) = T_o(x). \tag{29}$$

Normally $X_{Io}(x) = X_{Jo}(x) = X_{Po}(x) = 0$, so that only the functions $X_{Fo}(x)$ and $X_{Oo}(x)$ arise in the initial concentration profiles. The boundary values given in the fuel and oxidizer streams are

$$X_j = X_{jF}(t)\ ,\ T = T_F(t) \tag{30}$$

and

$$X_j = X_{jO}(t)\ ,\ T = T_O(t), \tag{31}$$

respectively. Normally $X_{jF}(t) = 0$ for $j \neq F, X_{jO}(t) = 0$ for $j \neq 0$, and $X_{FF}(t)$, $X_{OO}(t)$, $T_F(t)$ and $T_O(t)$ are specified constants, independent of t.

6.6 SIMPLIFIED PROBLEMS

The formulation completed above enables a number of different problems to be addressed. One is the problem of the steady, strained mixing layer, obtained by putting $\partial/\partial t = 0$ and $d/dt = 0$ and by deleting the initial conditions of Eq. (29). Another is the problem of the unsteady, unstrained, constant-pressure mixing layer, obtained by putting $A = 0$ and $dp/dt = 0$. A third is the homogeneous ignition problem with variable pressure, obtained by putting $\partial/\partial x = 0$ and by deleting the boundary conditions in Eqs. (30) and (31). The simplest problem is the homogeneous, constant-pressure ignition problem, obtained from the third problem by putting $dp/dt = 0$ as well. The solution to this problem, addressed previously,[5] needs to be discussed first, because it serves to expose the influences of the chemical kinetics specific to n-heptane and thereby provides information required in addressing the more complicated problems. This problem is defined by Eqs. (23) through (29) with

$$dX_j/dt = W_j \ , \ j = F, I, J, O, P, T, \tag{32}$$

where $X_T \equiv T$.

6.7 CHEMICAL TIMES

Characteristic reciprocal times can be defined for each step and plotted as functions of temperature by use of Eqs. (6), (7) and (8). To address ignitions in air, it is best to include the initial oxygen mole fraction X_{O_o} in the definitions of these times, so that the relevant reciprocal times become $k_1, k_2 n X_{O_o}$, $k_{3f} n X_{O_o}, k_{3b}$ and $k_4 n X_{O_o}$. Figure 5 shows these times as solid lines for an initially stoichiometric mixture ($X_{F_o} = 0.0187, X_{O_o} = 0.2061$) at $p = 40\,\text{atm}$. In Fig. 5, the factor n is proportional to pressure p.

Relatively small temperature changes are seen in Fig. 5 to lead to large changes in ratios of the characteristic times. This produces corresponding changes in ignition regimes with changing temperature. These changes can be discussed by investigating isothermal concentration histories at different temperatures.

6.8 ISOTHERMAL CONCENTRATION HISTORIES

Different regimes of isothermal chemistry arise in different temperature ranges. It is convenient to address these regimes beginning at the lowest temperature and proceeding to the highest.

6.8.1 $T < T_-$

Although Fig. 5 shows step 2 to have the highest rate constant at the lowest temperatures, this is irrelevant because step 2 cannot occur until the intermediate I is produced by step 1, and the rate of step 1 is negligible there because k_1 is extremely small. Therefore, only steps 3 and 4 influence the rate. At the lowest temperature, the rate constant for step 4 is seen in Fig. 5 to be high enough that during an initial

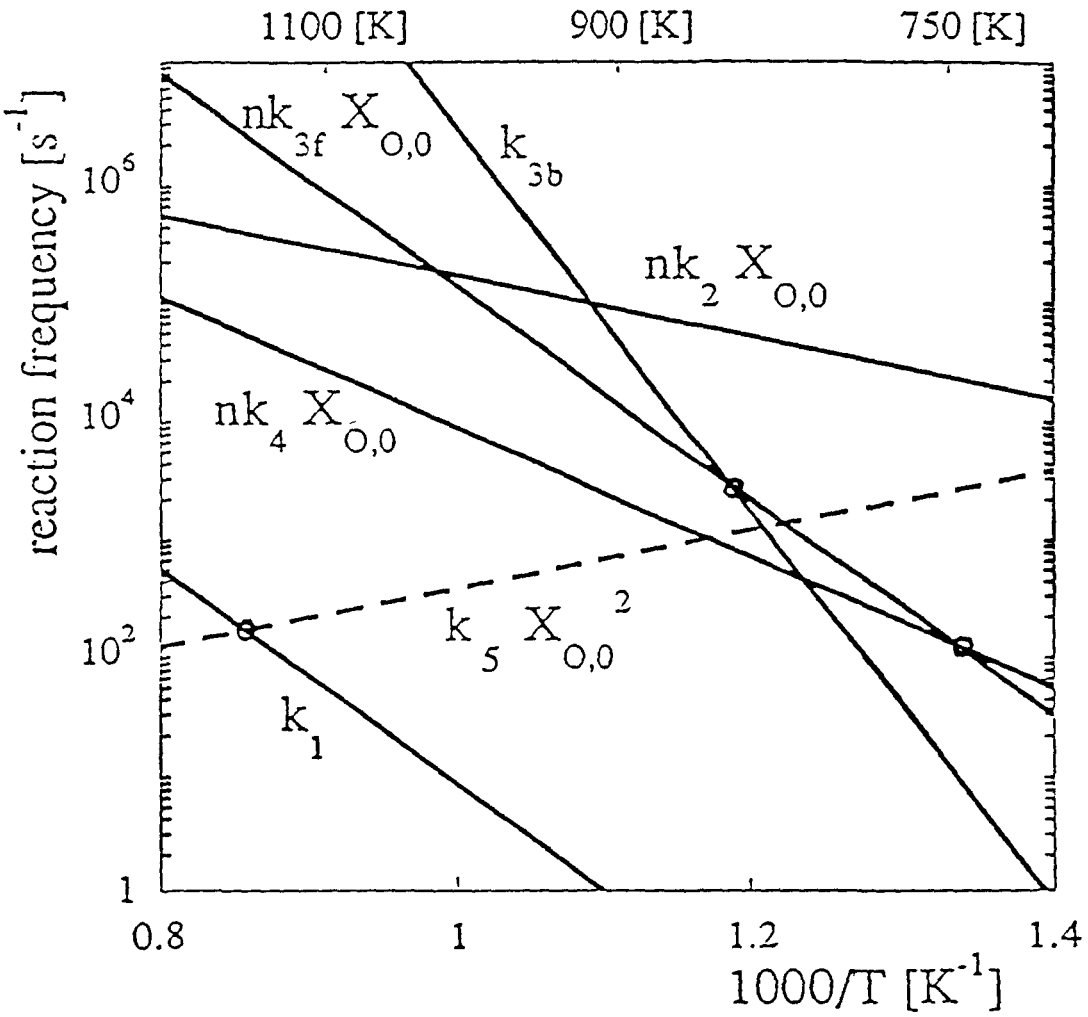

Figure 5: An Arrhenius plot of the reciprocal times for the different reaction steps.

stage the intermediate J may be anticipated to rapidly achieve a steady state, yielding from Eq. (25)

$$X_J = (k_{3f}/k_4)X_F, \tag{33}$$

since step 3 is seen from Fig. 5 to be very slow in this regime. Equation (32) readily gives

$$X_O = X_{Oo} - 11(X_{Fo} - X_F) \tag{34}$$

and

$$dX_F/dt = -k_{3f}nX_OX_F, \tag{35}$$

which may easily be integrated. This regime ends when T becomes large enough that the rate of step 4 is no longer large enough compared with the forward rate of step 3 for J to maintain its steady state,

$$k_{3f}(T_-) = k_4(T_-), \tag{36}$$

the crossover point of the k_{3f} and k_4 curves in Fig. 5, about 750 K. At temperatures above this value, Eq. (33) in inapplicable because it gives $X_J > X_F$.

6.8.2 $T_- < T < T_t$

For temperatures somewhat above T_- step 4 is slow enough to allow the concentration of the intermediate J to increase above that of the fuel. There are then two stages, an initial stage in which step 4 can be neglected and only step 3 is important, followed by a second stage, of longer duration, in which step 4 must be considered as well. If the reverse of step 3 were negligible, then fuel would be converted completely to the intermediate J in the initial stage, while J would be converted to product in the second stage. Figure 5 indicates that in fact the reverse of step 3 is not negligibly slow in this regime, so that in the initial stage the fuel mole fraction is reduced to its partial-equilibrium value

$$X_F = X_Jk_{3b}/(k_{3f}nX_O), \tag{37}$$

and the fuel-intermediate pool, with effective mole fraction $X_K = X_F + X_J$, is converted to products in the second stage. The oxygen balance leads to

$$X_O = X_{Oo} + 9(X_K - X_{Fo}) - 2(X_{Fo} - X_F), \tag{38}$$

which with Eq. (37) enables the relevant mole fractions to be expressed in terms of X_K. The general differential equation for the second stage is

$$dX_K/dt = -k_4nX_OX_J. \tag{39}$$

In view of Fig. 5, Eq. (37) shows that near T_- the value of X_F is small compared with X_J, so that $X_K \approx X_J$ and $X_O \approx X_{Oo} + 9X_J - 11X_{Fo}$, and Eq. (39) is again readily integrated analytically subject to $X_J = X_{Fo}$ at $t = 0$ for the second stage. This solution will continue to apply up to a transition temperature T_t defined by crossover of the forward and backward rates of step 3,

$$k_{3b}(T_t) = (nX_O)k_{3f}(T_t), \tag{40}$$

about 850 K in Fig. 5. For $T > T_t$ Eq. (37) indicates that $X_J < X_F$, that is, a steady state for the intermediate J again becomes valid, now because it is consumed sufficiently rapidly by the reverse of step 3, rather than by step 4.

6.8.3 $T_t < T < T_+$

When the steady state applies for the intermediate J as a consequence of the forward and backward steps 3 being fast, Eq. (37) give $X_J < X_F$, so that the approximation $X_K = X_F$ may be employed, and Eq. (39) for the second stage becomes

$$dX_F/dt = -k_4 K_3 n^2 X_O^2 X_F, \tag{41}$$

where $K_3 = k_{3f}/k_{3b}$ is the equilibrium constant for step 3. Equation (38) indicates that, in Eq. (41), Eq. (34) may again be used as a simplification for X_O. Since Eqs. (6) and (8) show that the effective activation temperature in this regime is $T_c + T_a - T_b = -2405$ K, a negative value, the reaction rate here decreases with increasing temperature. This is a consequence of the decrease in the steady-state concentration of the intermediate J, which is a reactant in the controlling step 4. The effective rate constant for Eq. (41) will be denoted by

$$k_5 = k_4 K_3 n^2 \tag{42}$$

The dashed line in Fig. 5 shows $k_5 X_{O_o}^2$ in the Arrhenius graph.

As yet, steps 1 and 2 have not played any role in the kinetics because the rate of step 1, the essential initial step for these two processes to occur, has been too small. The decrease in the rate of fuel consumption in the second stage with increasing temperature according to Eq. (41) eventually results in the rate of fuel consumption by step 1 becoming comparable with that through steps 3 and 4. Equality of these two rates occurs at the crossover temperature T_+, defined by

$$k_1(T_+) = X_O^2 k_5(T_+) \tag{43}$$

and seen from Fig. 5 to be about 1150 K. Above this temperature, it is no longer permissible to neglect steps 1 and 2.

6.8.4 $T > T_+$

For $T > T_+$ there is an initial stage in which the fuel consumption occurs rapidly by step 3. This process produces partial equilibrium of step 3 in the very short time k_{3b}^{-1}, while a second stage begins, in which the dominant fuel consumption occurs through step 1. Since Fig. 5 shows that the rate constant for step 2 exceeds that for step 1, for this second stage there is a short transition stage in which the concentration of the intermediate I quickly increases to its steady-state value,

$$X_I = (k_1/k_2) X_F/(n X_O). \tag{44}$$

Subsequently, the rate of step 1 dominates both the rate of removal of fuel and the rate of production of products, giving the overall one-step reaction $F + 11O \rightarrow P$ (applicable in fact in all second stages, except that for $T_- < T < T_t$, for which the reaction is $J + 9O \rightarrow P$) with the differential equation

$$dX_F/dt = -k_1 X_F. \tag{45}$$

6.9 ESTIMATES OF HOMOGENEOUS, ISOBARIC IGNITION TIMES

Explosion theory may be used to estimate ignition times on the basis of the chemical-kinetic histories discussed above. It is relevant to observe at the outset, from Eqs. (1)-(4), that the chemical mechanism can be no more complicated than a straight-chain process and that therefore branched-chain explosions cannot occur in this model. The theory of thermal explosions therefore provides the only candidate for obtaining simple estimates of ignition times. According to this theory,[6,8] for a one-step, Arrhenius process releasing the amount of energy $c_p\overline{W}T_Q$ per mole of fuel consumed, the ignition time is

$$t_{ign} = T_o^2/(T_Q T_A k_o X_{Fo}), \tag{46}$$

where T_A is the activation temperature associated with the heat release, and k_o is the effective first-order specific reaction-rate constant at the initial temperature T_o. This formula arises by defining the ignition time as the time required for T to increase by an amount T_o^2/T_A. It is of interest to apply Eq. (46) to each of the four regimes just identified.

6.9.1 $\underline{T_o < T_-}$

In this regime, Eqs. (28) and (32) readily give

$$dT/dt = (T_3 + T_4)k_3 n X_O X_F = -(T_3 + T_4)dX_F/dt, \tag{47}$$

where Eq. (35) has been employed in the last equality. For this one-step process, Eqs. (6), (8) and (10) imply that $T_Q = 129,400$ K and $T_A = 21,650$ K, and $k_o = k_{3fo} n_o X_{Oo}$ in Eq. (46). The overall activation energy for t_{ign}^{-1} in this regime is about 45 cal/mole.

This simple reasoning is based on the presumption that ignition occurs in the second stage, rather than in the initial stage of radical buildup – a presumption motivated by observing from Eq. (9) that the heat release associated with fuel consumption (described by T_3) is negligible compared with that associated with the intermediate consumption (described by T_4). It is necessary, however, to test whether sufficient intermediate consumption may occur during its buildup to cause ignition. For this purpose, the buildup time

$$t_{build} \approx X_J/(k_{3f} n X_O X_F) \approx (k_4 n X_O)_o^{-1} \tag{48}$$

may be compared with the ignition time obtained above. The criterion $t_{build} \ll t_{ign}$ is then found to be $k_{3f}/k_4 \ll T_o^2/(T_Q T_A X_{Fo})$, which is satisfied only at very low temperatures. At higher temperatures, Eqs. (28) and (32) give, approximately,

$$dT/dt = T_4 k_4 n X_O X_J, \tag{49}$$

since T_3 is negligibly small, and coupled with the approximation

$$dX_J/dt = k_{3f} n X_O X_F, \tag{50}$$

from Eqs. (25) and (32), results in the order-of-magnitude estimate $\Delta T/t_{ign} = T_4 k_4 n X_O (k_{3f} n X_O X_F t_{ign})$, which with $\Delta T = T_o^2/T_A$ produces

$$t_{ign} = T_o (T_4 T_A)^{-1/2} (k_{3fo} k_{4o})^{-1/2} (n_o X_{Oo})^{-1} X_{Fo}^{-1/2}, \tag{51}$$

in which $T_A = (T_a + T_c)/2 = 17,440$ K, from Eqs. (6) and (8). The consequent lower activation energy, of about 35 kcal/mol, will be more representative of most of this regime. A gradual transition from Eq. (46) to Eq. (51) with increasing temperature in this regime may be anticipated, although as an approximation a sharp transition from the higher to the lower activation energy may be presumed to occur when T_o increases through a critical value T_* at which the two ignition times are equal. The value of T_* is then defined by

$$k_{3f}(T_*) = \frac{T_*^2 T_4 (T_a + T_c)}{2 X_{Fo} (T_3 + T_4)^2 T_a^2} k_4(T_*), \tag{52}$$

which falls within this regime but below 600 K, the low-temperature limit for the validity of the kinetic-model correlation.

6.9.2 $T_- < T_o < T_t$

The estimate in Eq. (51) equally applies in this regime in the vicinity of $T_o = T_-$. In the estimate in Eq. (48) for the duration of the initial stage, Eq. (37) must now be employed in place of Eq. (33) in deriving the last equality, and the revised result is $t_{build} \approx k_{3bo}^{-1}$, so that Eq. (51) holds when it gives $t_{ign} \ll k_{3bo}^{-1}$. Otherwise, the second stage is entered prior to ignition, and Eqs. (28) and (32) with T_3 neglected give

$$dT/dt = T_4 k_4 n X_O X_J = -T_4 dX_J/dt, \tag{53}$$

where Eq. (39) was used in the second equality; the resulting one-step process conforms with Eq. (46) with $T_Q = T_4 = 127,850$ K, $T_A = T_c = 13,230$ K, and $k_o = k_{4o} n_o X_{Oo}$, yielding an overall activation energy of about 28 kcal/mol. This last result requires $k_{4o} n_o X_{Oo}/k_{3bo} \ll T_o^2/(T_4 T_c X_{Fo})$ for its validity, which improves with increasing T_o. The activation energy may thus be expected to continue to decrease with increasing temperature in this regime, although as an approximation Eq. (51) may be considered to hold below a critical temperature T_s and Eq. (46) above, where T_s is again defined by equality of the two ignition times,

$$k_4(T_s) = \frac{T_s^2 (T_a + T_c)}{2 X_{Fo} T_4 T_c^2} k_3(T_s). \tag{54}$$

Numerically, the resulting T_s typically exceeds T_t, so that this transition is not observed, mainly because this regime itself is too narrow to be distinguished very clearly, as may be seen in Fig. 5. The partial equilibrium of step 3 is not well established in this regime, and Eq. (51) typically may be used throughout the regime.

6.9.3 $\underline{T_t < T_o < T_+}$

In this regime, Eqs. (28) and (32) with T_3 neglected produce

$$dT/dt = -T_4 dX_F/dt, \tag{55}$$

with dX_F/dt given by Eq. (41). The negative activation energy, indicated after Eq. (41), implies then that a thermal explosion in fact cannot occur in this regime. The reaction rate will decrease with increasing temperature, until the temperature reaches T_+ and the high-temperature path through steps 1 and 2 begins, exhibiting a positive activation energy. The time required for this to occur may be roughly estimated from Eqs. (41) and (55) to be

$$t_{delay} = (T_+ - T_o)/(T_4 X_{Fo} k_{5o} X_{Oo}^2), \tag{56}$$

where k_5 is defined in Eq. (42) and shown in Fig. 5. This delay time will provide the major contribution to the ignition time if it is large compared with the ignition time of the regime in which $T > T_+$, as it indeed is, except when T_o approaches T_+ to within about 50 K. Away from this limit, Eq. (56) gives an activation energy for the ignition time of about -5 kcal/mol. When $T_s > T_t$, there is a critical initial temperature T_r at which t_{delay} of Eq. (56) equals t_{ign} of Eq. (51), and above this temperature it will be better to employ Eq. (56) than Eq. (51). This temperature, defined by

$$(n_o X_{Oo})^2 k_{3f}(T_r) k_4(T_r) = \frac{(T_+ - T_r)^2 (T_a + T_c)}{2 X_{Fo} T_4 T_r^2} k_{3b}^2(T_r), \tag{57}$$

typically lies near T_t and within the present regime.

Especially in this regime, ignition times may be expected to be strongly dependent on the particular definition of ignition that is adopted. For example, a full-chemistry calculation employing a critical radical concentration level to define ignition may give times quite different from those based on attainment of a specified temperature rise, and these, in turn, may differ from times based on an eventual thermal runaway. The present estimates are geared to thermal runaway. Figure 6 illustrates representative temperature histories in different regimes.

6.9.4 $\underline{T_o > T_+}$

In this high-temperature regime, the early stages are nearly energetically neutral according to Eq. (9), so ignition may be expected to occur after the steady state of Eq. (44) is established, as may be verified *a posteriori* by comparing the ignition time with the relevant times k_{3b}^{-1} and $(nk_2 X_O)^{-1}$. Equations (28), (32) and (45) show that

$$dT/dt = -(T_1 + T_2) dX_F/dt, \tag{58}$$

to be used with Eq. (45). The ignition time is then given by Eq. (46), with the substitutions
$k_o = k_{1o}, T_Q = T_1 + T_2$ and $T_A = T_a$. The transition between Eq. (56) and this result may be estimated to occur at an initial temperature T^* obtained by equating ignition times,

$$k_{3b}(T^*) k_1(T^*) = \frac{(T_+ - T_r)(T_3 + T_4) T_a}{T^{*2} T_4} (n_o X_{Oo})^2 k_{3f}(T^*) k_4(T^*), \tag{59}$$

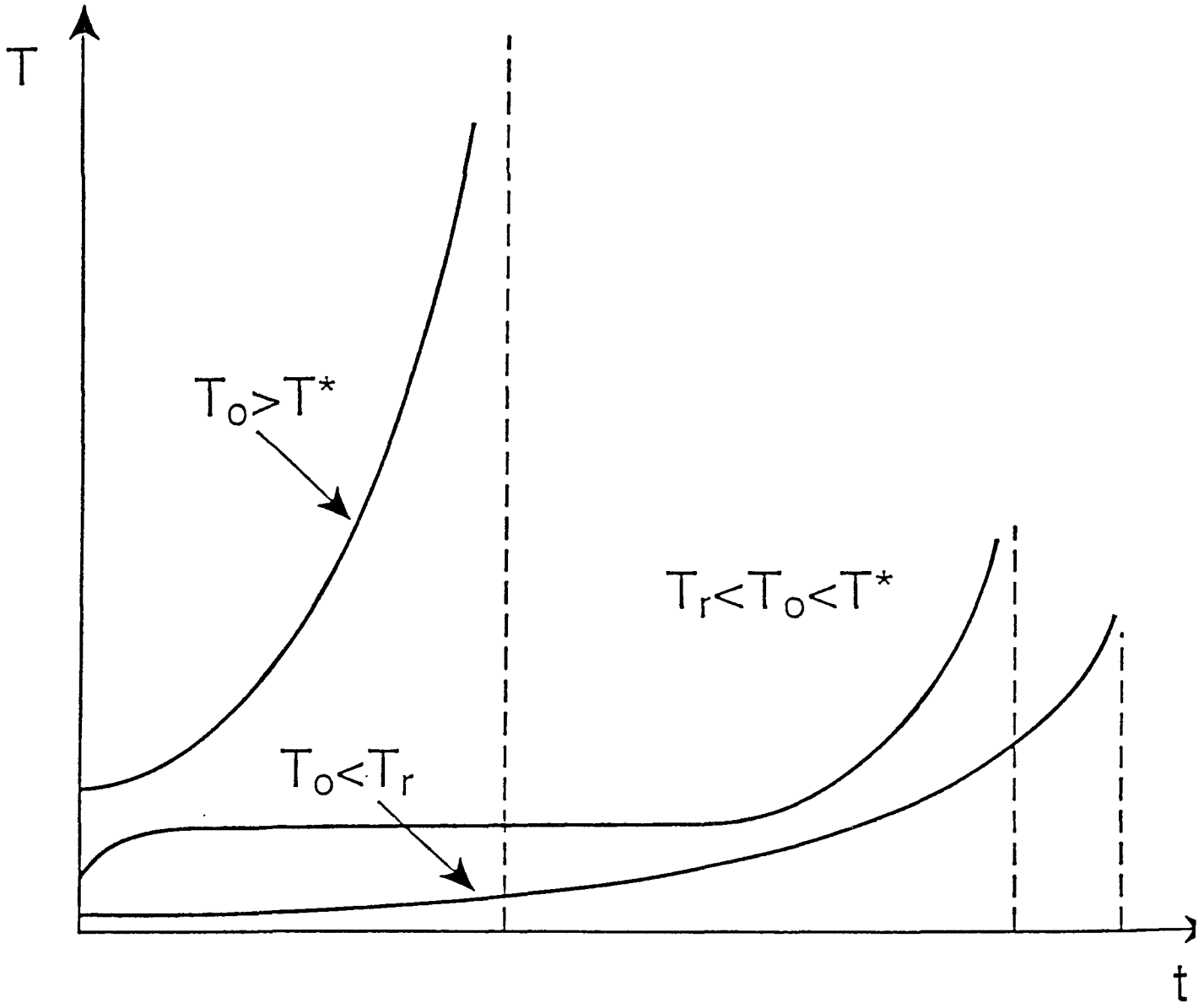

Figure 6: A schematic illustration of temperature-time histories during ignition in different regimes.

giving T^* close to T_+. The activation energy for t_{ign} in this regime is about 45 kcal/mol. Figure 5 suggests that at higher temperatures the activation energy will decrease again because nk_2X_O will become too small, but this occurs well above 1500 K, outside the range of the correlation.

6.10 ACTIVATION-ENERGY ASYMPTOTICS FOR HOMOGENEOUS, ISOBARIC IGNITION

The solid straight lines in Fig. 7 illustrate the reciprocal ignition times obtained in the previous section. Improved results can be derived through a formal application of activation-energy asymptotics. Such analyses and their results have been reported previously.[5] Efficiencies of the analyses are aided by including more than one of the preceding regimes in a common formulation. Thus, a single low-temperature regime, extending up to a temperature T_o of about 900 K, and a single high-temperature regime, extending down to about 900 K, are considered separately. In the low-temperature regime, steps 1 and 2 are ignored, but steps 3 and 4 are included completely, without any approximation of a steady state for the intermediate J or of partial equilibrium for step 3. In the high-temperature regime, all four steps are included, but steady-state approximations are employed for both intermediates, I and J. As a consequence, there are, in effect, two sequential reactions in the low-temperature regime and two parallel reactions in the high-temperature regime. The changing relative importance of the different steps with changing T_o causes the smooth variations illustrated by the dashed curves in Fig. 7. The agreement with results of numerical integrations for the model chemistry are good, except the regime $T_t < T_o < T_+$ (roughly between 800 K and 1100 K), where the predictions are most sensitive to the particular ignition criterion employed. Although the numerical integrations with the four-step model chemistry have not shown a reversal in the intermediate range giving rise to an increase in t_{ign} with increasing T_o, both experiment and numerical integrations with full chemistry do show such a reversal, in qualitative agreement with the asymptotic predictions for the four-step model.

6.11 EFFECTS OF DEPARTURES FROM HOMOGENEITY AND ISOBARICITY

The simplifications identified above for different regimes help to simplify analyses of ignition behavior under more complex conditions. It has been seen that it is never necessary to consider more than two steps in obtaining good qualitative descriptions, and at high temperatures (or at very low temperatures) one-step approximations suffice. The effects of pressure changes for one-step, Arrhenius chemistry have previously been clarified in homogeneous systems;[9] by introducing the entropy variable $T/p^{(\gamma-1)/\gamma}$, a formulation like that for isobaric ignition is recovered, and the ignition enhancement through the temperature increase produced by a pressure increase is automatically included.[10] Slow rates of pressure increase in systems starting at low temperatures, such that the characteristic time for pressure change is long compared with ignition times in low-temperature regimes, allows the ignition process to be described by the preceding results for low-temperature ignition.

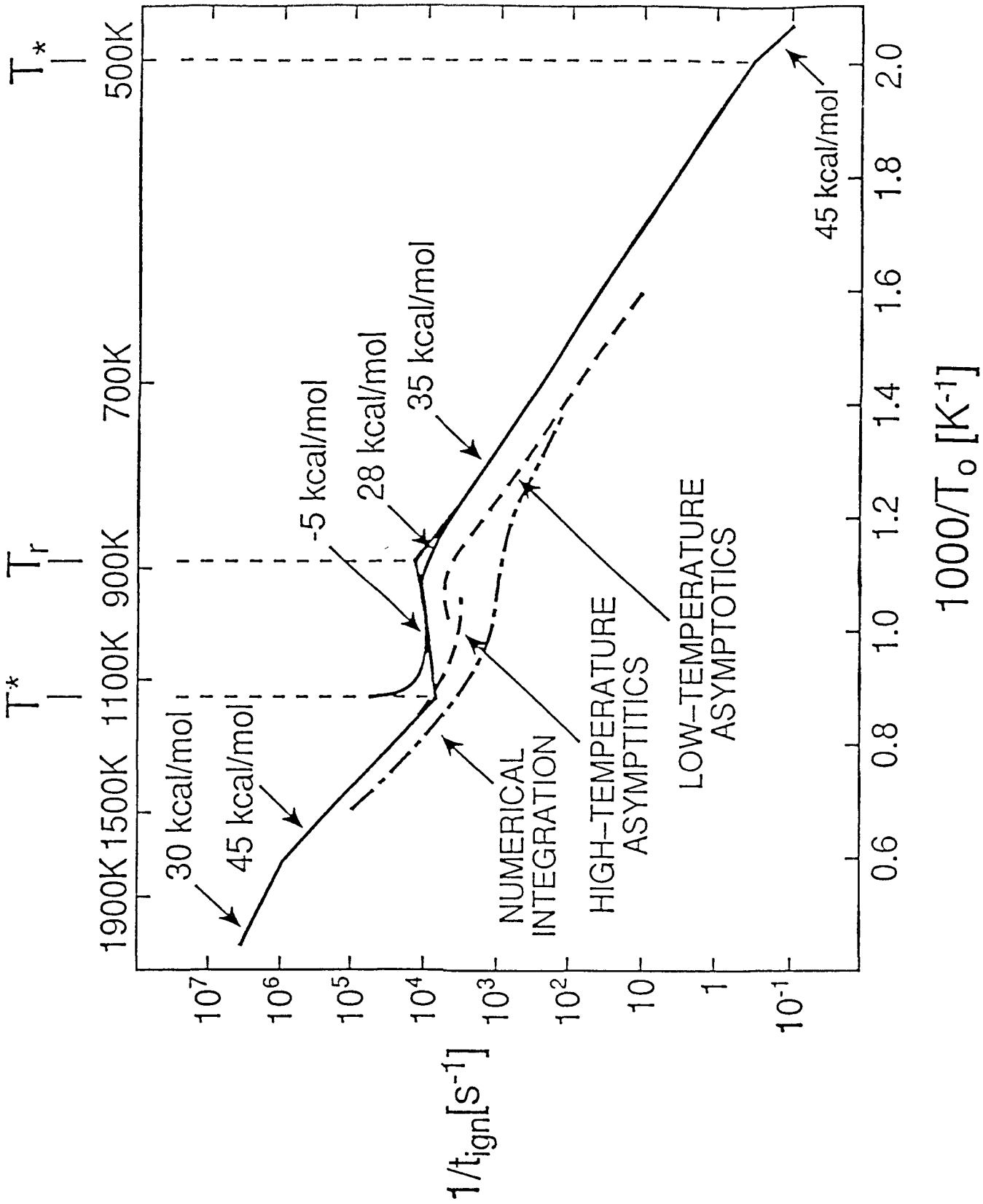

Figure 7: A schematic Arrhenius plot of reciprocal ignition times based on a criterion of thermal runaway.

More rapid rates of pressure increase, such that the relevant pressure-change time is short compared with low-temperature ignition times, places the ignition process in the high-temperature regimes described above. More detailed analyses for specifically prescribed pressure histories can be developed.

In unstrained mixing layers, characteristic inert diffusion times typically are long compared with ignition times, and relevant analyses of ignition stages in such nonhomogeneous systems can make use of the preceding chemical-kinetic descriptions. Imposing strain on mixing layers can reduce characteristic diffusion times substantially. For steady, strained mixing layers, ignition cannot occur if the strain rate is too large. Relevant parameters here will be Damköhler numbers related to $(At_{ign})^{-1}$, for the A of Eq. (18). At sufficiently high temperatures, analyses[7] based on one-step activation-energy asymptotics can be employed directly; at lower temperatures, the dependence of the peak temperature on Damköhler numbers may be more complex because of the two-step chemistry, and further analysis is needed.

6.12 CONCLUSIONS

The model mechanism for heptane ignition does not involve chain branching and therefore needs thermal explosion theory for describing its ignition process. Different chemical-kinetic simplifications arise in four different temperature ranges, as explained in Section 8. These ranges can be combined into a high-temperature regime (above roughly 900 K), in which reaction intermediaries maintain steady states and two parallel reactions effectively occur, and a low-temperature regime (below 900 K), in which two sequential reactions occur, the other two steps being negligible. Simplified ignition-time formulas, Eqs. (46) and (56), enable estimates of adiabatic, isobaric, homogeneous ignition times to be obtained over three different temperature ranges. The results provide basic information needed for pursuit of asymptotic analyses of n-heptane ignition in nonhomogeneous systems with variable pressure.

Of particular use in modeling that involves computation with finite rates is the reduced version of Eqs. (1) thorugh (5), obtained through asymptotic analysis,[5] that corresponds to a two-reaction description of the chemistry, applicable over the temperature range from about 800 K to 1500 K, which includes essentially all temperatures of practical interest. In this range, the reaction becomes simply[5]

$$F + 11O \rightarrow P, \tag{60}$$

with the rate

$$\omega = k_1 n_F + k_4 K_3 n_O^2 n_F, \tag{61}$$

the first term of which is dominant in the high-temperature portion of this range, and the second term of which is dominant in the low-temperature portion. This rate expression has been indicated[5] to exhibit a minimum around 1180 K. This result can thus be used quite readily in computational simulations of ignition.

6.13 REFERENCES

1. D.J. Vermeer, J.W. Meyer and A.K. Oppenheim, Combustion and Flame 18, 327 (1972).

2. C.M. Coats and A. Williams, Seventeenth Symposium (International) on Combustion, The Combustion Institute, Pittsburgh, 1979, pp. 611-621.

3. H. Cieski and G. Adomeit, Combustion and Flame, to appear, 1992.

4. C.K. Westbrook, J. Warnatz and W.J. Pitz, Twenty-Second Symposium (International) on Combustion, The Combustion Institute, Pittsburgh, 1989, pp. 893-901.

5. U.C. Müller, N. Peters and A. Liñán, "Global Kinetics for n-Heptane Ignition at High Pressure," Twenty-Fourth Symposium (International) on Combustion, The Combustion Institute, Pittsburgh, to appear, 1992.

6. A. Liñán and F.A. Williams, Fundamental Aspects of Combustion, Oxford University Press, New York, 1993.

7. A. Liñán and F.A. Williams, "Ignition in an Unsteady Mixing Layer Subject to Strain and Variable Pressure,"IDEA Report, 1990.

8. F.A. Williams, Combustion Theory, Second Edition, Addison-Wesley, Menlo Park, CA, 1985, p. 580.

9. A. Liñán, "Ignition of a Nonuniform Mixture in a Chamber of Variable Volume," unpublished, 1990.

10. A. Liñán and F.A. Williams, "Turbulence Interactions in Diesel Ignition," IDEA Report, 1991.

7 CONCLUSIONS AND RECOMMENDATIONS

Specific conclusions have been given in the preceding chapters. Here only general conclusions and recommendations are stated.

One general observation concerns the importance of the mixture fraction for describing Diesel ignition and combustion processes. This is a useful and underutilized variable in code development. The present work showed how to extend mixture-fraction formulations to account for Lewis numbers differing from unity and demonstrated the relevance of the instantaneous scalar dissipation to Diesel ignition.

Another general observation concerns the surprising ease with which pressure variations can be taken into account in analyzing Diesel ignition. The best temperature variable to use when pressure varies with time is the ratio of the temperature to that produced by isentropic compression. Although not yet implemented in codes, this variable was used extensively in the present work to obtain ignition conditions and ignition times.

A surprising result is that strong time-dependent pressure variations associated with compression can significantly simplify ignition descriptions in ignition theory. Basically, these variations tend to cause ignition processes to occur homogeneously in local advantageous spots, so that spatial variations during ignition stages produce small influences. In other words, the asymptotic analyses often are easier to perform under strong compression than under other conditions. This greatly facilitated obtaining many of the results in the present program.

The importance of ignition-front propagation, in contrast to flame propagation, in contributing to the initial combustion-induced pressure rise, was identified in the present study. In this ignition-propagation stage the pressure increases in proportion to the two-thirds power of the time increment. The statistical turbulent properties that influence ignition histories in nonuniform mixtures under compression were identified here.

Flame propagation mechanisms in mixing layers during triple-flame regimes were clarified in the present work. In particular, conditions for positive and negative rates of spread of flame edges have now been determined.

Finally, different ignition regimes exist in different ranges of pressure and temperature when a four-step description of n-heptane ignition kinetics is employed. Different overall activation energies apply in different regimes, and there is a range of temperatures (typically between roughly 800K and 1100K) over which the asymptotics give negative overall activation energies and peculiar ignition histories resulting in ignition times strongly dependent on adopted ignition criteria.

Pursuit of further asymptotic analyses of ignition times in unsteady, strained mixing layers is recommended, as indicated in Chapter 3. Also, further analyses along the lines of the simplifications in Chapter 4 could profitably be developed. During the temperature range of negative overall activation energy of Chapter 6, cool flame propagation may readily develop and contribute significantly to the ignition transient; conditions for this to occur, as well as methods for describing it, can readily be identified and therefore are worthy of further work. Finally, the mixture fraction, scalar-dissipation and relative-temperature variables of the present work are recommended to be given further consideration for use in code development.